ABSTRACT

Title of Document:	INFLUENCE OF ENVIRONMENTAL CONDITIONS ON THE AGE, HATCH DATES, AND GROWTH OF JUVENILE ATLANTIC MENHADEN IN THE CHOPTANK RIVER, MD
	Alexandra Nicole Atkinson, Master of Science Degree, 2016
Directed By:	Professor David H. Secor Marine, Estuarine, and Environmental Science

Since 1993 Atlantic menhaden has experienced sustained low juvenile production (recruitment) in the Chesapeake Bay. Factors controlling growth, abundance, and mortality of larval and juvenile menhaden change throughout ontogeny such that larval growth rates could carry over to juvenile growth and survival. The effects of winter thermal conditions on the hatch dates and growth of larval and juvenile Atlantic menhaden in Atlantic shelf and Chesapeake Bay habitats were examined using otolith (ear-stone) increment analyses and growth models. For 2010-2013, truncated hatch-date distributions provided evidence for a winter recruitment bottleneck in Atlantic menhaden caused by cold temperatures. Hatch-dates of surviving juveniles were skewed towards warmer months for years characterized by colder temperatures. Reduced larval growth rates, influenced by

reduced temperature and food availability, carried over to juvenile growth rates. A growing degree-day model performed well in simulating observed juvenile growth rates in the Choptank River tributary of Chesapeake Bay.

INFLUENCE OF ENVIRONMENTAL CONDITIONS ON THE AGE, HATCH DATES, AND GROWTH OF JUVENILE ATLANTIC MENHADEN IN THE CHOPTANK RIVER, MD

By

Alexandra Nicole Atkinson

Thesis submitted to the Faculty of the Graduate School of the
University of Maryland, College Park, in partial fulfillment
of the requirements for the degree of
Master of Science
2016

Advisory Committee:
Professor Dr. David H. Secor, Chair
Professor Edward Houde
Associate Professor Lora Harris

Acknowledgements

First, I would like to thank my committee chair and major advisor, Dr. David Secor. You have been a joy to work with and I am inspired everyday by your unending enthusiasm for everything that you do. Thank you for providing me the opportunity to join your lab and for offering your guidance throughout this process of self-discovery. Thank you to Drs. Ed Houde and Lora Harris for sharing your expertise and valuable feedback.

Secor lab members, past and present, were instrumental throughout the thesis process. Thank you to Matt Siskey, for guiding me through the world of tiny menhaden otoliths, and to Mike O'Brien, for serving as an amazing student mentor and R coach. Without help from you both, and Brian Gallagher, I also wouldn't have any menhaden samples, so thank you for all your hard work in the field.

I'd also like to thank Carlos Lozano for your assistance in learning otolith polishing and ageing and Cara Simpson for helping me work through many a mind-bending menhaden puzzle. You are both engaging soundboards off which I've bounced many ideas. Thank you to Eric Annis for guiding me through bioenergetics model Excel spreadsheets and to Jennifer Humphrey for allowing me to apply the GDD model. I've learned so much from working with you, Slava Lyubchich, thank you for recommending statistical methods and helping me to apply them. Thank you to Nicole Millette, at the Horn Point Laboratory, for generously sharing your winter chlorophyll *a* data.

I'd like to also thank my boyfriend, Justin Warrenfeltz, for your continued support and inspiration, from near or far, throughout this process. Finally, I'd like to thank my family: Terri, Dale, and Colby. You've encouraged me to always pursue my dreams and never doubted my passion for one second (no matter how far away from home it guided me).

Table of Contents

List of Tables

List of Figures

Figure 11 Winter water temperature (°C) from 1 December – 31 March time series for the Chesapeake Bay Bridge Tunnel NOAA Tides and Currents site at the bay mouth for 2010 – 2013.

Figure 12 Cumulative frequency of winter temperature (°C) as measured at the Chesapeake Bay Bridge Tunnel NOAA Tides and Currents site near the bay mouth 2010-2013.

Figure 13 Mean winter temperature experienced by aged YOY menhaden (°C) vs. hatch date. Experienced temperature estimated by averaging daily water temperatures measured at the Chesapeake Bay Bridge Tunnel site between the date of hatch and the estimated date of ingress (50 days post hatch).

Figure 14 Boxplot of YOY Atlantic menhaden otolith increment widths before (gray bars) and after (white bars) 50 days (ingress) for all years sampled in the Choptank River, MD. Sample sizes from 2010 – 2013 are 45, 41, 37, and 44, respectively. Box covers from 25^{th} – 75^{th} percentile, horizontal bar marks the mean, and whiskers extend to the highest/lowest value within 1.5 * inter-quartile range.

Figure 15 Pre- and post-ingress water temperatures (°C) calculated per individual based on dates of hatch, approximated dates of ingress (50 days after hatch), and capture dates for 2010 – 2013 Atlantic menhaden samples (N=167). Sample sizes from 2010 – 2013 are 45, 41, 37, and 44, respectively. Box covers from 25^{th} – 75^{th} percentile, horizontal bar marks the mean, and whiskers extend to the highest/lowest value within 1.5 * inter-quartile range. Pre-ingress temperatures from Chesapeake Bay Bridge Tunnel (NOAA Tides & Currents site # 8638863) and Stingray Point and First Landing sites (Chesapeake Bay Interpretive Buoy System). Post-ingress temperatures from Goose's Reef (CBIBS) and Cambridge, MD (NOAA Tides & Currents) sites. Different years, as measured by Tukey HSD, are marked with differing letters (post-ingress: above; pre-ingress: below).

Figure 16 Length at age for 2010 – 2013 sample of YOY Atlantic menhaden from the Choptank River, MD. All 2013 specimens are plotted with solid figures with slow growing individuals denoted by triangles and others are denoted by circles.

Figure 17 YOY menhaden otolith increment widths before (gray bars) and after (white bars) 50 days (ingress) for the two growth sub-cohorts observed in 2013. Box covers from 25^{th} – 75^{th} percentile, horizontal bar marks the mean, and whiskers extend to the highest/lowest value within 1.5 * inter-quartile range.

Figure 18 Pre- and post-ingress growth rates of YOY Atlantic menhaden. Different years, as measured by Tukey HSD, are marked with differing letters (pre-ingress: above; post-ingress: below). Box covers from 25^{th} – 75^{th} percentile, horizontal bar marks the mean, and whiskers extend to the highest/lowest value within 1.5 * inter-quartile range.

Figure 19 Pre- and post-ingress chlorophyll concentration ($\mu g\ L^{-1}$) calculated per individual based on dates of hatch and approximated dates of ingress for 2010 – 2013 Atlantic menhaden samples (N=167). Box covers from 25^{th} – 75^{th} percentile, horizontal bar marks the mean, and whiskers extend to the highest/lowest value within 1.5 * inter-quartile range. Pre-ingress chlorophyll measures from Chesapeake Bay Bridge Tunnel (NOAA Tides & Currents site # 8638863) and Stingray Point and First Landing sites (Chesapeake Bay Interpretive Buoy System). Post-ingress chlorophyll measures from Goose's Reef (CBIBS) and

Cambridge, MD (NOAA Tides & Currents) sites. Different years, as measured by Tukey HSD, are marked with differing letters (post-ingress: above; pre-ingress: below).

Figure 20 Pruned regression tree of factors that influence post-ingress mean otolith increment widths for Atlantic menhaden. Variables tested included: pre/post-temperature, pre/post-chlorophyll densities, pre-ingress mean otolith increment width and biweekly hatch date. For specific estimates of terminal group characteristics see Table 8.

Figure 21 Box whisker plots of growth rates (mm d^{-1}) from length at age data for summer-captured YOY Atlantic menhaden in the Choptank River, MD 2010 – 2013. Box covers from 25^{th} – 75^{th} percentile, horizontal bar marks the mean, and whiskers extend to the highest/lowest value within 1.5 * inter-quartile range.

Figure 22 Growing degree-day model simulation results for three dates of ingress (right y-axis: 1 November, 1 February, and 1 April) and for three dates of capture (lower x-axis: 1 June, 1 July, and 1 August) for Chesapeake Bay Atlantic menhaden YOY. Upper x-axis represents three growth temperature thresholds tested (10°, 12°, 14°C).

Figure 23 Length at age for YOY Atlantic menhaden from growing degree-day (GDD) model for December - April ingress months, July capture month (see Tables 10-13), and 10, 12 and 14°C growth thresholds (red, blue, and green symbols). Overlain are empirically observed (July capture month) data (black symbols) from 2010 – 2013.

Figure 24 Bioenergetics model length predictions for Atlantic menhaden YOY in 2010 – 2013 with constant or variable consumption.

Figure 25a Length at age for observed (black symbols) and modeled (red, green, and blue symbols) YOY Atlantic menhaden in 2010-2013. Observed lengths are plotted as a mean ± 2 standard deviations and, when possible, multiple sampling months means are regressed to infer growth rates (mm d^{-1}).

Figure 25b Length at age for observed (black symbols) and modeled (red, green, and blue symbols) YOY Atlantic menhaden in 2010-2013. Observed lengths (black symbols) represent the mean length ± two standard deviations collected during monthly sampling events. A regression was performed on all years combined to infer growth rate from the slope (mm d^{-1}).

Introduction

Marine fish populations are known for dynamic changes in abundance and distribution, which are often linked to recruitment variability (Rothschild, 1986; MacCall, 1990; Houde, 2009; Secor, 2015). Pelagic planktivores regularly show low frequency oscillations in their recruitments (Bakun et al., 2009; Alheit and Bakun, 2010). For example, recruitments of Norwegian spring-spawning herring, *Clupea harengus,* vary by three orders of magnitude and are characterized by decadal oscillations (Sætre, 2002). Similarly, anchovy and sardine exhibit multi-year abundance oscillations, which are associated with the Pacific Decadal Oscillation (Schwartzlose et al., 1999; Alheit and Bakun, 2010). Atlantic menhaden recruitments in Chesapeake Bay vary >20 fold according to juvenile abundance indices, but have been persistently low for the past 20+ years (Figure 1a). Herring, anchovy, sardines, and menhaden, commonly referred to as forage fish, support valuable and large-scale commercial fisheries worldwide (Pikitch et al., 2012). Much research has been devoted to identifying the causes of high recruitment variability in forage fishes. An improved understanding of factors contributing to this variability will translate to better predictions of population fluctuations, assessment strategies, and overall management of this important species guild.

Atlantic Menhaden Fluctuations

Atlantic menhaden, *Brevoortia tyrannus,* is a forage fish found in the northwest Atlantic Ocean ranging from Nova Scotia to Florida (Hildebrand, 1948; Reintjes, 1960). Population dynamics of Atlantic menhaden are believed to be

controlled by processes that affect juvenile recruitment in Chesapeake Bay, the center of its distribution and historical fishery (Maryland Sea Grant [MDSG], 2009). Lack of a strong stock-recruitment relationship for Atlantic menhaden indicates that environmental fluctuations are a primary driver of recruitment variability in Chesapeake Bay and coast-wide (SEDAR, 2015). Specifically, climate fluctuations indexed by inter-annual winter-spring conditions in the mid-Atlantic, are suggested as a primary cause of menhaden recruitment variability (Kimmel et al. 2009; Buchheister et al., *in* press). In a multivariate analysis of Chesapeake Bay juvenile finfish abundances, Wood and Austin (2009) documented a negative relationship between recruitment of anadromous (e.g., coastal species that spawn in freshwater including striped bass) and coastal shelf-spawning (e.g., Atlantic menhaden) species. This pattern caused oscillations in young-of-the-year (YOY) abundances of anadromous and coastal shelf-spawning species at both decadal and interannual scales. Additionally, Austin (2002) proposed that warm-wet and cold-dry decadal regimes in Chesapeake Bay were associated respectively with higher recruitments of shelf- and anadromous- spawning species. The 1960s was a cold-dry period, which shifted to warm-wet conditions in the 1970s. Atlantic menhaden recruitments, represented by the Maryland juvenile index, showed a dramatic increase from the 1960s to the 1970s (Figure 1a). However, Wood (2000) proposed that high menhaden recruitments generally coincide with warm-*dry* late-winter conditions. When the Azores-Bermuda high pressure system dominates the mid-Atlantic Bight, it may provide favorable shoreward larval transport and feeding conditions or favorable

within-nursery conditions for young-of-the-year (YOY) menhaden (Wood and Houde, 2003).

Atlantic menhaden have a complex life cycle that results in opportunities for both coastal and estuarine conditions to influence recruitment variation. Starting early life as larvae in coastal shelf waters, menhaden exhibit particle feeding on zooplankton. Upon metamorphosis, gill-rakers lengthen and body depth and mass increase. With increased filtering and swimming abilities, their food source shifts from zooplankton to primarily phytoplankton, corresponding to a decrease in their trophic level (Friedland et al., 1984). In addition to this trophic shift, YOY juveniles transition from shelf waters to estuaries, bays, and tributaries (Friedland et al., 1996). Associated with this ingress to estuarine habitats are large shifts in the amplitude and variability in water temperature, salinity, currents and flow, predation, food source, and oxygen level.

Chesapeake Bay Atlantic Menhaden

Chesapeake Bay is one of the most important nursery estuaries contributing to the coast-wide production of Atlantic menhaden (Nicholson, 1978). Juveniles occur in all tidal portions of Chesapeake Bay, but are concentrated in sub-estuaries and open water habitats (Friedland et al., 1996; Houde, 2009). The Chesapeake Bay, including coastal Virginia, is estimated to contribute 69% of the annual recruits to the coast-wide stock, based on a calculation normalizing relative menhaden production to estuarine area (Ahrenholz et al., 1989; Atlantic States Marine Fisheries Commission

[ASMFC], 2004). Thus, understanding the dynamics of menhaden within Chesapeake Bay is essential for understanding coast-wide stock fluctuations.

Menhaden spawning has been documented in all months of the year. However, spawning over US mid-Atlantic shelf waters occurs from August – January (Higham and Nicholson, 1964; Berrien and Sibunka, 1999; Lozano et al., 2012). Most larvae ingress into Chesapeake Bay from November to April, resulting from spawning that occurred from August – January (Lozano, et al. 2012). The transport of larvae from shelf waters into estuaries depends on winds, ocean currents, temperature, as well as spawning time and location (Quinlan et al., 1999; Rice et al., 1999; Warlen et al., 2002; Epifanio and Garvine, 2001). Ingressing larvae enter estuaries and will soon transform into YOY juveniles. Once inside the estuary, menhaden (6-40 mm TL) feed and grow during the spring, summer, and fall months (Lozano, et al. 2012; Lozano and Houde 2013). Thus, during their first year of life, menhaden will experience the full seasonal range of temperatures in Chesapeake Bay (~1°C to 29°C) (Murdy et al. 1996).

Abundances of age-0 juvenile menhaden (i.e., recruitments) in Chesapeake Bay have varied >20-fold and since 1993 have persisted at less than 10% of recruitment levels for the period 1974-1981 (Figure 1a). Owing to their abundant biomass among juvenile ichthyofaunal surveys (Jung and Houde, 2003), sustained low recruitments likely have had food web effects on predators such as striped bass, *Morone saxatillis,* and osprey, *Pandion haliaetus,* and indirect impacts due to their mid-trophic role. At low abundance, primary production consumed by young menhaden is not as efficiently transferred to higher trophic levels when menhaden

abundance is low (Ahrenholz, 1991; Uphoff, 2003; Bakun et al., 2009). Low YOY recruitments in Chesapeake Bay also likely affect subsequent coast-wide fishery yields for age 1-2 menhaden, which are largely concentrated in the lower Chesapeake Bay and southern mid-Atlantic shelf waters (ASMFC, 2004).

In general, processes that influence menhaden recruitment can be classified as those occurring in (1) shelf waters, including reduced egg production, poor growth and survival of larvae, and reduced transport and ingress of larvae into Chesapeake Bay, and (2) within Chesapeake Bay, including poor growth and survival, and high predation of late-stage larvae and juveniles. Previous work, focused on shelf processes, documented 9-fold variability in larval abundance at the mouth of Chesapeake Bay (Lozano et al., 2012; Lozano and Houde, 2013). However, the observed variability in larval abundance did not correlate with subsequent juvenile abundance as estimated by Maryland Department of Natural Resources (MDNR), suggesting strong control over production may occur on post-ingress larvae and YOY juveniles within Chesapeake Bay.

Environmental Conditions Experienced by YOY Atlantic Menhaden

Environmental conditions vary greatly between offshore, coastal, and estuarine habitats experienced by Atlantic menhaden throughout their life cycle. Around 50 days-post-hatch, larvae transition from inhabiting coastal shelf waters to shallow bays and estuaries. This shift exposes transforming larvae and YOY juveniles to changes in temperature, mixing, dissolved oxygen, and salinity as well as plankton and nutrient concentrations. In addition, predator densities are likely higher in more

productive estuarine waters. Offshore sea surface temperatures in the Mid Atlantic Bight range from 4°C in winter to 26°C in summer (NOAA National Data Buoy Center, site #44014). Water temperatures within Chesapeake Bay range from 1° to 29°C and exhibit high variability, seasonal stratification, and increased productivity when compared to oceanic waters (Flemer, 1970; Murdy et al. 1996). Thermal conditions act directly and indirectly to control recruitment and survival of fishes. Temperature directly influences mortality, growth, and metabolic rates at the individual level (Lewis, 1965; Secor and Houde, 1995; Houde, 2009), while indirectly controlling ecosystem-level productivity that fluctuates on decadal cycles (Austin, 2002; Wood and Austin, 2009). Salinities in Chesapeake Bay range from 0.5 at the mouth of the Susquehanna River to 30 at the bay mouth, while well-mixed offshore salinities range from 25 – 32 (data from CBIBS First Landing site, Murdy et al. 1996). Zooplankton and phytoplankton stocks vary seasonally and serve as the primary food source for larval and juvenile menhaden. . Due to bloom dynamics, plankton is a highly patchy and pulsed resource. The timing as well as spatial extent and variability of plankton resources (indexed here as primary production) in Chesapeake Bay likely affect growth and distributions of incoming menhaden cohorts as they transition to filter-feeding juveniles. Although larvae primarily feed on zooplankton, information on zooplankton concentrations are largely unavailable so I focused on chlorophyll *a* measures as a proxy for phytoplankton densities to test their influence on juvenile menhaden growth. Positive correlations between phytoplankton stocks and YOY juvenile menhaden abundance and growth have been detected (Friedland et al., 1989; 1996; Annis et al., 2011; Houde et al., *in review*). Overall,

larvae move from stable water quality but diffuse forage resources in offshore habitats to an estuarine habitat characterized by higher variations in water quality and forage concentrations, the latter ephemerally more concentrated. Menhaden embryos, larvae, and juveniles experience contrasting environments throughout their life history which influence their growth and survival to the next life stage.

Although Atlantic menhaden shift habitats early in life, both coastal and estuarine environments are crucial in setting the stage for growth, feeding, and survival beyond the larval stage. Predator densities, food availability, and thermal conditions vary greatly, depending on timing of hatch and larval ingress into Chesapeake Bay. Larvae hatched from October – December experience different conditions than those hatched from January – March. Their complex life cycle thus entails carryover effects where processes acting on larvae, such as hatch timing and larval ingress, indirectly influence YOY juvenile growth and recruitment. Carryover effects have been documented in many taxa including fish, crustaceans, birds, and mammals. Pechenik (2006) defines carryover effects as, "characteristics that originate in embryonic and larval experiences but become visible only in juvenile or adult stages." More generally, these ecological effects occur when past experiences influence current outcomes (O'Connor et al., 2014). They may also be referred to as "latent effects" because they remain latent until later expressed in juveniles or adults. Thus, a condition or stressor during the larval stage in fish, for example a food deficiency, could be displayed later as depressed juvenile or adult growth. For example, larval growth and mortality rates in Patuxent River white perch, *Morone americana,* indirectly influenced adult migratory behavior outcomes through

carryover effects (Kerr and Secor, 2010). Early spawned, slower growing larval cohorts were disproportionately represented in the adult migratory contingent; whereas faster growing larvae were more likely to contribute to the resident contingent (Kerr and Secor, 2010). Once established, migratory behaviors typically persist throughout the organism's lifetime (Kerr and Secor, 2009).

Recruitment success has also been linked to carryover effects originating in the larval stage. Bergenius et al. (2002) detected positive correlations between larval otolith increment widths (corresponding to somatic growth) and settlement rates in a Caribbean reef fish. Faster larval growth correlated with earlier settlement and, subsequently, enhanced recruitment. Similarly, increased larval growth rates in kelp bass corresponded to increased survival post-settlement (Shima and Findlay, 2002). Both these studies in reef fish demonstrate the influence of larval life on juvenile and adult outcomes. This expanding area of research on carryover effects has the potential to explain recruitment variations, especially in forage fish like Atlantic menhaden.

Objectives

My thesis focuses on the effects of thermal conditions and phytoplankton stocks on recruitment through its direct and indirect influences on survival, growth, and hatch-date patterns of juvenile Atlantic menhaden in Chesapeake Bay. I aimed to further investigate the mismatch of larval- and juvenile-derived hatch dates described by Lozano et al. (2012) for years with varying winter conditions. Otolith microstructure was employed to estimate hatch-date distributions and juvenile growth, while two menhaden-specific growth models were employed to compare

empirically observed growth outcomes with model predictions. The Choptank River was selected as the focal tributary of this four-year study because of its pronounced recruitment signal in the Maryland Department of Natural Resources bay-wide menhaden index of YOY abundance (Figure 1b). Though I am primarily interested in the influence of wintertime environmental conditions on the early life stages of Atlantic menhaden, early stage juveniles are not easily sampled in Chesapeake Bay during winter. Thus, my analysis focuses on "wintertime survivors" collected as juveniles during summer, and inferences about wintertime growth were made using their otoliths as record-keeping structures, which enabled evaluation of early life carryover effects.

Objective 1: Test the influence of winter temperature on juvenile-derived hatch-date distributions.

Winter conditions are important for Atlantic menhaden because spawning primarily occurs from August – January (Higham and Nicholson, 1964; Berrien and Sibunka, 1999; Lozano et al., 2012). Thus, embryos and larvae are exposed to offshore conditions during winter months. Environmental variability, specifically inter-annual changes in winter-spring conditions, has been suggested as a main controller of menhaden recruitment variability due to the lack of a strong stock-recruitment relationship (MDSG, 2009; SEDAR, 2015). This objective focuses on examining the influence of winter temperature on the hatch dates of surviving juvenile menhaden in the Choptank River. Owing to the prominent influence and high range (~1°C to 29°C) of thermal conditions experienced by Atlantic menhaden during

their first year of life, hatch-date distributions of sampled juveniles will reflect survivors of prior thermal conditions. Previous research identified the importance of temperature in controlling recruitment and growth of YOY menhaden (Schwartlose et al., 1999; Wood and Houde, 2003; I aim to compare menhaden hatch-date distributions of surviving juveniles for years with varying winter thermal conditions.

By using otolith microstructure analyses to investigate hatch dates of YOY menhaden along with concurrent winter temperatures, distributions may inform which conditions favored larval and juvenile survival. If larval survival to the juvenile stage is similar across all hatch dates, then I would expect juvenile-derived hatch dates to overlap with observed larval-derived hatch dates occurring from October – March. However, this was not observed in the Lozano et al. (2012) study, which documented that juvenile hatch dates in three years of observations occurred mostly from January – March, while those of ingressing larvae predominately had hatched from October – December. This mismatch between larval- and juvenile-derived hatch dates suggests decreased survival of early-hatched individuals to the juvenile stage.

I hypothesize that cold winter conditions depress growth and survival of early-ingressed larvae and early stage juveniles during winter months causing this mismatch between larval- and juvenile-derived hatch dates. Conversely, greater overlap is expected during warmer winter conditions. I will test this hypothesis by examining hatch dates and concurrent thermal conditions from juvenile menhaden sampled from 2010 – 2013 in the Choptank River across a range of winter temperature conditions. In addition, I hypothesized that later-hatched individuals would exhibit increased survival when compared to early-hatched individuals, which

would be evident based on proportion of early- versus late-hatched individuals from all juvenile samples.

Objective 2: Examine pre- and post-ingress growth dynamics and the potential for a carryover effect of larval thermal and feeding conditions to juvenile stage growth rates.

Forage fishes are highly fecund and produce thousands of small eggs per spawning event (Lewis et al., 1987; Winemiller and Rose, 1993). However, the majority of eggs spawned will not survive (Hjort, 1914; 1926). What sets apart the embryos and larvae that survive from those that perish? Food availability, currents, and predation all control egg and larval survival and growth at the individual level (Houde, 2009). Subtle variability in growth, in addition to episodic events, affect survival and recruitment rates of cohorts (Houde, 1989). Additionally, individual growth and cohort recruitment at later life stages may also be influenced by effects that carryover from the larval stage. This objective aims to identify whether larval menhaden characteristics, specifically hatch timing and early growth, carry over to affect YOY juvenile growth rates. Larval and juvenile growth rates were compared with the expectation that fast larval-stage growth enhances juvenile growth. With prior research suggesting recruitment controls act on the menhaden juvenile stage (MDSG, 2009; Houde et al., *in review*), I aimed to identify if carryover effects are present from larval to juvenile menhaden. In order to examine this question, individual growth histories were reconstructed.

I retrospectively tracked changes in growth throughout ontogeny by measuring otolith increment widths that provide a proxy for somatic growth in many fish species including Atlantic menhaden (Maillet and Checkley, 1990; Ahrenholz et al., 1995; Chambers and Miller, 1995). Widths of daily rings change depending on somatic growth and environmental conditions (Maillet and Checkley, 1990; 1991; Fitzhugh et al., 1997). Menhaden ingress (at a total length [TL] between 20 – 30 mm) occurs before larvae metamorphose into juveniles (at a total length [TL] between 30 – 40 mm) and represents a potential survival bottleneck in the menhaden life history. Depending on when ingress occurs, the latent effect of coastal shelf conditions on larvae may influence juvenile growth and subsequent recruitment differently. By examining larval and juvenile growth in addition to hatch dates of sampled juveniles, I expected to potentially see evidence of these latent effects.

Temperature and phytoplankton densities have been identified as key factors influencing Atlantic menhaden growth. For example, Fitzhugh et al. (1997) found that laboratory-reared menhaden larvae kept at a higher-than-ambient temperature (25°C) reached metamorphosis one month earlier and had wider otolith increments beyond metamorphosis than those raised at ambient temperatures. In addition to timing of metamorphosis, temperature also indirectly influences juvenile growth through its effect on consumption. At higher spring and summer temperatures, YOY menhaden are poised to exploit warming conditions by increasing their consumption and growth. Laboratory studies of juvenile Atlantic menhaden consumption rates showed a rapid increase in consumption when ambient water temperature is increased from 18 to 25°C (Rippetoe, 1993). This temperature-associated increase in consumption may

lead to juvenile growth rates during summer months as high as 0.70 or 0.83 mm d^{-1} (Pacheco and Grant, 1965; Kroger et al., 1974). Individuals that experience warm temperatures may have an advantage over those that experience colder conditions because of improved feeding and swimming abilities associated with earlier metamorphosis. Larger size and associated increased swimming ability will improve ability of menhaden to search for prey resources, primarily phytoplankton. In this regard, Friedland et al. (1989) documented a positive correlation and overlap between phytoplankton concentrations and menhaden abundances in estuarine creeks.

This objective has two goals; (1) to compare pre- and post-ingress growth with environmental histories, and (2) examine a potential carryover effect of larval thermal and feeding conditions to post-ingress growth rates. Otolith increment widths and environmental data allow the reconstruction of growth and environmental histories of sampled juveniles. To test carryover effects, I examined growth during the juvenile stage relative to prior growth during the larval stage as well as concurrent (spring within the Bay) and past (winter on the coastal shelf) environmental conditions. I expected early-hatched individuals to exhibit slower larval growth rates owing to reduced shelf temperatures, which would carry over into juvenile growth rates. Conversely, I expected later-hatched larvae to exhibit faster larval growth rates, due to improved thermal conditions, that also carried over to juvenile growth rates.

Objective 3: Evaluate predictions of YOY growth derived from temperature degree-day- and bioenergetics-models against observed growth rates.

Growth models that integrate influential environmental factors with individual energetics permit evaluation of different growth scenarios. To examine possible causes of decreased menhaden recruitment to Chesapeake Bay, models have been developed to analyze and evaluate juvenile Atlantic menhaden growth. The application of temperature degree-day and bioenergetics models has provided opportunities to predict Atlantic menhaden growth across a range of environmental conditions (Annis et al., 2011; Humphrey et al., 2014). In this objective, growing degree-day and bioenergetics models were employed to further examine winter, spring and summer growth dynamics. Models simulated differing months of ingress. Growth predictions were compared between the two models to evaluate the influence of winter conditions on juvenile menhaden growth. To test possible model bias and limitations, predicted growth rates were compared with observed growth rates. When employing the growing degree-day model, I predicted that its simple temperature threshold for growth would not capture the subtleties of wintertime menhaden growth dynamics. I hypothesized that the bioenergetics model would predict observed growth outcomes more accurately because of its inclusion of both chlorophyll and temperature influences.

Methods

YOY Menhaden Sampling

YOY Atlantic menhaden were sampled during June, July, and August from 2010-2013 in the tidal Choptank River. Seven sampling sites were distributed from river km 11 to river km 63 (Figure 2). Mean salinity at the most down and upriver sites were 9.8 and 1.4, respectively (Table 1). Two gear types (operated simultaneously from two vessels for 2012 and 2013 collections) were deployed: a midwater trawl targeted channel and open water habitats (≥3 m deep), and a beach seine targeted adjacent shallow shore areas <1.5 m deep. The midwater trawl, with an 18 m^2 mouth-opening and a 4 mm mesh cod end, was towed from the R/V Rachel Carson obliquely from surface to bottom in two-minute time steps for a total of 20 minutes. The beach seine, 30 m long by 1.2 m deep with a 6 mm mesh and a ~ 1 m^3 bag, was deployed from the beach in a quarter sweep.

When menhaden were present in the catch, up to 30 were measured for TL (mm) and either frozen or preserved in 100% ethanol and brought to the laboratory. During processing, individuals were randomly selected for dissection. A minimum of 15 specimens from each gear type for each year were selected for otolith analysis, including all sites where menhaden were sampled, for a total of 167 specimens. An effort was made to subsample equally from all years, for both gear types, and from a representative diversity of sites. However, during otolith preparation many samples were rendered unusable for ageing, hence there occurred an unequal distribution of samples across years, gear types, and sites (Table 2). July-collected samples were prioritized over those collected during other months. The July samples consisted of

younger juveniles, sampled in mid-summer, that were relatively easy to age (i.e., count increments accurately).

Otolith Processing

Preserved menhaden were measured for total length (mm) and wet weight (g). Both sagittal otoliths were removed from the fish using protocol from Secor et al. (1991), and embedded in EpoxFix resin. A transverse section containing the core region (earliest formed portion of the otolith) was obtained using a slow speed metallurgical saw. Sections were mounted on glass slides, hand polished until the core was visible, and a digital image was captured (Figure 3). In Adobe Photoshop ©, daily rings were demarcated and enumerated from the core to the edge along the clearest axis. Sometimes, two images of the same otolith were used to improve resolution of daily growth rings. In these cases, one image was taken with the core in the focal plane and the other with the edge in the focal plane. An obvious landmark (e.g. crack, mark or distinct ring) was used to combine the series from the two annotated images (Figure 3). Ages in this study were adjusted by adding two days to the total number of rings (the initial ring circumscribing the core is counted as one), based on the expectation that the first growth ring forms 2-3 days after hatching (Maillet and Checkley, 1990). Precision and bias in growth ring interpretations were evaluated for a set of 30 otoliths, which were each randomly and blindly aged twice. If significant differences between the reads existed (paired t-test), an additional, randomly ordered read was performed. This was repeated until a paired t-test showed no significant difference between the last two age interpretations. Three age

interpretation trials were needed to achieve no significant difference between ageing trials. Precision between trials 1 and 2 was ± 14.5 rings and differed significantly when tested by a paired t-test ($p < 0.05$). Trials 2 and 3 estimated age with a precision of ± 13.2 rings and did not differ significantly ($p > 0.05$). As a proportion of the mean estimated age, this error was 10%. By convention, the age obtained during the third ageing trial was used as the final age count in days.

Otolith Increment Width Measures

Adobe Photoshop © was used for age interpretations and increment width analyses. The otolith growth axis of juvenile menhaden changes throughout ontogeny, making it difficult to delineate a single, linear radius from the core to the edge of the otolith (Figure 3). In an analysis on the effects of temperature on juvenile menhaden otolith microstructure, Fitzhugh et al. (1997) described two transitions in the direction of otolith growth axes: one that marks the onset of larval-YOY metamorphosis and another that demarcates the onset of juvenile growth. Initial trials to evaluate whether these landmarks could be consistently identified in my samples failed to consistently identify the two transitions. Rather, these trials supported consistency in a single transition point, which was defined to occur at the most pronounced change in the otolith growth axis (Figure 4). This transition point occurred at different ages for each individual, but on average occurred at 62 ± 11 estimated days-post-hatch (mean ± standard deviation) and divided the otolith into 2 growth axes or radii: one from the core to the transition and the other from the transition to the edge (Figure 4).

I used the otolith transition as a preliminary morphological proxy for changes in growth associated with ingress from shelf waters into Chesapeake Bay. Age at this transition varied widely (range 38-98 days). Lozano et al. (2012) found the average age of menhaden larvae ingressing into Chesapeake Bay was 46 (± 8.7 SD; range 9 – 96) days-post-hatch. In the interest of preserving 10-day bins for increment measures and consistency across all individuals, I selected an age of 50 days to represent the age at ingress. Thus, up to age 50 or pre-ingress, individuals were assumed to inhabit shelf waters. Beyond age 50 or post-ingress, individuals were assumed to inhabit Chesapeake Bay. A Principal Component Analysis (PCA) showed that a stipulated age at ingress (50 days) provided similar explanatory power as age at ingress estimated directly from the otolith transition point (Appendix Figure A1). Back-calculated lengths at 50 days-post-hatch were compared to the observed length distribution of ingressing menhaden from Lozano et al. (2012). Based on the overlap of length distributions it is likely that, on average, the assigned otolith dimension at 50 days post-hatch aligned approximately with ingress of larvae into Chesapeake Bay (Figure 5).

All aged otolith samples (2010-2013) were measured for pre- and post-ingress radii (to the nearest 0.01 micron), delineated by 50 days post-hatch. Mean increment widths were calculated by dividing the radii by the number of days pre- and post-transition. To compare slow- and fast-growing modes observed in 2013, every 10 increments were measured. Differences in increment widths were examined by comparing pre- and post-ingress radius lengths, pre- and post-ingress mean increment widths, and overall growth rates estimated from length at age data (growth

rate = $[TL_t - TL_0]$ age $^{-1}$; where TL_0 = length at hatch = 4.0 mm). Relationships between otolith radius, age, and total length were also examined.

Statistical Analyses

Statistical tests were performed in R version 3.2.0 (R Development Core Team 2015) using an alpha value of 0.05. Normality assumptions were checked using a Shapiro-Wilk test. If data were non-normal, log-transformation was applied and normality was re-checked.

Winter Temperature and Hatch-date Distributions

I hypothesized that in years characterized by cold winter temperatures, a greater proportion of later hatched individuals would be represented in samples of YOY juveniles. Thus, annual hatch dates distributions were expected to be ordered in time, earlier to later as winter temperatures declined. For the purposes of this study, "winter" was defined as the period between 1 December and 31 March. Mean winter temperatures, derived from the Chesapeake Bay Bridge Tunnel NOAA site, during the study were ordered from lowest to highest 2011, 2010, 2013 and 2012; with mean temperatures ranging from 5.5° – 9.2°C (Figure 6). Hatch dates were obtained by subtracting interpreted daily ages from the known date of capture. Because age interpretation precision was estimated at ± 13.2 days, hatch dates were combined to provide bi-weekly hatch-date distributions. Hatch-date frequencies were also adjusted for cumulative daily mortality using M = 0.01 d^{-1} (Lozano et al., 2012) and annual hatch-date distributions were compared using analysis of variance. Proportions of

hatch dates before and after 1 January were compared using a chi-squared test. Hatch-date distributions were further tested for asymmetry using the lawstat package (Gastwirth et al., 2015) in R version 3.2.0 (R Development Core Team 2015).

Pre- and Post-ingress Growth Dynamics

I hypothesized that individuals with slow, pre-ingress growth, as measured by otolith increment width, retain slow growth later into the juvenile period (post-ingress) as a latent effect. Individual growth histories can be matched with approximate environmental chronologies, assuming that the bay mouth temperature represents the pre-ingress time period and he Choptank River data represents the post-ingress period (Townsend et al., 1989; Campana and Thorrold, 2001). Measurements, made in Adobe Photoshop ©, of 10-ring bins along the otolith axis were compared to detect when a potential change in growth occurs. Pre- and post-ingress mean increment widths were compared across years using analysis of variance. Additional comparisons tested for differences between pre- and post-ingress mean increment widths of slow and fast growth sub-cohorts detected in 2013.

Back-calculation via the biological intercept method was used to determine the approximate size at ingress. To test whether the otolith transition was a sound approximation of ingress, back-calculated lengths at transition were compared with larval lengths at ingress measured by Lozano et al. (2012). The biological intercept method equation is

$$TL_a = T\,L_c + (((O_a - O_c)\,(TL_c - TL_0)) / (O_c - O_0))$$

where TL_a is the TL at age a (e.g., length at ingress), TL_c is the TL at capture, and L_0 is the TL at hatch (3.0 - 4.5 mm, MDSG, 2009), O_a is the otolith radius at age a, O_c is the otolith radius at capture (or total radius), and O_0 is the otolith radius at hatch (4.8 ± 0.3 microns, from Maillet and Checkley, 1990). Length at ingress was compared across years and 2013 sub-cohorts using analysis of variance. Instantaneous growth rate from ingress to capture was calculated as

$$IGR = ln\ (TL_c - TL_i) / (age_c - age_i)$$

where TL_c is the TL at capture, TL_i is TL at ingress (28 mm, Lozano et al., 2012), age_c is the age at capture, and age_i is the age at ingress. Here 46 days, rather than 50 days, was used to represent age at ingress, the former estimate empirically derived from Lozano et al., 2012.

Temperature, chlorophyll, and growth analyses were divided into pre- and post-ingress periods. Mean daily water temperature (°C) and chlorophyll concentrations ($\mu g\ L^{-1}$) pre- and post-ingress were calculated for each individual included in the ageing analysis (N=167) based on their hatch dates, calculated date of ingress, and known date of capture. For the pre-ingress period, environmental data were obtained from the Bay Bridge Tunnel NOAA Tides and Currents site (#8638863) and the Chesapeake Bay Interpretive Buoy System (CBIBS) Stingray Point and First Landing sites (Table 3; Figure 7). For the post-ingress period, environmental data were obtained from the CBIBS Goose's Reef buoy (#44062) supplemented by Cambridge, MD NOAA Tides and Currents buoy (#8571892) and the Chesapeake Bay Program site EE2.1 (Table 3; Figure 7). These sites were selected because the conditions are representative of pre- and post-ingress conditions.

Gaps in the post-ingress water temperature data (Goose's Reef site) were interpolated by regressing this time series against Cambridge, MD NOAA Tides and Currents buoy (#8571892) data. Pre- and post-ingress chlorophyll conditions were supplemented with Chesapeake Bay Program data for the 2010-2011 portion of the time series (Table 3; Figure 7).

To further examine the influence of winter temperature on hatch dates of juvenile Atlantic menhaden, mean winter water temperatures for each individual was estimated for the period bounded by the hatch date and 31 March, the stipulated end of winter. This way, each individual included in my ageing analysis had a unique mean winter water temperature. Water temperature data was drawn from the NOAA National Data Buoy Center Bay Bridge Tunnel site.

Classification and regression trees (CART) were used to develop a model to predict mean post-ingress increment width. In CART, data are classified into groups and subgroups through recursive partitioning. Starting with the full dataset, models are fit at each node to determine the most discriminating variable which then divides the data into branches based on a threshold value. This process continues until subgroups reach a minimum size or no classification improvements can be made. The results are depicted with a tree diagram and cross-validation is used to prune the full tree to avoid overfitting the data. Resultant groups at each node of the regression tree are compared using univariate analyses. This analysis was performed using the rpart package (Therneau et al., 2015) in R version 3.2.0 (R Development Core Team 2015). A regression tree was constructed for the post-ingress mean increment width with the

following predictors: pre-ingress mean increment width, hatch date, and pre- and post-ingress mean temperature and chlorophyll concentration.

Growth Estimates

Observed YOY growth rates were estimated using two methods; 1) by dividing growth increment between two ages by days between those ages [*Growth rate* = $(TL_2 - TL_1) / (age_2 - age_1)$] (N= 167) and 2) by regressing length at date for all menhaden collected on summer cruises for the June to August sampling period. The latter length-based growth rates permitted growth inferences on a much larger sample than the number of directly aged fish. Laird-Gompertz curves by Warlen (1992) and Lozano et al. (2012) show nonlinear larval menhaden growth with linear growth in the early YOY juvenile period (~80-100 days post-hatch). Accordingly, YOY growth was modeled as a linear function of age.

Growing Degree-Day Model

Observed size-at-age and growth rate estimates were compared to sizes and rates estimated from a growing degree-day (GDD) model (Humphrey et al., 2014). This linear model, derived from 49 years of YOY juveniles length frequency data (surveys conducted by: Virginia Institute of Marine Science, MDNR, University of Maryland Center for Environmental Science), determines whether or not growth occurs on a particular day due to a threshold temperature according to the expression

$$TL_t = TL_0 + \beta (\Sigma\, GDD)$$

where TL_t is the final predicted length, TL_0 is the initial starting length, β is an estimated constant, and Σ GDD is the sum of the growing degree-days that occur during a particular time period. A length distribution of larval menhaden (N= 10,524, μ = 28 mm) measured by Lozano et al. (2012) at the mouth of Chesapeake Bay from 2005-2008 was used as input for the starting lengths (TL_0). Three temperature thresholds were explored in this analysis (10°, 12°, 14°C) and β was held constant at 0.05 (Humphrey et al., 2014).

Temperature data used in model simulations were from CBIBS Goose's Reef site with gaps interpolated using Horn Point Laboratory Pier temperature records (Figure 7; see previous section). A suite of start dates (monthly from 1 November to 1 March), representing ingress dates, were simulated to explore the influence of winter conditions on summer growth predictions. End dates were selected based on dates YOY menhaden were sampled in the Choptank River. Thus, model simulations coincided with the period of summertime juvenile growth represented by my samples. Observed sizes at collection dates were compared to the model predictions for differing start dates and temperature thresholds.

Bioenergetics Model

A bioenergetics model developed for Atlantic menhaden in Chesapeake Bay by Annis et al. (2011) was applied to the Choptank River. This model couples a foraging model (Luo et al., 2001) with a Wisconsin bioenergetics model (Kitchell et al., 1977; Hanson, et al. 1997) to predict YOY juvenile menhaden growth outcomes. Sub-models describe consumption, swimming speed, gill-raker filtering efficiency,

respiration, excretion and carrying capacity as they influence YOY growth. The model was calibrated by Annis et al. (2011) to field-collected samples from Trophic Interactions in Estuarine Systems (TIES) and Chesapeake Bay Fishery-Independent Multispecies Survey (CHESFIMS; Miller, 2002; Jung and Houde, 2005) surveys over an 11-year period and successfully predicted observed menhaden lengths. The bioenergetics model requires an initial length and daily temperatures and chlorophyll concentrations to predict growth outcomes.

Inputs for my application of this model included daily water temperatures and chlorophyll concentrations, obtained from the Horn Point Laboratory Pier time series and Annapolis CBIBS site (Figure 7). When possible, winter chlorophyll data gaps were interpolated with weekly winter chlorophyll measurements collected by Horn Point Laboratory (Cambridge MD) student Nicole Millette at the Choptank River Fishing Pier (Table 3). The starting menhaden length was set at 28 mm (0.2 g predicted mass), the average length of ingressing menhaden larvae (N = 10,524) (Lozano et al., 2012). Model simulations began on the average date of ingress (day of year) from 2010-2013 and ended on days corresponding with cruise-collected menhaden samples and 31 August. The average date of ingress (28 March) over all the four years represented individual year averages, which ranged between 24 and 31 March.

The original model was calibrated by Annis et al. (2011) to 11 years of bay-wide observed length data by adjusting the percent chlorophyll available for consumption. The best fit occurred when 9.2% of available chlorophyll was

consumed, which was used in model applications. Consumption was calculated according to the formula

$$Consumption\ wt^{-1} = phy\ x\ gape\ x\ u\ x\ eff$$

where *phy* is phytoplankton concentration (g m^{-3}), *gape* is open mouth area (m^2), *u* is swimming velocity (m d^{-1}), and *eff* is filtering efficiency (dimensionless). So that the potential maximum consumption would not be exceeded, consumption used in the model was selected as the minimum value of either the calculated consumption or maximum possible consumption. Dissolved oxygen saturation was assumed to be normoxic and was held constant at 100%. All metabolic functions included in the full model were size-specific (consumption, swimming speed, gill-raker filtering efficiency, respiration, excretion and carrying capacity). Model output included daily growth projections of mean individual length at date for each of the four years of interest (2010-2013). Final fish length, mass, and growth potential throughout the season were estimated.

The model was highly sensitive to spikes in chlorophyll concentrations. Orders of magnitude pulses (i.e. blooms) in chlorophyll led to unrealistic short term increases in growth. These types of abrupt excursions were not observed in the original model runs by Annis et al. (2011) because chlorophyll inputs represented integrated, bay-wide estimates (Harding et al., 1994, 2005). The simulations in this study focused on one tributary and utilized more highly resolved data. To accommodate this model sensitivity, additional simulations were run with less varied chlorophyll conditions. These included a constant consumption rate (8% maximum

consumption) simulation to represent a scenario where YOY consumption was less responsive to ephemeral excursions in chlorophyll concentrations.

Growth Comparisons

Growth outcomes (length-at-age data) from the growing degree-day and bioenergetics models were plotted and compared with observed growth outcomes. Modeled and observed data consisted of lengths from June, July, and August. Regressions were fit to each year's empirical or simulated growth outcomes to estimate summertime juvenile growth rate. Because YOY menhaden were only collected in one month in 2010, linear regression could not be used to infer a juvenile growth rate. Instead, the mean overall growth rate across aged individuals (N = 45) was calculated for 2010 using length at age and size at hatch information (TL_0 = 4.0 mm).

Results

Ages and Hatch Dates

For all sample years, capture dates of aged YOY menhaden (N = 167) were centered in July, typically encompassing the 8 weeks from early June to early August (Table 4). Estimated ages ranged from 98 to 223 days with a mean 146 ± 24 days (SD). Ages did not differ across years, gear type, or sampling site (ANOVA on $\log_e$-transformed dates, $p_{year} = 0.16$, $p_{gear} = 0.10$, $p_{site} = 0.36$, N = 167). Ages differed significantly by capture month (ANOVA on $\log_e$-transformed dates, $p < 0.005$); earlier months exhibited younger ages than later months (Tukey HSD, $p_{Jun\text{-}Aug} < 0.001$, $p_{Jun\text{-}July} < 0.01$), although ages of July-caught menhaden were not significantly different than those of August-caught individuals (Tukey HSD, $p = 0.15$).

Hatch-date distributions adjusted for cumulative mortality effects showed relatively few juvenile "survivors" in samples with hatch dates before 1 January. Hatch-date frequencies before 1 January (overall = 7%) did not differ between years (range 0-15%; Table 5) (Chi Square, $p_{adj} = 0.58$). Unadjusted hatch dates ranged from late November to early April with the overall mode and mean occurring in the first two weeks of February (Figure 8). Hatch dates, adjusted for cumulative mortality effects, were shifted slightly earlier but the mode in hatch dates remained early February (Figure 8). Mortality-adjusted mean biweekly hatch dates did not differ among years (ANOVA, $p = 0.9$; Figure 9). Mortality-adjusted hatch-date modes in the 2010 and 2011 occurred in early and late February, respectively, and in 2012 and 2013 occurred in late January (Figure 9; Table 5). The earliest adjusted hatch date

was late November 2009 and the latest was early April 2013. Hatch dates showed more curtailed distributions during 2010-2011 than 2012-2013 (Figures 9, 10). The 2010 and 2011 hatch-date distributions exhibited gaps in early and late December with very low frequency of hatch dates detected in late November (2010) and early December (2011). Hatch-date distributions in 2010 and 2011 were also curtailed after February compared to 2012 and 2013 with sharp declines in hatch-date frequencies after their modes in early (2010) and late (2011) February (Figure 10). The hatch-date distribution in 2011 was significantly right-skewed (Symmetry test, $p < 0.05$). The hatch-date distribution in 2012 was broad with hatch dates spanning the late November to early April period and no gaps. Hatch dates in 2013 ranged from late December to early April with a mortality-adjusted mode in late January. Hatch-date distributions from 2010, 2012, and 2013 showed no significant asymmetries (Symmetry test, $p > 0.05$).

Winter Temperature and Hatch-date Distributions

Mean winter temperatures (1 December – 31 March), measured at the Chesapeake Bay Bridge Tunnel site, were warmer during the latter two years of the study (2011 – 2012: 9.2° ± 1.7°C; 2012 – 2013: 7.3° ± 1.5°C) than during the first two study years (2009 – 2010: 7.2° ± 3.0°C; 2010 – 2011: 5.6° ± 2.9°C) (Figures 4, 11). The 50th percentile winter temperatures were ordered similarly (2011-2012: 8.8°C; 2012-2013: 7.0°C; 2009-2010: 5.9°C; 2010-2011: 5.0°C) (Figure 12). Winter temperatures from 2010 – 2013 ranged from 1.9 to 14°C with an overall mean of 7.3°C. The most frequent hatch dates across all years were in the mid-January to

early-February period with 43% of all individuals hatched during this time. For 2010 – 2013, mid-January to early February dates encompassed or occurred shortly after the winter temperature minima. During the two warmer years, relative frequencies of hatch-date distributions were similar (Figure 10). In the two cooler winters, smaller fractions of hatch dates occurred prior to 1 January when compared to the two warmer winters, although the differences were not significant.

Mean experienced winter water temperatures calculated for each individual, using water temperatures from the Chesapeake Bay Bridge Tunnel site bounded by their hatch date and 31 March, showed an expected pattern of increasing experienced temperature with seasonal warming (Figure 13). Substantial interannual differences in experienced temperatures occurred for early hatch dates 1-30 December, with colder conditions during 2010 – 2011 and warmer conditions during through 2012-2013. One outlier in 2010 was hatched significantly earlier than all other samples (27 November) and experienced warmer late fall and early winter temperatures (Figure 13). A second noteworthy difference in experienced temperatures occurred for individuals hatched after 1 January, where temperature conditions for an assigned "warm" year, 2013, were actually depressed compared to other years, although temperatures remained above juvenile sub-lethal (3°C) levels (Lewis, 1965). During 2012, the other "warm" year in this study, the experienced winter temperatures were highest among all years (Figure 13).

Otolith Increment Widths

Mean pre-ingress increment widths were 2.4, 2.5, 2.7 and 2.5 µm in 2010 – 2013, respectively. Mean post-ingress increment widths were 3.3, 3.3, 3.4 and 3.2 µm in 2010 – 2013, respectively (Table 6). Mean otolith increment widths, pre- and post-ingress, did not differ significantly among years (Figure 14; Table 6; ANOVA; p_{pre} = 0.19, p_{post} = 0.56), but their variances showed some correspondence with differences in experienced temperature (Figure 15). Pre-ingress increment widths ranged from 1.5 – 4.4 µm, with greatest widths occurring in the warmest winter, 2012. The two warmer years, 2012 and 2013, had a greater fraction of mean pre-ingress increment widths ≥ 3.0 microns (32% and 18%, respectively) than in 2010 and 2011 (11% and 5%, respectively). Still, in all years, increments < 2 microns were similarly represented (Figure 14). Post-ingress increment widths ranged from 2.1 – 5.6 µm and their variances broadly overlapped. Corresponding with mostly higher experienced temperatures before ingress in 2012 and some in 2013, post-ingress increment widths regularly exceeded 3.5 microns (38% and 41%, respectively), whereas post-ingress increments less commonly exceeded this width in 2010 and 2011 (24% and 29%, respectively). Carryover effects from pre- to post-ingress mean increment widths did not differ across years (ANCOVA, factor: year; covariate: pre-ingress increment width; p = 0.77).

Examination of size-at-age data indicated an anomalous group of slow-growing individuals in 2013, which was examined separately to evaluate whether pre- or post-ingress processes were associated with reduced juvenile growth (Figure 16). All slow-growing individuals were less than 60 mm in length and ranged between 98 and 156 days old with evidence of only minor growth over the post-ingress period.

The other 15 individuals from the 2013 sample exhibited length at age distributions, which overlapped broadly with other years, ranging from 66 to 118 mm over an age range of 98 to 189 days (Figure 16). Mean increment widths, pre- and post-ingress, of the slow- and fast-growing 2013 sub-cohorts differed significantly (t-test, $p_{pre} < 0.05$, $p_{post} < 0.001$, Figure 17). Slow-growers ingressed at a significantly smaller length than fast-growers (t-test on $\log_e$-transformed lengths, $p < 0.0001$; Table 7). Carryover from pre- to post-ingress increment widths differed between 2013 slow and fast growth sub-cohorts (ANCOVA, factor = sub-cohort; covariate = pre-ingress increment width; $p < 0.0005$). The narrower pre-ingress increment widths of the slow growth sub-cohort were associated with narrower post-ingress increment widths, while wider pre-ingress increment widths were associated with wider post-ingress increment widths in the fast growth sub-cohort.

Size at Ingress & Growth Rates

Back-calculated length at ingress (50 days) during 2010 – 2013 ranged from 14 to 51 mm with a mean of 26 mm (Figure 5). Mean length at ingress in 2012 and 2013 differed significantly from each other (Tukey HSD, $p < 0.05$), however all other years were not statistically different (ANOVA on $\log_e$-transformed lengths, $p > 0.05$). Mean length at ingress of the 2013 slow-growing mode was significantly smaller than the fast-growing mode (t test on $\log_e$ transformed lengths, $p < 0.0001$). The mean length at ingress observed in this study corresponds well with the mean length at ingress directly observed by Lozano et al. 2012 (28 ± 2.9 mm, range: 7 – 40 mm, N = 10,124). Pre-ingress (larval) growth rates ranged from 0.21 to 0.93 mm d^{-1}. In 2012,

the year with warmest winter temperatures, mean pre-ingress growth rate was the highest (0.54 ± 0.15 mm d^{-1}) and significantly higher than in 2013 (0.45 ± 0.16 mm d^{-1}) (ANOVA on $\log_e$-transformed growth rates, $p < 0.05$; Figure 18). A similar trend occurred in the post-ingress growth rates. Post-ingress growth rates in 2010 and 2012 were significantly higher than in 2013 (ANOVA and Tukey HSD, $p < 0.05$; Figure 18).

Environmental Variables and Post-ingress Increment Widths

During their larval period, ingressing individuals experienced temperatures that ranged from 2.9 to 17°C with an overall mean of 8.2 ± 2.7°C (Figure 13). Mean pre-ingress water temperatures were significantly different across years (ANOVA, $p < 0.001$); mean temperature in 2012 (9.7 ± 2.7°C) was significantly higher than all other years sampled (7.7 ± 2.6°C) (Tukey HSD, $p < 0.05$). Following ingress, juveniles experienced a mean temperature of 20 ± 3.1°C. Post-ingress mean water temperatures were significantly lower in 2013 (18 ± 3.9°C) when compared to each of the other three years (combined mean, 2010-2012: 21 ± 2.5°C) (Tukey's HSD, $p < 0.05$).

Chlorophyll concentrations measured at the Chesapeake Bay Bridge Tunnel for the pre-ingress larval period ranged from 1.9 to 7.4 µg L^{-1} with an overall mean of 3.6 ± 1.7 µg L^{-1} (geometric means reported; Figure 19). Pre-ingress chlorophyll concentrations differed significantly between sample years (ANOVA, $p < 0.0001$) and post-hoc tests showed that all years differed from each other (Tukey HSD, $p < 0.005$) except for 2011 and 2013, which were similar ($p = 0.27$). Mean chlorophyll

concentrations measured at the mouth of the Choptank River for post-ingress juveniles ranged from 2.5 to 21.3 µg $L^{-1}$with an overall mean of 10.7 ± 3.1 µg L^{-1}. Mean post-ingress chlorophyll concentrations differed significantly; all years differed (ANOVA, $p < 0.0001$; Tukey HSD, $p < 0.005$) except 2011 and 2012, which were similar ($p = 0.11$). In 2011, both pre- and post-ingress chlorophyll concentrations were lowest among years. In 2012, pre- and post-ingress chlorophyll concentrations were both relatively high. The largest range of post-ingress chlorophyll concentrations occurred in 2013 when values ranged from 9.7 to 21.3 µgL^{-1}.

Regression tree analysis was conducted to hierarchically evaluate the influence of environmental variables on post-ingress (Chesapeake Bay) juvenile growth, indexed by post-ingress mean increment width. Each node on the resultant tree (Figure 20) divides the dataset into two groups based on a factor threshold value. The right branch is followed if the condition at the node is false and the left node is followed if the condition is satisfied. The tree from this analysis includes pre- and post-ingress temperature as the top 3 nodes (of 10 total nodes), reflecting the important influence of past and concurrent temperatures on juvenile menhaden growth. The left branch has 8 terminal groups while the right branch has 3 terminal groups. Characteristics of terminal groups labelled A – K are summarized in Table 8. The top node divides the post-ingress increment data based on mean pre-ingress temperature; with cooler pre-ingress temperatures, I observed smaller post-ingress increment widths and with warmer pre-ingress temperatures, I observed greater post-ingress increment widths (means 3.1 and 3.9 µm, respectively). The next nodes progressing down the tree divide increment data based on post-ingress temperature

and a different threshold for pre-ingress temperature (13°C). Biweekly hatch date was included as a node at the next level; those with hatch dates before February having lower mean post-ingress increment widths (2.9 µm) than those hatched after February (3.3 µm). Mean pre-ingress increment width was also included at the same level. The final unique node was mean pre-ingress chlorophyll concentration, dividing individuals at that node into those that experienced mean pre-ingress concentrations above or below 3.2 µg L^{-1}. Individuals that experienced higher pre-ingress chlorophyll densities, had lower post-ingress mean increment widths than those which experienced lower pre-ingress mean chlorophyll densities. The remaining 4 nodes included factors that occurred previously. Note that the regression tree model did not select post-ingress chlorophyll concentration at any branch point.

When comparing the characteristics of terminal groups (groups A-K in Figure 20; Table 8), several trends emerge. In general, when moving from terminal groups with lower pre-ingress temperatures (A-H) to terminal groups with warmer pre-ingress temperatures (I-K), mean age decreases and mean increment widths for both pre- and post-ingress periods increase. Also, instantaneous growth rate increases with increasing pre-ingress temperatures (as classified by nodes). Finally, larger post-ingress mean increment widths coincide with warmer post-ingress conditions.

Growth Rates

Mean overall (larval and juvenile) growth rate from length at age data of the 2010 – 2013 sample was 0.59 ± 0.12 mm d^{-1}. Growth rates broadly overlapped between years, although 2013 had a much broader range of growth rates (0.30 to 0.93

mm d^{-1}) due to the incidence of the anomalously slow-growing group detected in the sample (Figures 17, 21; see *Otolith Increment Width*). Growth rates (mm d^{-1}) differed significantly between years (ANOVA, $p < 0.005$); with 2013 rates being significantly slower than 2010 and 2012 growth rates (Tukey HSD, $p_{2013\text{-}2010} < 0.005$, $p_{2013\text{-}2012} < 0.01$). Mean growth rate in 2013, excluding the slow-growing individuals, was 0.63 mm d^{-1}, aligning closely with mean growth rates from other years. Mean growth rates of YOY Atlantic menhaden observed in this study were intermediate to the range of growth rates reported in the literature (0.35-0.97 mm d^{-1}; Table 9).

Growing Degree Day Model

Model scenarios included varying months of ingress (November to April), capture (June to August) and temperature threshold for growth (10, 12, 14°C). Results of all model scenarios tested are described in Figure 22 and Appendix 1. Of the different growing degree-day model temperature thresholds tested, growth estimates produced by simulations with a 10°C growth threshold best fit observed menhaden lengths across all years. The 10°C growth threshold model-predicted lengths in 2010 – 2013 that all were within the range of observed lengths of juvenile Atlantic menhaden and were closest to the mean observed length relative to other growth thresholds tested (Figure 23). Thresholds of 12 and 14°C resulted in substantially smaller lengths at month than those observed (Figure 23). For the 10°C threshold, the mean predicted length from the 2009 – 2010 February or March ingress and July capture was 75.0 mm. The same scenario produced mean lengths of 77.6 mm in 2010 – 2011, 75.9 mm in 2011 – 2012, and 64.5 mm in 2012 – 2013 (Figure 23). In a

contrasting scenario with a 1 November ingress and 1 August capture, projected mean length was 108 mm, 109 mm, 108 mm, and 93.6 mm in 2010, 2011, 2012, and 2013, respectively. Only the highest threshold (14°C) scenario corresponded with model outcomes within the range of the observed lengths from the anomalous slow-growing sub-cohort in 2013 (< 60 mm). The flat response of scenario outcomes to age for the July sample is likely due to model insensitivity to growth at temperatures below the threshold. Varying months of ingress from November to March, results in very few additional growing degree-days during which growth occurs. Thus in these scenarios, individuals age, but do not increase in length due to lack of sufficiently warm conditions.

Bioenergetics Model

Predicted length and weights from bioenergetics model simulations were sensitive to assumptions on consumption rates (constant or variable; Table 10). Under the scenario of a variable consumption rate predicted lengths were quite high in 2013 (217 mm) and variable among years: 140 mm in 2012, 111 mm in 2010 and 62 mm in 2011. Higher predicted growth in 2013 resulted from higher chlorophyll concentrations. Chlorophyll concentrations in 2013 ranged 6.08 to 94.9 µg L^{-1} (mean: 23.4 µg L^{-1}). Chlorophyll concentrations in 2010 - 2012 ranged from 0.96 to 47.9 µg L^{-1} (means: 9.34, 6.83, and 10.3 µg L^{-1} respectively). Conversely, small predicted lengths in 2011 under the variable consumption condition were associated with consistently low chlorophyll concentrations in comparison to other study years (Figure 19). For simulations run with a constant consumption rate, 2010 resulted in

the greatest predicted length (144 mm) followed by 2011 (127 mm), 2013 (101 mm), and 2012 (70.7 mm) (Figure 24). In the constant consumption rate simulations, chlorophyll was less influential resulting in less variation in predicted lengths between years (Figure 25a).

The bioenergetics model simulations with variable consumption predicted much higher than observed sizes at age in 2013, whereas the constant consumption scenario better matched observed data (Figure 25b). The opposite pattern was observed in 2011; simulations with variable consumption were substantially less than observed YOY growth outcomes. Variable consumption simulations also performed relatively well in 2010 and 2012, only slightly underestimating observed lengths. Constant consumption rate simulations performed well in 2010 but not in 2012. Clearly, phytoplankton dynamics, particularly blooms, which naturally occurred with varying consumption rates had a strong influence on model predictions.

Empirical and Modelled Growth Rates

Observed and modeled summer YOY growth rates were highly variable (Table 11; observed mean: 0.86 mm d^{-1}; GDD model mean: 0.74 mm d^{-1}; bioenergetics model mean: 0.86 mm d^{-1}; observed and model range: 0.12 – 1.16 mm d^{-1}). Because YOY menhaden were only collected in one month in 2010, linear regression could not be used to infer a juvenile growth rate. Instead, the mean overall growth rate across aged individuals (N = 45) was calculated for 2010 using length at age data (0.63 mm d^{-1}; Table 11). For combined years (2011 – 2013), the mean growth rate obtained from observed length at age data was 0.92 mm d^{-1}. The growing

degree-day model with a 10°C threshold from 2010 – 2013 produced a mean growth rate of 0.84 mm d^{-1}. And those estimated by bioenergetics model simulations with variable and constant chlorophyll inputs were respectively 0.85 and 0.45 mm d^{-1}. Mean growth rates across years from empirically observed data, the growing degree-day model, and the bioenergetics model (variable chlorophyll simulations) were within 0.08 mm d^{-1} of each other and fell within the range of growth rates reported for other studies (Table 9). Overall, the growing degree-day model with the 10°C growth threshold best estimated observed growth rates of the three thresholds tested (10°, 12°, and 14°C), while the bioenergetics model simulations with constant consumption rates were closer to observed YOY growth than simulations with variable consumption.

Discussion

I hypothesized that winter thermal conditions experienced by larval Atlantic menhaden shape hatch-date distributions, influence present larval and future juvenile growth, and could serve to predict within-bay juvenile growth and survival. Hatch-date distributions from four years with varied winter conditions contained few individuals that hatched before 1 January, although prior research had indicated most larvae ingressing into the Chesapeake Bay originate from fall and early winter spawning (Lozano et al. 2012). The presumed cause of the absence of fall and early winter cohorts is winter mortality owing to lethal and sub-lethal exposure to cold temperatures. As circumstantial evidence of temperature-induced mortality, the broadest distribution of hatch dates, ranging from November to April, occurred during 2011-2012, the year with the warmest mean winter temperature and the highest juvenile abundance in the Choptank River (Figure 1b). Although, hatch-date distributions in other years did not differ significantly from those estimated for 2012-collected YOY juveniles, they were more truncated, with gaps in the incidence of early hatch dates. Otolith increment width analysis detected carryover effects from larval to juvenile growth, particularly within the two contrasting 2013 sub-cohorts. Distinct environmental conditions experienced by these cohorts early in life contributed to their differences in sizes and growth rates as YOY in the Choptank River. Carryover effects of pre-ingress temperature and chlorophyll on YOY growth were detected in samples pooled across study years. Finally, YOY growth predictions from the growing-degree-day model (GDD) were insensitive to winter conditions below the selected threshold temperature (10°C), while the bioenergetics model was

constrained by the data available, which yielded over-resolved responses to daily variations in chlorophyll concentrations. The increased sensitivity and complexity of the bioenergetics model is perhaps better suited for estimating growth across broad geographic regions with averaged chlorophyll data inputs, rather than at the tributary-scale with more resolved data. Predicted sizes from the GDD model performed better against observed summer sizes of Choptank River YOY than did those predicted from bioenergetics model scenarios.

Influence of winter temperature on hatch dates

A rich history of research supports the important role of survival and growth of the earliest life stages (i.e. eggs and larvae) on resultant recruitment (Hjort, 1914; Cushing, 1990; Lasker, 1975; Iles and Sinclair, 1982; Miller, et al. 1988; Cury and Roy, 1989; Houde 1989, 2009). Influenced by a suite of biotic and abiotic factors, egg and larval life stage dynamics are still central to hypotheses explaining recruitment variability (Houde, 2008). Among abiotic conditions, temperature likely has the most influence on early vital rates through direct physiological, developmental, and indirect food web effects (Houde, 1989; Fuiman et al. 1998). Effects of temperature on survival, and subsequent recruitment, are likely mediated by changes in phytoplankton and zooplankton production (Polgar, 1982; Cushing, 1990; Logan, 1985).

I propose that the lack of early-hatched menhaden juveniles that I observed in the Choptank River was caused by larval mortality due to direct or indirect effects of exposure to cold winter temperatures. Overall, only a small fraction (7%) of hatch

dates was observed before 1 January in years with varied winter conditions. Winter temperatures during these years ranged from 1.9 to 14°C with an overall mean of 7.3°C. The minimum lethal temperature for Atlantic menhaden is reported as 3°C (Lewis, 1965). However, larvae have been sampled near the Bay mouth in water as cold as 2°C (E. Houde, University of Maryland Center for Environmental Science, unpublished data). Still, the outcome for these larvae is uncertain. As an example, cohorts of striped bass eggs and larvae were collected in sub-lethal temperatures, but otolith analyses of survivors indicated that subsequent mortality of cohorts exposed to the cold temperatures was high (Secor and Houde, 1995; Rutherford et al., 1997). Here it is suggested that many larvae ingressing during winter months may experience mortality owing to exposure to sub-lethal temperatures.

Temperature also influences other aspects of larval physiology that are important for survival such as consumption rate and swimming performance. Additionally, larval fish have little ability to actively disperse towards improved thermal conditions, aside from controlling their vertical position in the water column (Houde, 2009). Mean swimming speed of large larval Atlantic herring, *Clupea harengus,* (a species similar in ecomorphology to Atlantic menhaden) decreases at low temperatures due to decreased stride lengths, although, this relationship did not hold for small herring larvae (Fuiman and Batty, 1997). Kauffman and Wieser (1992) found reduced swimming performance of Danube bleak larvae when the temperature was reduced from 20 to 15°C. Because of the interdependency of feeding, growth, and swimming, the negative effects of cold temperature on swimming and larval duration likely render larvae vulnerable to predation and sub-lethal effects such as

short-term starvation. Cold, sub-lethal, temperatures could cause larval mortality through two main mechanisms; acute thermal stress or starvation (Lankford and Targett, 2001). Exposure to prolonged cold temperatures can prevent an individual from maintaining homeostasis by interrupting protein function and ion transport causing acute thermal stress which can result in death (Lankford and Targett, 2001; Hurst, 2007). Starvation occurs when an individual depletes their energy reserves due to poor feeding conditions or inability to pursue prey (Lankford and Targett, 2001). Thus, although temperatures throughout winter remained above the 3°C lethal temperature, the prolonged exposure to temperatures near this limit, could have negative implications on growth and survival.

Transitions between life history stages and the time spent at each stage are also dependent on temperature (Houde, 2009). Specifically, larval stage duration in many fish species is shown to be inversely related to temperature (Houde, 1989; Pepin, 1991). The larval stage duration of Atlantic menhaden is likely lengthened by depressed winter temperatures, increasing cumulative mortality during this life stage (Houde, 1987; Anderson, 1988). Larval stage duration of the slowest growing pre-ingress larvae in this study (76 days, 0.026 d^{-1}) is twice as long as that of the fastest growing pre-ingress larvae (37 days, 0.051 d^{-1}). Cumulative larval survival pre-ingress calculated using a mortality rate of 0.05 d^{-1} resulted in an 8-fold higher cumulative survival for the fastest growing larvae (16%) when compared to the slowest (2%).

Thermal conditions not only influence larval vital rates, but also the timing and spatial extent of spawning events and larval distributions (Warlen, 1994). The

spatial extent of larval menhaden has been largely consistent from the 1970s to recent years with spawning concentrations from Long Island to Cape Hatteras (C. Simpson, Chesapeake Biological Laboratory, pers. comm.). Years with high adult abundance and biomass correspond with the greatest spatial extent of larval incidence (C. Simpson, Chesapeake Biological Laboratory, pers. comm.). As they seasonally migrate southward during fall, each Atlantic menhaden adult produces multiple clutches of eggs (Lewis et al., 1987). This type of spawning can be described as a "bet-hedging" strategy; where multiple batches of eggs are spawned resulting in a succession of larval cohorts (Lambert and Ware, 1984). The advantage to employing this strategy is that some (but not all) eggs and larvae will encounter environmental conditions sufficient for growth and survival. These multiple clutches also are differentially transported to nursery habitats depending on spawning location. Due to their limited larval swimming ability, menhaden larvae rely primarily on wind and ocean currents to be transported from their spawning grounds offshore to estuarine nurseries (Checkley et al., 1988; Quinlan et al., 1999; Rice et al., 1999; Epifanio and Garvine, 2001; Warlen et al., 2002), although vertical movements will also affect their dispersal (Hare et al., 1999; Rice, et al., 1999). Larger adults are more northerly distributed throughout spring and summer (Nicholson, 1978; Reish et al., 1985; SEDAR, 2015) and could spawn larvae in more northerly spawning regions. Such larvae would likely experience colder temperatures throughout their development.

In addition to spatial extent, spawning phenology is also crucial in determining conditions for early life stages (Lewis, 1965; Stegmann et al., 1999). It is hypothesized that the variation in age at ingress is caused by the diversity of

spawning locations and times along with transport routes and rates (Quinlan, et al., 1999). Northern estuaries may receive predominately early-spawned eggs as the adult stock migrates southward, which could result in decreased larval survival due to poor environmental or transport conditions. Warlen et al. (2002) observed this contrast between hatch distributions of a northern estuary, New Jersey, which were shifted earlier than hatch distributions of a southern estuary, North Carolina. Early spawned Atlantic menhaden may represent "ecological overhead", due to the combination of high fecundity and migration and spawning behaviors (Secor, 2015). However, variability in environmental conditions could permit survival of some early-hatched individuals in years with sufficient conditions. Additionally, larvae entering the estuary from February to April when temperatures are rising, are likely entering a more prey-rich environment in which predator, larval fish, and invertebrate competitor abundances are low (Warlen, 1994). Even subtle differences in the timing or location of spawning could have important consequences for the transport and environmental conditions experienced by larvae along with subsequent growth and survival.

The combination of slowed growth during winter and size-selective mortality could serve as a powerful regulator of larval and juvenile survival and have significant recruitment implications for Atlantic menhaden. Size- and growth-dependent mortality have been documented in many fish species (Sogard, 1997; Takasuka et al., 2003). Meekan and Fortier (1996) found evidence of strong growth-dependent mortality in Atlantic cod, *Gadus morhua*, larvae. Size-selective mortality was also observed in a slow-growing cohort of yellow perch, *Perca flavescens*;

although these results depended on the composition of predators present (Post and Prankevicius, 1987). The severely stunted size-at-age of the slow-growing sub-cohort detected in 2013 experienced very low larval growth rates. Interestingly this sub-cohort was not sampled beyond the month of June. Lack of representation of this sub-cohort in later summer months could be indicative of size-selective mortality.

Winter temperatures in Chesapeake Bay could serve as a recruitment bottleneck for Atlantic menhaden because of its effects on growth and size-selective mortality. Lozano et al. (2012) observed that the majority of juvenile-derived hatch dates sampled throughout Chesapeake Bay occurred in January and February while an average of 95% of larval-derived hatch dates from 2005-2008 occurred before 31 December. This mismatch of larval- and juvenile-derived hatch dates and the new evidence of a truncated distribution presented herein is suggestive of a winter recruitment bottleneck (Ludsin and DeVries, 1997; Hurst, 2007). Evidence of this phenomenon has been documented through empirical and modeling studies on hatch dates and larval mortality. Callihan et al. (2008) documented hatch-date distribution gaps in bluefish that were associated with spawning during sub-lethal temperatures. Hare and Able (2007) showed evidence that Atlantic croaker year-class strength is determined by overwinter survival of juveniles; with warm winter temperatures associated with higher adult catches. Observations of increased overwinter survival of larger smallmouth bass led Shuter et al. (1980) to model the relationship between temperature and first-year survival of smallmouth bass. Not only does the severity of winter temperatures affect survival, but the duration of winter conditions is also important. Post and Evans (1989) suggested that a combination of size-dependent

overwinter mortality and variable winter duration explain recruitment success in yellow perch. Overwinter mortality in bluefish, Atlantic croaker, smallmouth bass, and yellow perch all represent possible case studies where overall recruitment outcomes are regulated by mortality associated with winter temperature conditions.

Despite a large range in winter temperatures across study years, no statistical difference in YOY menhaden hatch dates was detected. Still, differences in the shape of the hatch-date distributions were consistent with broader representation in the warmest year and major gaps in hatch-date distributions in other years. Such gaps potentially represent non-surviving larvae owing to periods of thermal stress. Because of the protracted spawning period of Atlantic menhaden, it is highly unlikely that no larvae were hatched in those two week gaps; rather they were undetected in summer-collected samples. The small to moderate sample sizes in this study could under-represent some biweekly cohorts, particularly those represented by low abundance. Increased sample sizes coupled with increased ageing precision could uncover interannual hatch-date differences obscured in the current analysis. Within the limits of my study – four years of contrasting winter conditions and a modest sample size – I infer that broad hatch-date distributions and an overall higher juvenile abundance in 2012 provide circumstantial evidence for the role of winter temperature in shaping early survival and recruitment in Chesapeake Atlantic menhaden. Of course, this is but one factor within a combination of local and regional conditions that influence survival of larvae during and beyond their ingress into Chesapeake Bay.

Overall, results from this study support the hypothesis that overwinter mortality, due to thermal stress, shapes hatch-date distributions of YOY Atlantic

menhaden. The mismatch between larval- and juvenile-derived hatch dates was further explained by differences in experienced temperatures inferred from this study. Since mortality often selects against the smallest members of a cohort, winter conditions could act as a recruitment control (Hurst, 2007).

Contribution of pre-ingress growth and environmental conditions to post-ingress growth (carryover effects)

Otolith increment width analyses allowed a retrospective view of YOY Atlantic menhaden growth before, during, and after the shift between shelf (larval) and Chesapeake (juvenile) habitats. In this study, I observed a positive correlation between pre- and post-ingress increment widths. This observation suggests that early larval growth rates are correlated with late larval and juvenile growth rates. For marine fishes with complex life cycles, including Atlantic menhaden, the influence of environmental factors on growth dynamics is complicated by habitat and trophic niche shifts that occur during the first year of life (Juanes, 2007). The ingress from the coastal ocean into the estuary by Atlantic menhaden is associated with a slight decrease in water temperature (coastal: 8.17 ± 2.8°C, within bay: 7.5 ± 3.1°C; data from NOAA Buoy #44009) and increased variability in temperature as the estuary is more susceptible to fluctuations in thermal conditions compared to coastal waters (Najjar et al., 2010). Shortly after ingressing into the Chesapeake Bay, menhaden larvae undergo transition to the juvenile stage (June and Carlson, 1971; Friedland et al., 1984). The transition from larval to juvenile stage is associated with a prey shift from zooplankton to smaller zooplankton and phytoplankton (Friedland et al., 1989).

Some have suggested that recruitment controls for Atlantic menhaden act on the ingressed juveniles (MDSG, 2009; Lozano et al., 2012; Houde et al. in review). My research indicates that that conditions experienced as larvae are linked with the fate of ingressed juveniles and overall juvenile growth outcomes. Subtle variation in early growth and mortality of fishes can have important implications for recruitment outcomes (Cushing, 1975; Houde, 1987; 2009). Furthermore, in a life table modeling study conducted by Quinlan and Crowder (1999), growth and mortality parameters of late larval stage and YOY stage menhaden were found to have the most influence on overall population growth rate. Thus, larval growth and mortality, and associated environmental drivers, can have far-reaching effects on population dynamics.

Otolith increment width analyses yielded evidence for a carryover effect of early growth to juvenile growth in Atlantic menhaden. Observed increment widths overlap broadly with increment widths reported by Fitzhugh et al. (1997) in laboratory-reared juvenile Atlantic menhaden (~1 to 5 μm) and did not vary significantly among years. However, the variance within otolith increment measures showed some correspondence with differences in experienced temperature. Specifically, a greater proportion of wider increments were observed in the two warmer years. Increment widths, both pre- and post-ingress, were significantly smaller for a slow-growing 2013 sub-cohort when compared to a fast-growing sub-cohort. The slow-growing sub-cohort also ingressed at significantly smaller sizes than fast-growing individuals.

Size and growth rate at ingress have implications for within-bay survival due to their direct connection with swimming ability, predator avoidance, and feeding

(Miller et al., 1988). During ingress, larvae move from the open coastal ocean to a spatially-defined bay. Thus, size and growth rate at ingress could be a strong indicator of potential for first year survival (Houde, 1989; Lozano et al., 2012). Support for a carryover effect in Atlantic menhaden was demonstrated by a regression tree analysis on factors contributing to post-ingress growth rates. Post-ingress growth rates, as measured by otolith increment widths, were associated with pre- and post-ingress temperature, hatch timing, and pre-ingress growth in this analysis (Figure 20). As noted previously, pre-ingress temperature likely affected feeding, swimming performance, and overall post-ingress growth outcomes. Spawning and hatch dates, similarly, were likely associated with transport and thermal conditions of eggs and larvae, resulting in differing growth rates.

Otoliths serve as record-keeping structures that document growth rates throughout development (Panella, 1971; Campana and Neilson, 1985; Secor et al., 1991; Ahrenholz et al., 1995). Because menhaden otolith growth is correlated with somatic growth, otoliths can be used to examine the growth history of individual fish (Ahrenholz et al. 1995; 2000). However, caution must be used in obtaining otolith-based growth estimates from short-at-age individuals due to independent temperature effects on otolith growth rates (Fey and Hare, 2012). In 2012, pre- and post-ingress increment widths corresponded with favorable growth conditions, which included warm temperatures and sufficient and less variable phytoplankton supply. In 2013, anomalously low pre-ingress larval growth of a sub-cohort carried over to very low YOY growth rates. Carryover effects, although not previously described for the early growth of Atlantic menhaden, have been documented in other studies. For example,

juvenile European eel, *Anguilla anguilla*, migratory behaviors were explained by glass eel activity levels, which are closely tied to thyroid hormone expression (Edeline, 2007). For Chesapeake Bay white perch and striped bass larval growth rates carried over to juvenile migration behaviors (Kerr and Secor 2010; Conroy et al. in review). In reef fish, Gagliano et al. (2007) observed that juvenile survival was associated with larval condition defined by body size and yolk-sac reserves. Because of this consistency in growth rates throughout development observed in my study (i.e., lack of compensatory growth), early stage growth in Atlantic menhaden may regulate growth potential later in life.

I posit that advantageous initial conditions as well as robust larval growth in Atlantic menhaden may have subtle influences on the subsequent growth of juveniles that could affect recruitment (i.e., first year survival). Improved larval menhaden growth, mediated by sufficient temperatures and food supply, could carryover to juvenile growth rates and thereby enhance overall survival. Such carryover effects would emphasize an important role in the timing and spatial extent of spawning in determining population dynamics of Atlantic menhaden. Interpretation of a carryover effect is complicated by the many factors influencing larval and juvenile growth of which this study only examined two (temperature and chlorophyll *a*). Many other external driving factors influence growth conditions including turbulence, salinity, oxygen levels, maternal effects, lipid storage, and disease (Hettler, 1976; Weatherly, 1990; Deegan 1990; Mackenzie et al., 1994).

Predicted growth rates from primary environmental drivers

The growing degree-day model better estimated summer juvenile growth outcomes compared to the bioenergetics model in this Choptank River application. Growing degree-day model-predicted growth rates ranged from 0.6 to 0.9 mm d^{-1} while bioenergetics model-predicted growth rates ranged from 0.1 to 1.2 mm d^{-1}. Observed growth rates of summer sampled YOY (i.e., estimated from size at age) ranged from 0.3 to 0.9 mm d^{-1} and overlapped between years, and with growth rates reported in the literature, which ranged from 0.4 to 1 mm d^{-1} (Table 9) These growth rates were better simulated by the growing degree-day model than the bioenergetics model. The differences in model performance are likely caused in part by the resolution of the input data and differences in model complexity. Both models were applied at a much finer scale than over that for which they were originally developed. Requiring multiple environmental inputs, the bioenergetics model was highly sensitive to fluctuations in chlorophyll *a* at the Cambridge, MD site. In particular, peaks in chlorophyll caused unrealistic growth outcomes. Further, a limiting assumption was required that these concentrations were representative of those encountered by YOY menhaden in the Choptank River. However, its application in years with more stable chlorophyll measures (e.g. 2012), resulted in growth outcomes that were more similar to observed lengths. The growing degree-day model growth predictions rely on temperature inputs only. Daily temperature fluctuations are more gradual and generally diminished when compared to chlorophyll *a* data because of the incidence of phytoplankton blooms. These differences in data inputs are magnified when measured at the tributary scale compared to the bay-wide scale.

The growing degree-day model, simulating July capture, does not predict individuals greater than 81 mm. However, 90% of my July-sampled individuals were longer than 81 mm. Growth of YOY menhaden estimated by a von Bertalanffy model that included temperature, primary production, and density-dependent effects also did not predict July growth outcomes greater than 80 mm (Houde et al., 2010). Similarly, mean length-at-date information reported for 1985 – 2004, rarely exceeded 80 mm (Houde et al. 2010). The wide range of length-at-age data from this study is also indicative of highly variable juvenile growth rates (range = 0.30 – 0.93 mmd^{-1}). Other studies have documented juvenile growth rates ranging from 0.35 to 0.97 mmd^{-1} (Table 9). Additionally, specific model assumptions and scenarios in the Choptank River could have accounted for the differences between observed and modeled growth outcomes. The bay-wide application of the bioenergetics model by Annis et al. (2011) showed the highest growth potential in the upper, oligohaline bay region followed by the mid- and lower regions. Although the Choptank River was classified by Annis et al. as a mesohaline tributary, it is possible that juveniles in the Choptank River exhibit a higher growth rate than in other tributaries. YOY menhaden growth rates were also observed to differ regionally; YOY in the lower bay reached 50% of their modeled maximum length sooner than those residing in the upper bay (Houde et al., 2010) Thus, evidence from size-at-age and size-at-date analyses in the Choptank River indicate higher and more variable growth rates than those simulated through GDD.

Fish growth is a multifaceted process influenced by many biotic and abiotic factors (Hettler, 1976; Weatherly, 1990; Deegan, 1990), which may be difficult to

simulate in predictive models. Further, growth in Atlantic menhaden and other marine fishes changes throughout ontogeny (Houde, 1997). Upon metamorphosis, menhaden grow more in mass than in length. Thus, it is important that growth modeling efforts consider many factors, including physiological changes, ontogenetic shifts, and fish allometry. The coupled foraging bioenergetics model applied in my study involved estimation of many parameters. This relatively complex model was developed to estimate YOY menhaden growth after menhaden had ingressed and underwent the habitat and trophic shift (Annis et al., 2011). In my application of the model, the highly variable nature of chlorophyll *a*, due to the extent and location of phytoplankton blooms, required special adjustments to the consumption parameter. One main assumption is that measured chlorophyll *a*, indicative of phytoplankton, overlaps with menhaden occurrences. Annis et al. (2011) noted in their model calibration that the best model fit was obtained by reducing the available phytoplankton to 9.2% of surface chlorophyll *a* values. Phytoplankton and Atlantic menhaden are both highly patchy within the environment, which can result in high uncertainty in forage availability. Additionally, neither model applied here considers density dependence in its estimation of growth. Houde et al. (in review) did observe that lower juvenile length-at-age were associated with years of high juvenile abundance.

Both menhaden growth models had utility in constructing growth outcomes based on environmental variables; however, there are some limitations to their application. Both models were applied to a finer scale than the scale at which they were originally constructed. Because very few growing degree-days are accumulated

during winter months, there was support for my hypothesis that the growing degree-day model application does not sufficiently capture winter growth dynamics of juvenile Atlantic menhaden. Varying month of ingress from November to March produced little variation in growth outcomes because temperatures rarely exceeded the growth temperature threshold during these months. Although the growing degree-day model estimates growth accurately, it completely discounts any growth that might occur below a designated temperature threshold. However, prior research shows evidence of larvae surviving and feeding in <10°C temperatures (Lozano, 2011). Further, the GDD model is not able to distinguish other potential causes of these differences such as density dependence, prey concentrations, and size-selective mortality. Even with its limitations, the growing degree-day model matched observed menhaden growth outcomes when applied at the tributary scale. For future bioenergetics model applications on a fine scale, dampening severe variation by applying an average consumption or smoothing the time series of chlorophyll data could produce more realistic growth outcomes. Further, chlorophyll inputs should rely on data, which was integrated across sites, representative of the Choptank River habitats occupied by YOY menhaden. Although the importance of the relationship between early growth, mortality, and recruitment is understood, it is complex (Post and Prankevicius, 1987; Hurst and Conover, 1998; Rankin and Sponaugle, 2011). The use of predictive models can reduce the need for costly *in situ* sampling and otolith analyses while permitting sufficient precision and realism to provide juvenile growth predictions. Development and application of growth models allow exploration of biotic and abiotic factors influencing growth outcomes. Because survival depends, to

an extent on growth, future recruitments potentially could be predictable based on juvenile growth measures (Houde 1987), with utility for Atlantic menhaden assessment and management.

Conclusion

Atlantic menhaden have exhibited > 20-fold recruitment variability with persistent, low recruitment levels in Chesapeake Bay since 1993. Forage fish, including menhaden, have particularly complicated recruitment dynamics because of their complex life histories, high fecundity, and trophic role. Thus, the cause of high recruitment variability in forage fish are not fully understood. Many studies, including this one, have confirmed the importance of thermal conditions for Atlantic menhaden recruitment and individual growth and survival. This study focused on the influence of winter conditions on YOY growth dynamics through larval carryover effects in the Chesapeake Bay, one of the most important nurseries contributing to the coast-wide adult stock. Due to the cold and food-limited conditions in winter, eggs and larvae are exposed to harsh conditions during critical developmental stages. If eggs are spawned and hatch early in winter, a recruitment bottleneck within the Chesapeake Bay may occur caused by thermal stress or starvation leading to larval mortality. However, if larvae survive, it is likely that depressed growth rates caused by exposure to poor thermal conditions carry over to juvenile growth and survival. Thus, timing of spawning, hatch, ingress, and metamorphosis are all critical to the successful development and growth of Atlantic menhaden recruits.

Incorporating overwinter mortality in population, recruitment or growth models has been suggested as a primary way to improve fisheries stock assessment and management tools, especially with impending climate change (Hurst and Conover, 1998; Hare et al., 2010; Shuter et al. 2012). With 2 to 6°C warming of water temperature predicted in Chesapeake Bay (Najjar et al., 2010), mortality rates of

Atlantic menhaden driven by winter temperatures could decrease. However, the impact of an increase in frequency and intensity of precipitation and sea level variability on menhaden within the bay is not certain. Climate-scale variables, including the Atlantic Multidecadal Oscillation, have also been shown to influence regional menhaden recruitment dynamics (Buchheister et al. *in* press). Finally, fishing effort and catch distributions are likely going to shift as a result of changing climate. Adaptive management of Atlantic menhaden is necessary to cope with the expected environmental and fishing changes in the coming decades.

Future research

Building upon the findings of this study, I suggest a more direct method should be pursued to examine the influence of winter conditions on the growth and survival of Atlantic menhaden. Targeted winter sampling of larval Atlantic menhaden on the coastal shelf and its approach to the main stem of the Chesapeake Bay along with collection of environmental variables would allow *in situ* observations of the age, growth and survival of ingressing menhaden. Otoliths can be used to collect age and hatch-date information while length-at-age measures could detect potential truncation of length distributions indicative of size-dependent mortality. These efforts would permit a more direct exploration of the potential winter recruitment bottleneck for Atlantic menhaden. The consequences of future climate change and warming water temperatures could be better anticipated with a more detailed knowledge of menhaden overwinter mortality. Additionally, winter mortality rates have utility in population dynamic models used to assess impacts of fishing on abundance and determine catch quotas.

Tables

Table 1 – Sampling site locations, river kilometer, and mean salinity in the Choptank River, MD

Site	Latitude	Longitude	River kilometer	Mean salinity
Castle Haven	38° 37’ 36”	76° 09’ 48”	11.3	9.8
Hambrook Point	38° 35’ 33”	76° 05’ 07”	20.9	8.7
Jamaica Point	38° 36’ 42”	75° 59’ 12”	32.5	6.5
Choptank Launch	38° 40’ 53”	75° 57’ 05”	41.6	5.3
Farm N. Frazier	38° 42’ 24”	75° 59’ 24”	46.0	4.3
Dover Bridge	38° 45’ 12”	76° 00’ 03”	52.6	2.9
Tuckahoe Creek	38° 48’ 57”	75° 53’ 51”	63.4	1.4

Table 2 – Composition of YOY menhaden samples for which otoliths were analyzed by year, gear type and site in the Choptank River, MD. MWT = midwater trawl. Due to otoliths being rendered unusable during preparation, there is unequal sample distribution across years and sites.

Site	River km	2010		2011		2012		2013	
		MWT	Seine	MWT	Seine	MWT	Seine	MWT	Seine
Castle Haven	11.3	4	-	-	-	-	-	-	12
Hambrook Point	20.9	-	-	15	-	-	9	--	-
Jamaica Point	32.5	7	12	-	13	5	-	2	11
Choptank Launch	41.6	-	-	-	-	3	2	8	2
Farm N Frazier	46.0	-	-	-	-	2	-	6	8
Dover Bridge	52.6	-	7	-	4	8	-	6	-
Tuckahoe Creek	63.4	-	15	-	9	-	-	-	-

Table 3 – Chesapeake Bay environmental data sources for winter temperature comparison and modeling efforts. Sites are plotted on Figure 7.

Site Name	Latitude	Longitude	Frequency	Time Range	Purpose	Source
CB Bridge Tunnel	36.967	76.113	Daily	12/1/09 – 11/28/13	Temperature	NOAA NBDC
First Landing	36.974	76.045	Daily	11/27/11 – 12/31/13	Chlorophyll	NOAA NBDC
Stingray Point	37.568	76.261	Daily	11/1/09 – 11/27/11	Chlorophyll	NOAA NBDC
Gooses Reef	38.556	76.415	Daily	7/27/10 – 12/31/13	Temperature, Chlorophyll	NOAA NBDC
Cambridge	38.573	76.068	Daily	10/7/11 – 10/31/14	Temperature, Chlorophyll	NOAA NOS
Annapolis	38.963	76.448	Daily	11/20/09 – 10/6/11	Temperature	NOAA CBIBS
Choptank River Fishing Pier	38.571	76.062	Weekly	1/23/12 – 3/10/14	Chlorophyll	HPL

Table 4 – Summary of sample collection dates, ages, and hatch dates for YOY Atlantic menhaden collected in the Choptank River, MD. Ranges, means and standard deviations are shown.

	Collection Date		Age (days)		Hatch Date	
	Range	**Mean ± SD**	**Range**	**Mean ± SD**	**Range**	**Mean ± SD**
2010		7/8 ± 1				
June	-		-	-	-	-
July	7/8-7/12		98 - 223	148 ± 21	11/27 - 4/1	2/10 ± 21
August	-		-	-	-	-
2011		7/8 ± 14				
June	6/10 - 6/28		112 - 185	147 ± 23	12/25 - 2/18	1/27 ± 18
July	7/18		110 - 192	147 ± 22	1/7 - 3/30	2/20 ± 22
August	-		-	-	-	-
2012		7/4 ± 26				
June	6/6		102 - 162	129 ± 18	12/27 - 2/25	1/30 ± 16
July	7/7-7/12		116 - 216	165 ± 32	1/15 - 3/18	2/3 ± 23
August	8/8		132 - 207	164 ± 25	1/14 - 3/29	2/25 ± 25
2013		7/3 ± 23				
June	6/7		98 - 156	130 ± 19	1/2 - 3/1	1/28 ± 19
July	7/10		98 - 172	140 ± 20	1/19 - 4/3	2/20 ± 20
August	8/7		129 - 189	153 ± 20	1/30 - 3/31	3/6 ± 20

Table 5 – Absolute and relative (in parentheses) frequencies of hatch-date distributions by biweekly periods for YOY Atlantic menhaden (N = 167) 2010 – 2013. Absolute frequencies are for data unadjusted for cumulative mortality. Relative frequencies are for data adjusted for cumulative mortality.

Month	Biweekly bin	2010	2011	2012	2013
November	1	1 (5%)	0 (0%)	0 (0%)	0 (0%)
Nov-Dec	2	0 (0%)	0 (0%)	1 (5%)	0 (0%)
December	3	0 (0%)	2 (7%)	3 (10%)	0 (0%)
January	4	4 (12%)	4 (13%)	4 (15%)	5 (13%)
January	5	6 (16%)	6 (18%)	8 (23%)	7 (17%)
February	6	15 (34%)	10 (23%)	8 (17%)	8 (21%)
February	7	12 (23%)	11 (25%)	5 (13%)	7 (15%)
March	8	5 (9%)	3 (6%)	4 (9%)	10 (20%)
March	9	1 (2%)	2 (4%)	3 (6%)	4 (9%)
April	10	1 (1%)	3 (5%)	1 (2%)	3 (6%)

Table 6 – YOY Atlantic menhaden otolith metrics, pre- and post-ingress growth rates, and size at ingress for 2010 – 2013.

		2010	2011	2012	2013
Pre-ingress increment widths	**Mean ± SD (µm)**	2.4 ± 0.5	2.5 ± 0.4	2.7 ± 0.7	2.5 ± 0.6
	Range (min, max)	1.5, 3.8	1.6, 3.8	1.7, 4.0	1.5, 4.41
Post-ingress increment widths	**Mean ± SD (µm)**	3.3 ± 0.7	3.3 ± 0.5	3.4 ± 0.7	3.2 ± 0.6
	Range (min, max)	2.1, 5.6	2.1, 5.0	2.3, 4.8	2.0, 5.5
Pre-ingress growth rate	**Mean ± SD (mm d^{-1})**	0.5 ± 0.1	0.5 ± 0.1	0.5 ± 0.2	0.5 ± 0.2
	Range (min, max)	0.3, 0.8	0.3, 0.8	0.2, 0.9	0.2, 0.9
Post-ingress growth rate	**Mean ± SD (mm d^{-1})**	0.7 ± 0.1	0.6 ± 0.1	0.7 ± 0.1	0.6 ± 0.2
	Range (min, max)	0.5, 1.0	0.4, 0.9	0.4, 1.0	0.3, 1.0
Back-calculated length at ingress (mm)		29 ± 5.4	28 ± 4.8	31 ± 7.5	26 ± 8.0
Total otolith radius (µm)		442 ± 47	431 ± 45	460 ± 57	403 ± 82
Mean ingress date ± SD (days)		4/1 ± 21	4/1 ± 24	3/29 ± 23	4/5 ± 24
					Slow mode: 3/21 ± 18
					Fast mode: 4/14 ± 23

Table 7 – Otolith metrics and size at ingress compared between the 2013 slow and fast growth modes of YOY Atlantic menhaden.

		2013 Fast Mode	2013 Slow Mode
Pre-ingress increment widths	**Mean ± SD (µm)**	2.637 ± 0.69	2.148 ± 0.38
	Range (min, max)	1.67, 4.08	1.39, 3.05
Post-ingress increment widths	**Mean ± SD (µm)**	3.44 ± 0.53	2.71 ± 0.54
	Range (min, max)	2.43, 4.63	2.18, 4.14
Back-calculated length at ingress (mm)		29.8 ± 7.73	20 ± 2.96
Total otolith radius (µm)		455 ± 52.2	313 ± 26.0

Table 8 – Summary characteristics for terminal groups resulting from regression tree (Figure 20) describing mean post-ingress increment widths for YOY Atlantic menhaden sampled in the Choptank River, MD 2010 – 2013. Unless otherwise indicated, values presented are mean ± standard deviation.

Group	Mean pre-ingress increment width (µm)	Mean post-ingress increment width (µm)	Biweekly hatch	Length (mm)	Length at ingress (mm)	Instantaneous growth rate	Age (days)	N
A	2.1 ± 0.34	2.5 ± 0.3	5	60 ± 18	21 ± 3.9	0.035	147 ± 29	17
B	2.4 ± 0.48	2.9 ± 0.3	5	94 ± 12	27 ± 5.9	0.036	165 ± 22	38
C	2.1 ± 0.24	3.0 ± 0.4	7	99 ± 8.6	26 ± 2.9	0.037	161 ± 10	17
D	2.3 ± 0.10	3.0 ± 0.3	7	90 ± 10	27 ± 2.3	0.041	149 ± 16	11
E	1.9 ± 0.15	3.4 ± 0.5	7	87 ± 22	21 ± 2.0	0.039	153 ± 22	11
F	2.8 ± 0.28	3.2 ± 0.3	7	93 ± 8.9	33 ± 4.1	0.043	144 ± 15	12
G	2.8 ± 0.24	3.3 ± 0.5	7	77 ± 22	29 ± 5.6	0.048	129 ± 25	7
H	3.0 ± 0.59	3.7 ± 0.5	7	91 ± 13	34 ± 6.6	0.051	128 ± 11	19
I	3.0 ± 0.47	3.5 ± 0.4	8	95 ± 11	35 ± 6.2	0.051	131 ± 15	15
J	2.2 ± 0.17	4.0 ± 0.3	7	93 ± 7.7	26 ± 3.1	0.05	130 ± 7	9
K	3.2 ± 0.64	4.4 ± 0.5	8	90 ± 12	34 ± 6.2	0.06	117 ± 14	11

Table 9 – Comparison of larval and juvenile Atlantic menhaden growth rates reported in the literature. Growth rate from Humphrey 2014 is marked with a * because different units of growth were applied (mm per growing degree-day).

Life Stage	Growth Rate (mm d^{-1})	Time of year	Source
Larval	0.48		Maillet and Checkley 1991
Larval	0.62		Lozano et al. 2012
Larval	0.49	Pre-ingress	Present study
Juvenile	0.35	June - August	Wingate (unpub.)
Juvenile	0.38	April – June	Annis et al. 2011
Juvenile	0.43	Hatch - June	Wilberg et al. 2012
Juvenile	0.49 – 0.95	Laboratory	Ahrenholz 1995
Juvenile	0.62	June - August	Present study
Juvenile	0.74		Present study – GDD
Juvenile	0.83	Summer	Kroger et al. 1974
Juvenile	0.86		Present study – observed
Juvenile	0.86		Present study – bioenergetics
Juvenile	0.90	June - October	Rippetoe 1993
Juvenile	0.97	July - August	Annis et al. 2011
Juvenile	0.044 mm/GDD*		Humphrey 2014

Table 10 – Bioenergetics model results for simulated YOY Atlantic menhaden growth. Simulations started on the mean day of ingress (28 March) and ended on 31 August. Chlorophyll data is from the Horn Point Laboratory time series with winter data supplemented by data collected off the Choptank River Fishing Pier. Mean temperature represents the mean daily water temperature at the Annapolis CBIBS site. L_0 = length at ingress. For more information on Consumption scenarios, see Methods.

Year	Consumption Assumption	L_0 (mm)	L_t (mm)	$Mass_t$ (g)	Mean temperature (°C)
2010	Variable	28	110.84	13.25	22.2
	Constant	28	144.18	29.71	22.2
2011	Variable	28	62.14	2.24	21.8
	Constant	28	126.50	19.88	21.8
2012	Variable	28	139.90	27.09	23.1
	Constant	28	70.71	3.33	23.1
2013	Variable	28	217.35	104.76	22.0
	Constant	28	101.17	10.01	22.0

Table 11 – Growth rates estimated from linear regressions of size at date for modeled and observed YOY Atlantic menhaden in 2010-2013. *Only one month of sampling was performed in 2010. Slope value was calculated as the average growth rate (length age^{-1}) across all aged 2010 individuals captured in the single sampling month, July (N = 45).

Year	Model	Regression slope (mm d^{-1})
ALL	Observed	0.59 ± 0.12
	GDD 10	0.83
	GDD 14	0.63
	Bioenergetics - variable	0.86
	Bioenergetics - constant	0.45
2010	Observed	0.63*
	GDD 10	0.86
	GDD 14	0.66
	Bioenergetics - variable	1.05
	Bioenergetics - constant	0.70
2011	Observed	0.94 ± 0.03
	GDD 10	0.87
	GDD 14	0.67
	Bioenergetics - variable	0.12
	Bioenergetics - constant	0.56
2012	Observed	0.88 ± 0.03
	GDD 10	0.83
	GDD 14	0.63
	Bioenergetics - variable	1.16
	Bioenergetics - constant	0.16
2013	Observed	0.94 ± 0.02
	GDD 10	0.79
	GDD 14	0.59
	Bioenergetics - variable	1.09
	Bioenergetics - constant	0.38

Figures

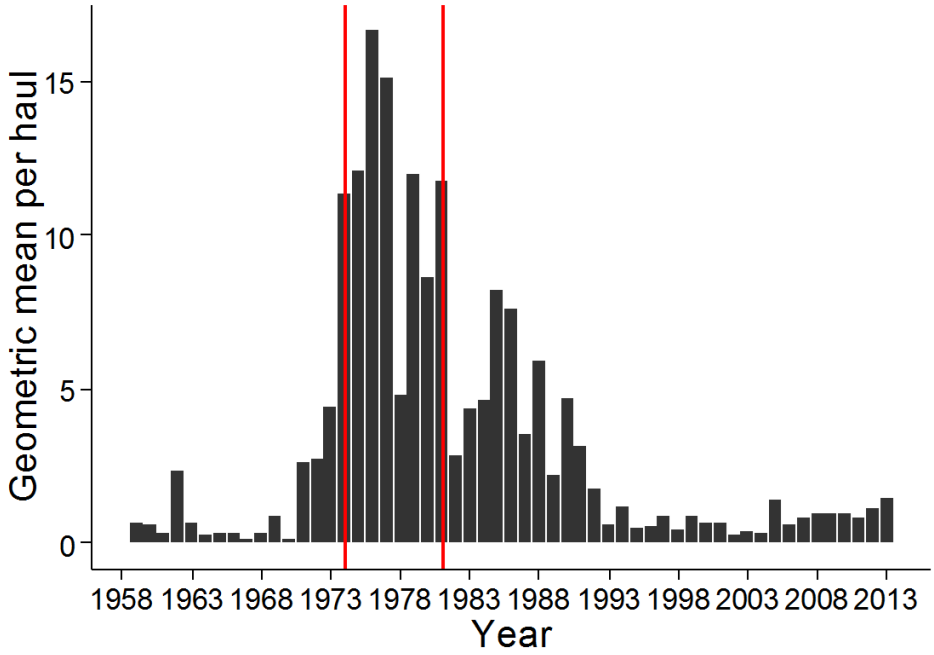

Figure 1a - Atlantic menhaden bay-wide juvenile abundance index for 1959 – 2013 (Maryland Department of Natural Resources http://dnr2.maryland.gov/fisheries/Pages/striped-bass/juvenile-index.aspx). Red lines demarcate 1974 – 1981 period of high menhaden recruitments in Chesapeake Bay. Since 1995 abundances have persisted at less than 10% of those observed from 1974 – 1981.

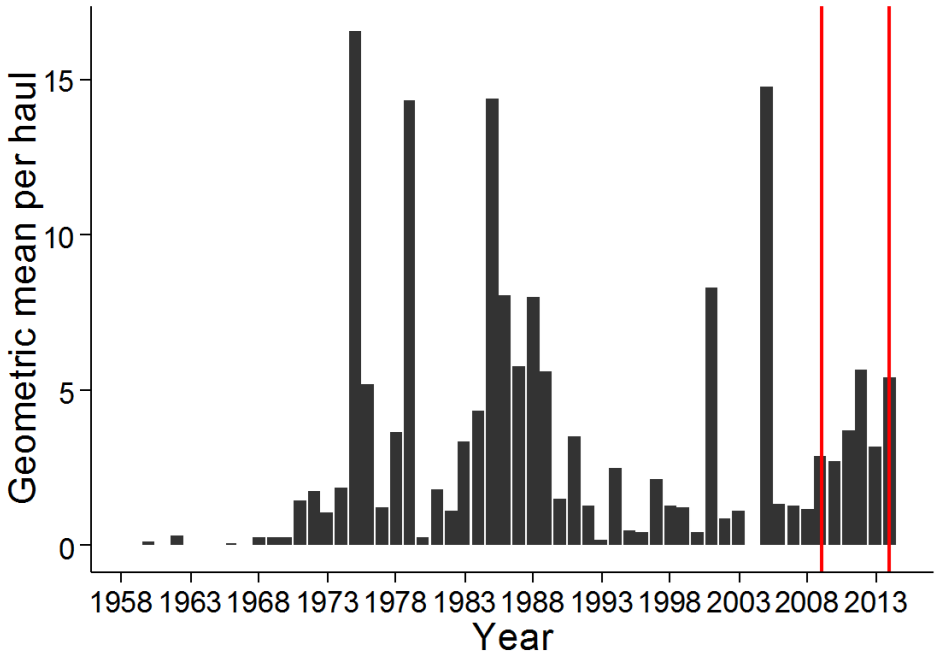

Figure 1b - Atlantic menhaden Choptank River juvenile abundance index for 1959 – 2013 (Maryland Department of Natural Resources). Red lines demarcate 2010 – 2013, the years encompassed in this study.

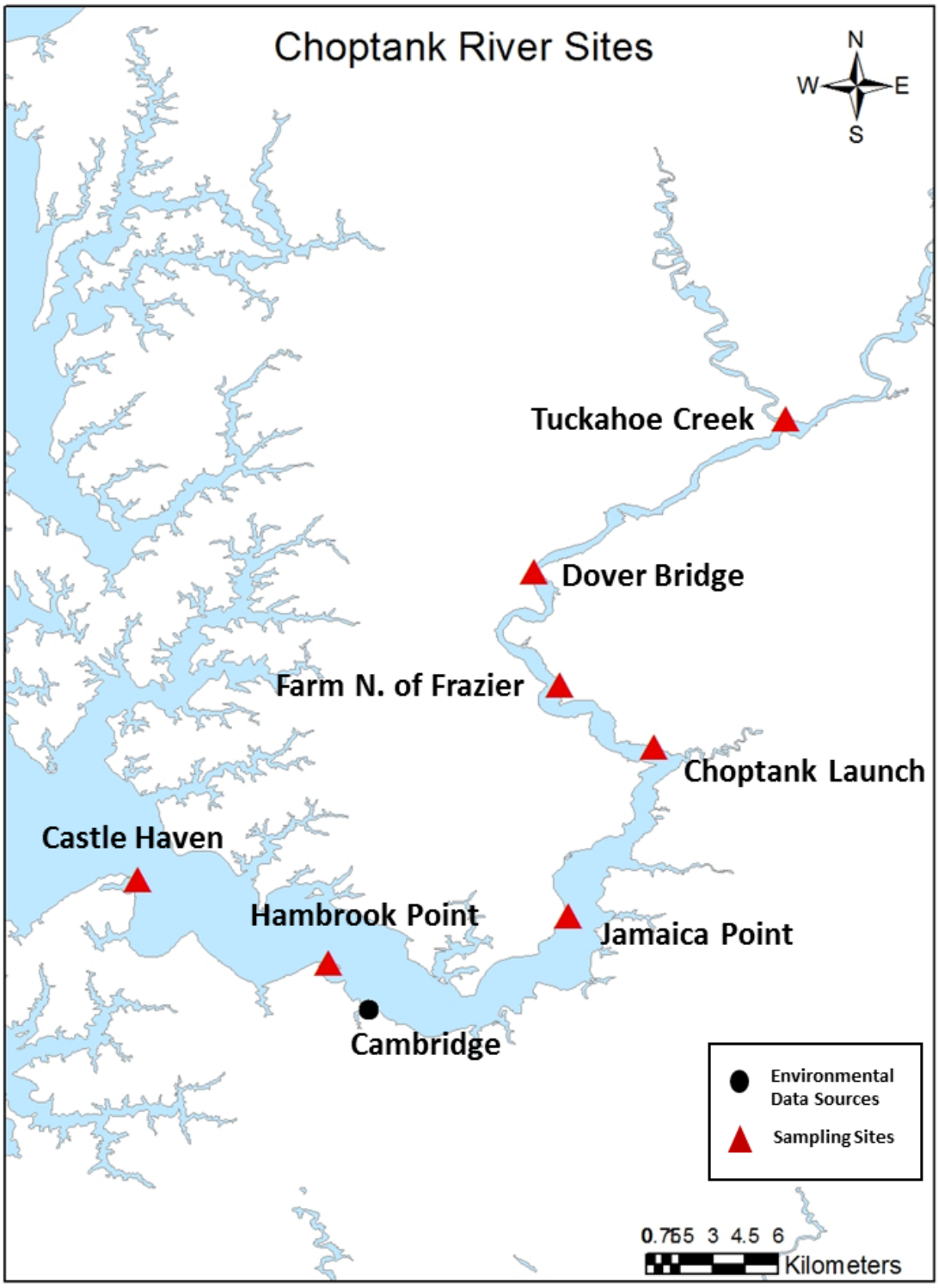

Figure 2 - YOY Atlantic menhaden sampling sites (red triangles) and environmental data sources (black circles) throughout the Choptank River.

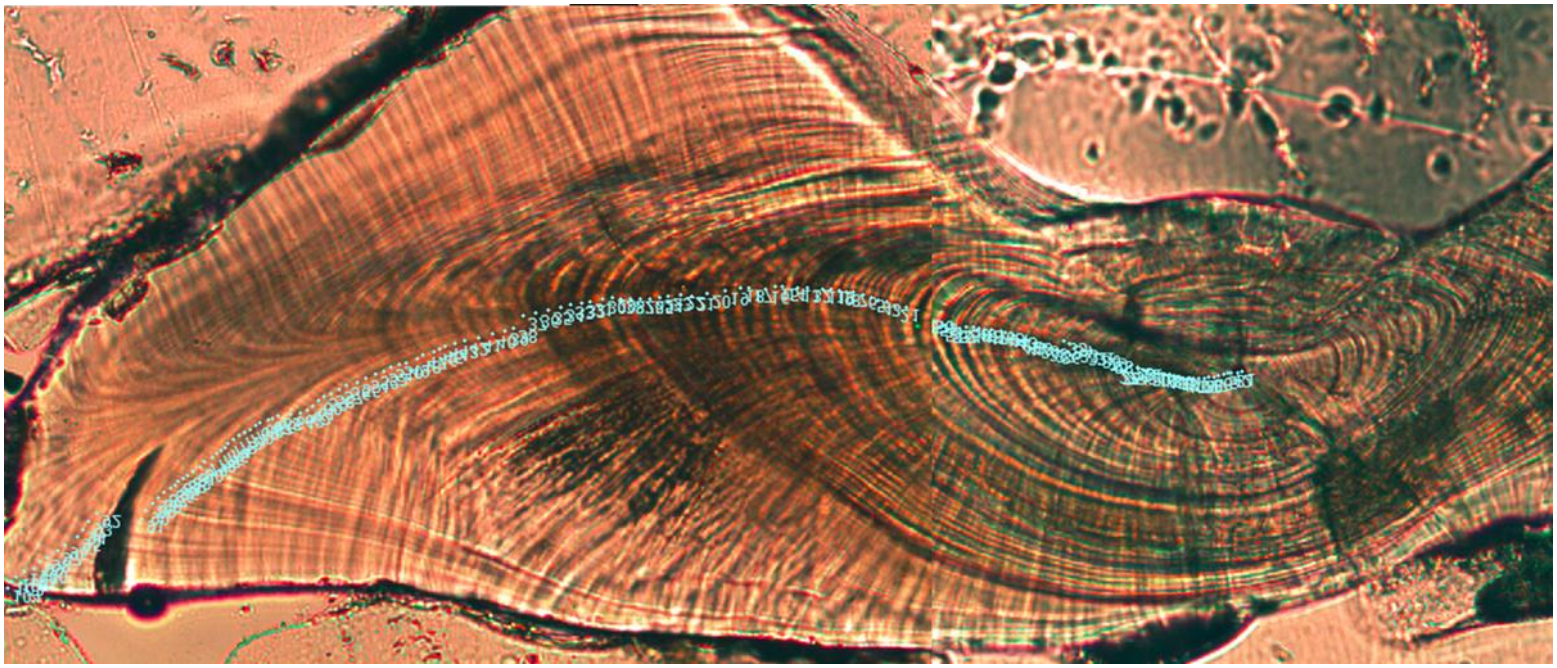

Figure 3 – Annotated image of sectioned YOY Atlantic menhaden otolith photographed at 200x magnification. Two images were combined in order to best resolve increments from the core and edge. This 2010 individual was estimated to be 161 days old and hatched on January 28, 2010.

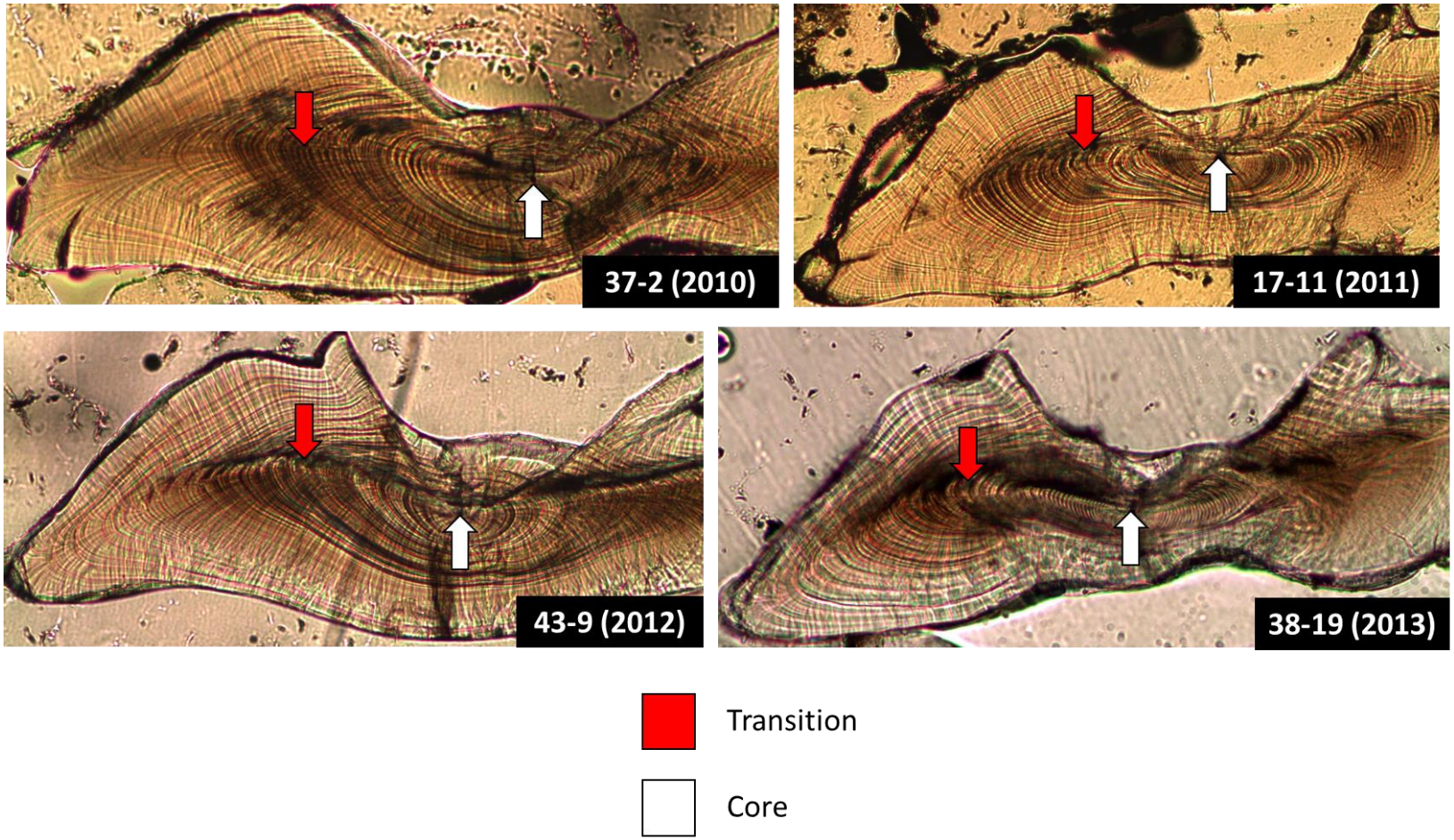

Figure 4 – YOY menhaden otoliths photographed at 200x magnification. Core is demarcated by the white arrow, while the otolith transition (a proxy for ingress) is demarcated by the red arrow. From the upper left to the lower right individuals represent 2010, 2011, 2012, and 2013 samples.

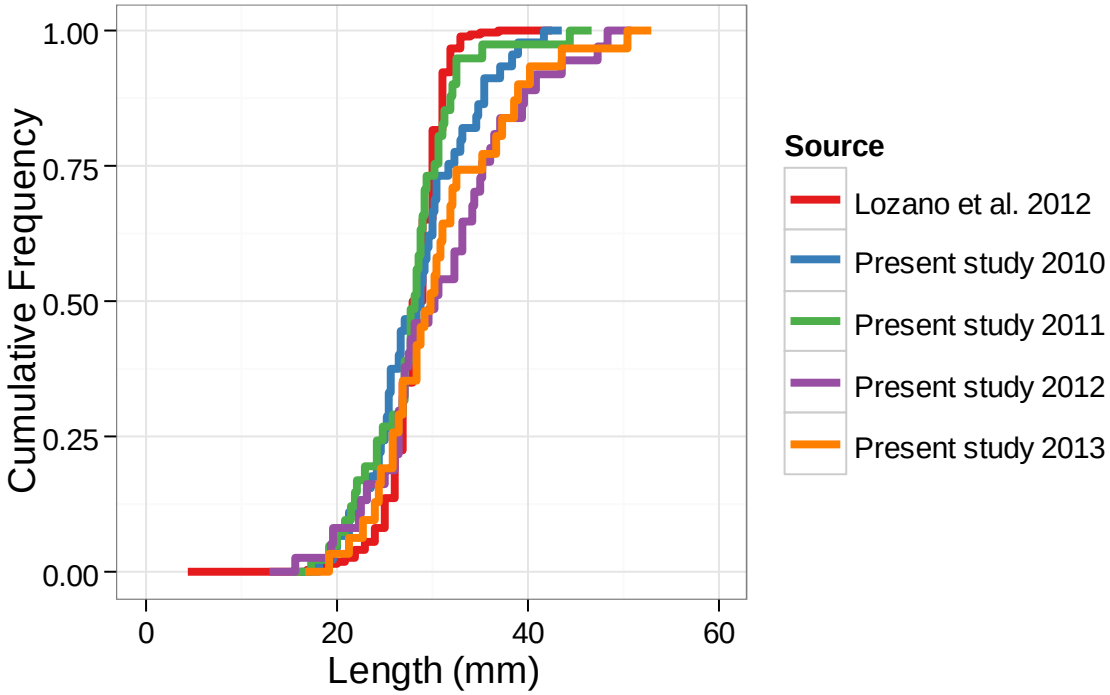

Figure 5 – Cumulative frequency of back-calculated length at 50 days post-hatch for 2010-2013 Atlantic menhaden YOY samples compared with length at ingress from 2005-2008 samples (Lozano et al. 2012).

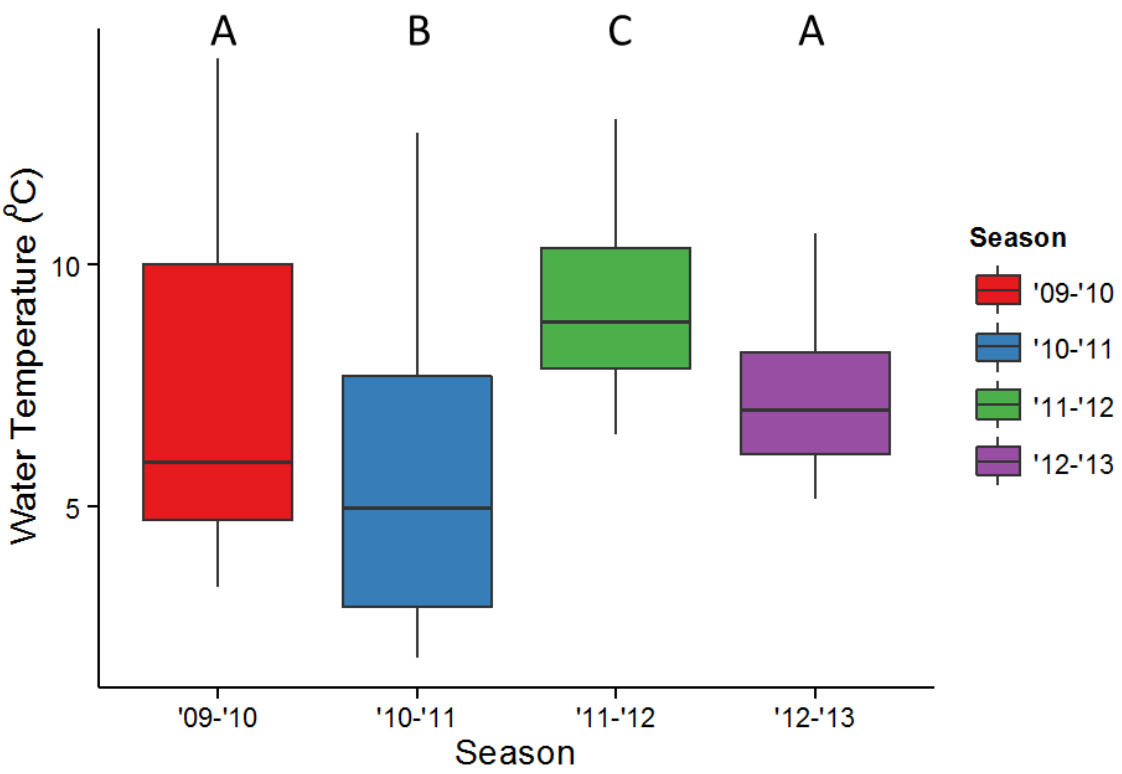

Figure 6 – Box whisker plots of winter water temperature from the Chesapeake Bay Bridge Tunnel NOAA Tides and Currents site from 2010 to 2013. Box covers from 25th – 75th percentile, horizontal bar marks the mean, and whiskers extend to the highest/lowest value within 1.5 * inter-quartile range. Seasons with similar means are marked with the same letter above bar (Tukey HSD $\alpha = 0.05$).

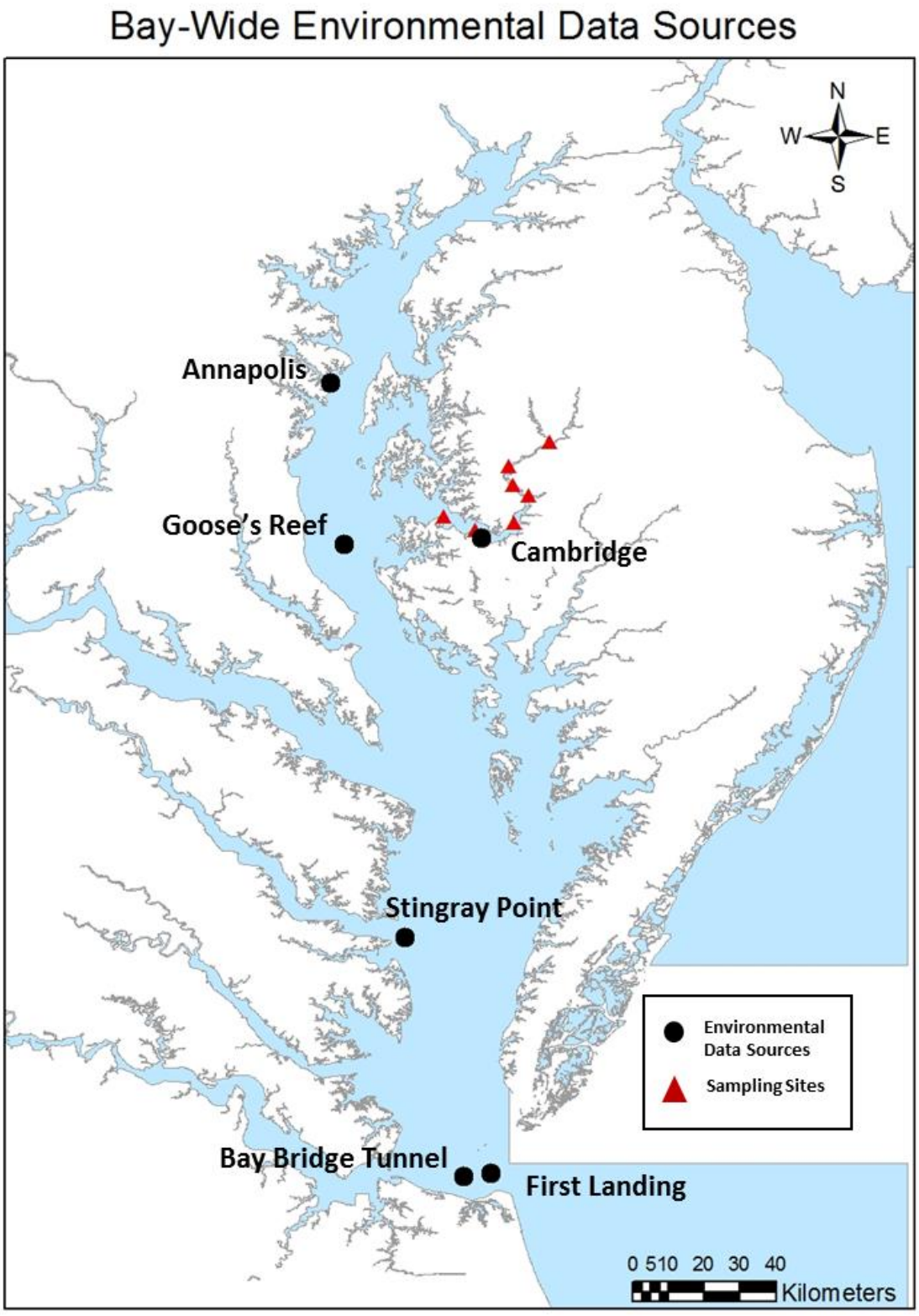

Figure 7 – Environmental data sources (black circles) throughout the Chesapeake Bay plotted with the YOY Atlantic menhaden sampling sites (red triangles) in the Choptank River.

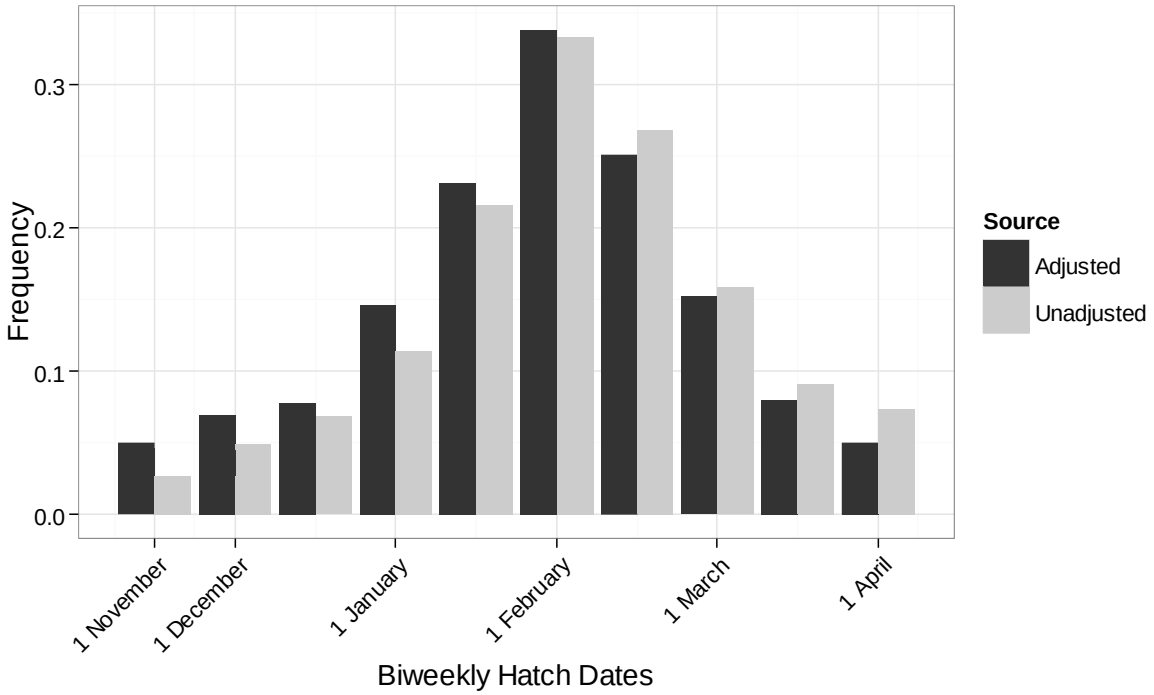

Figure 8 – Biweekly hatch-date distribution for summer-caught YOY Atlantic menhaden captured in the Choptank River, MD from 2010-2013. Unadjusted distribution shown in gray bars and daily mortality-adjusted hatch-date distribution (M = 0.010 d^{-1}) shown in black bars.

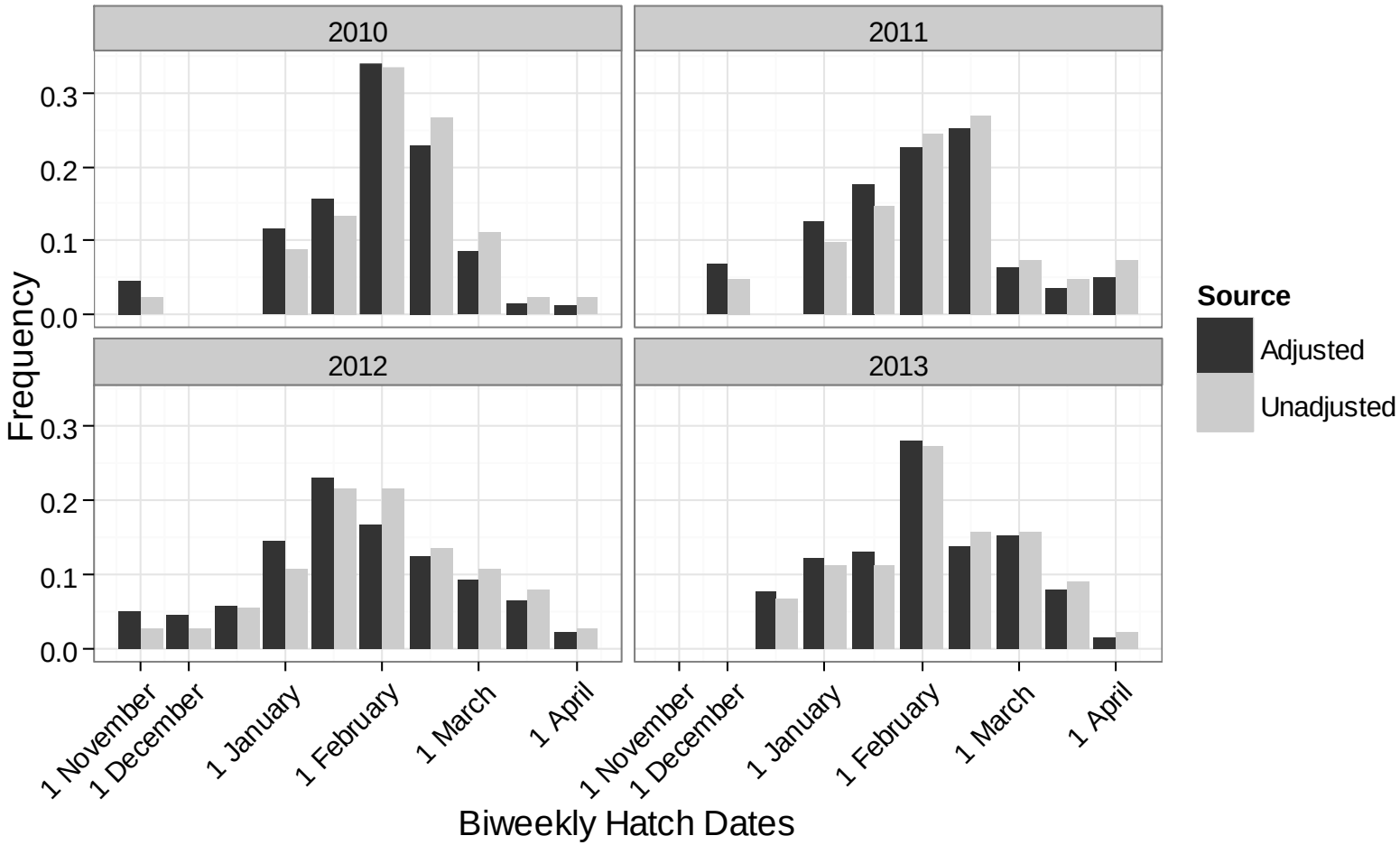

Figure 9 – Biweekly hatch-date distribution for summer-caught YOY Atlantic menhaden captured in the Choptank River, MD from 2010-2013. Unadjusted distribution is shown in gray bars and daily mortality-adjusted hatch-date distribution (M = 0.010 d^{-1}) and is shown in black bars.

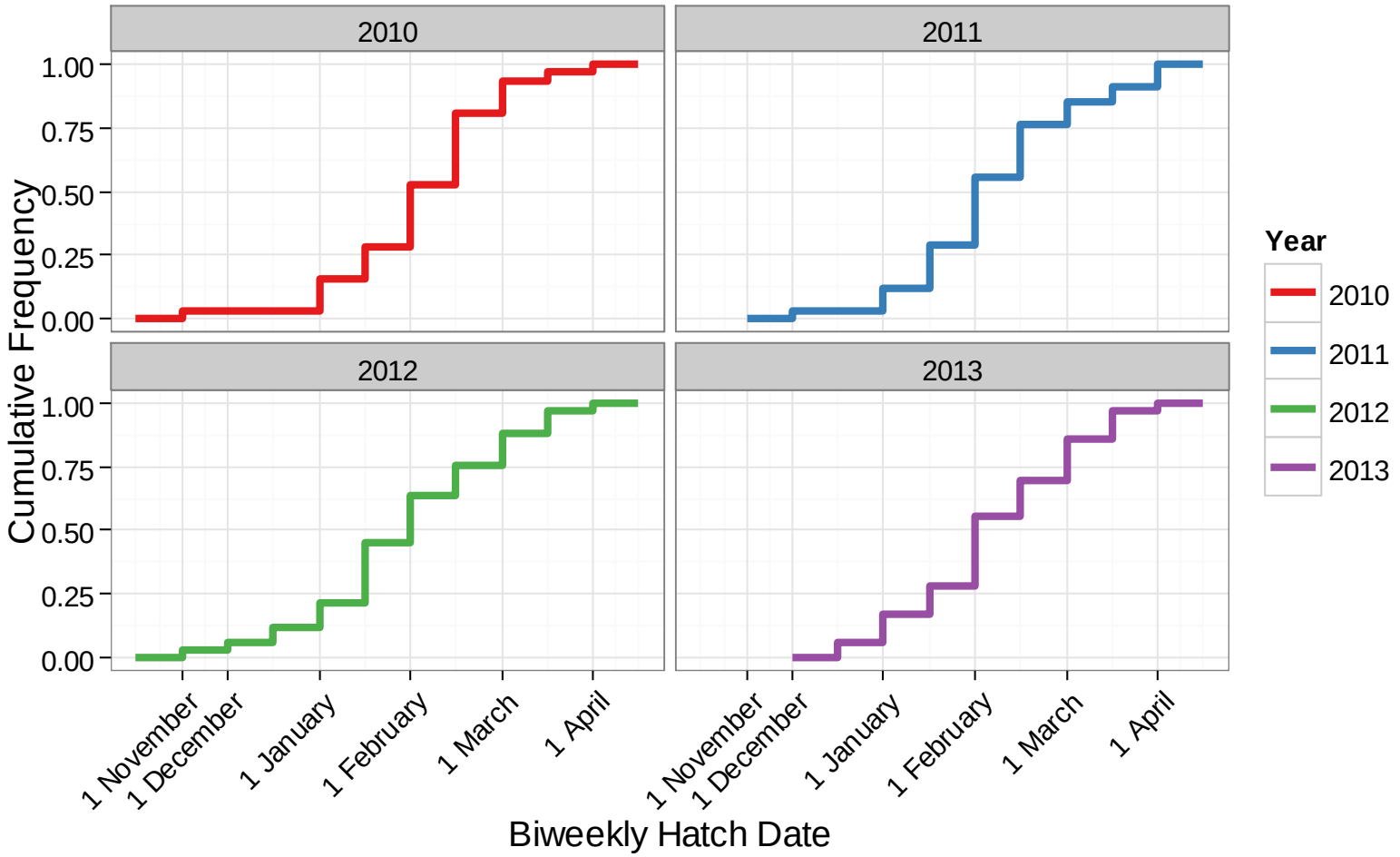

Figure 10 – Cumulative frequency of biweekly hatch dates of summer-captured YOY Atlantic menhaden for 2010 – 2013.

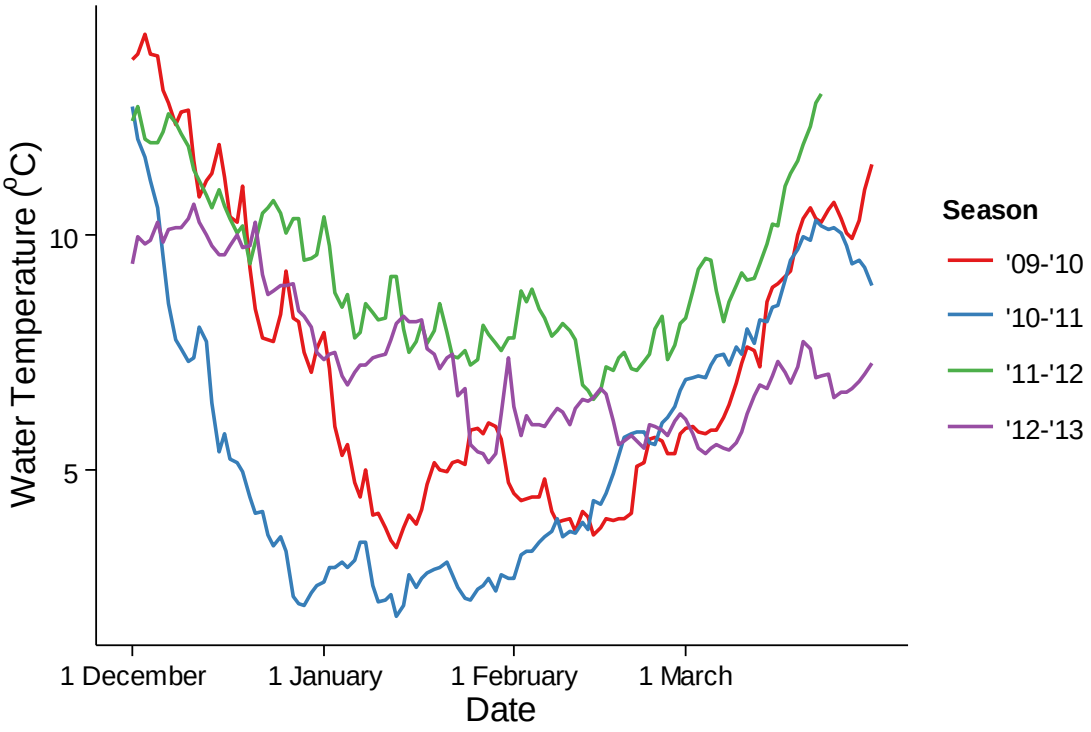

Figure 11 – Winter water temperature (°C) from 1 December – 31 March time series for the Chesapeake Bay Bridge Tunnel NOAA Tides and Currents site at the bay mouth for 2010 – 2013.

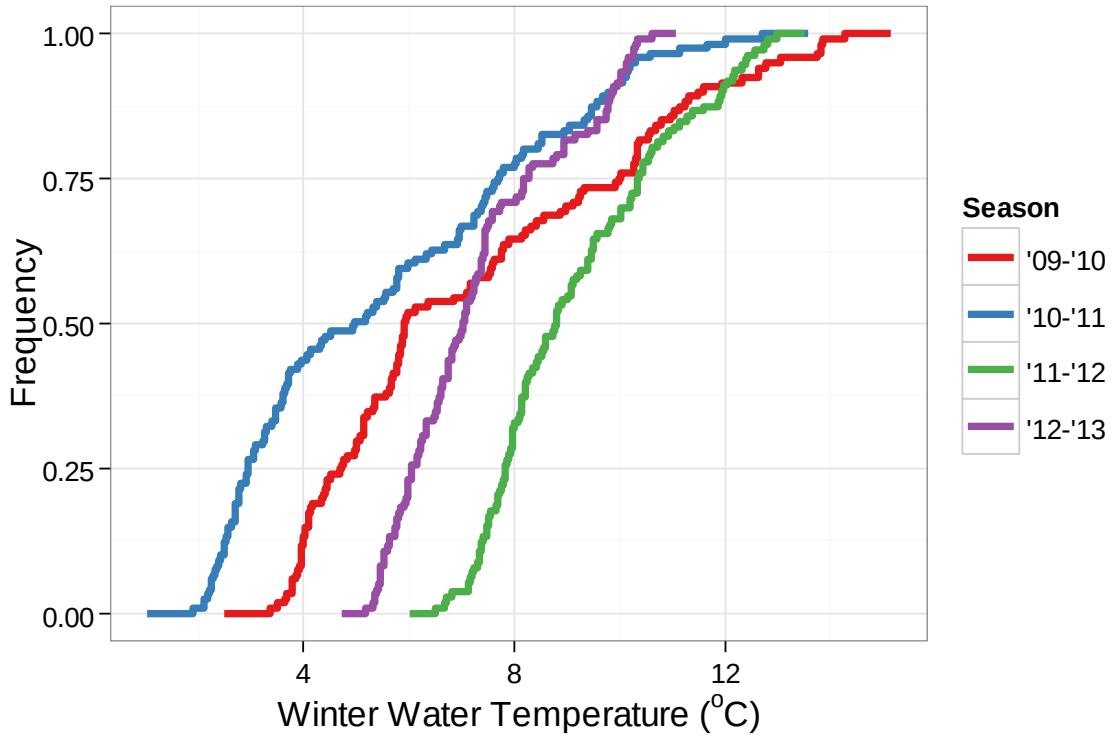

Figure 12 – Cumulative frequency of winter temperature (°C) as measured at the Chesapeake Bay Bridge Tunnel NOAA Tides and Currents site near the bay mouth 2010-2013.

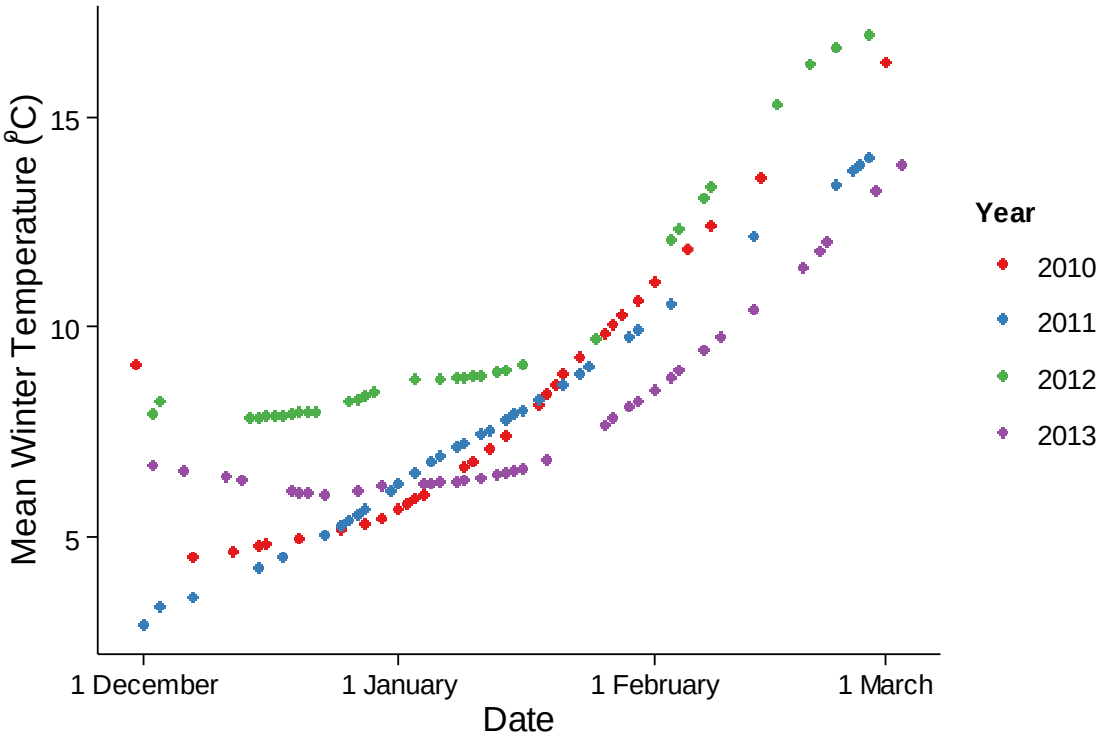

Figure 13 – Mean winter temperature experienced by aged YOY menhaden (°C) vs. hatch date. Experienced temperature estimated by averaging daily water temperatures measured at the Chesapeake Bay Bridge Tunnel site between the date of hatch and the estimated date of ingress (50 days post hatch).

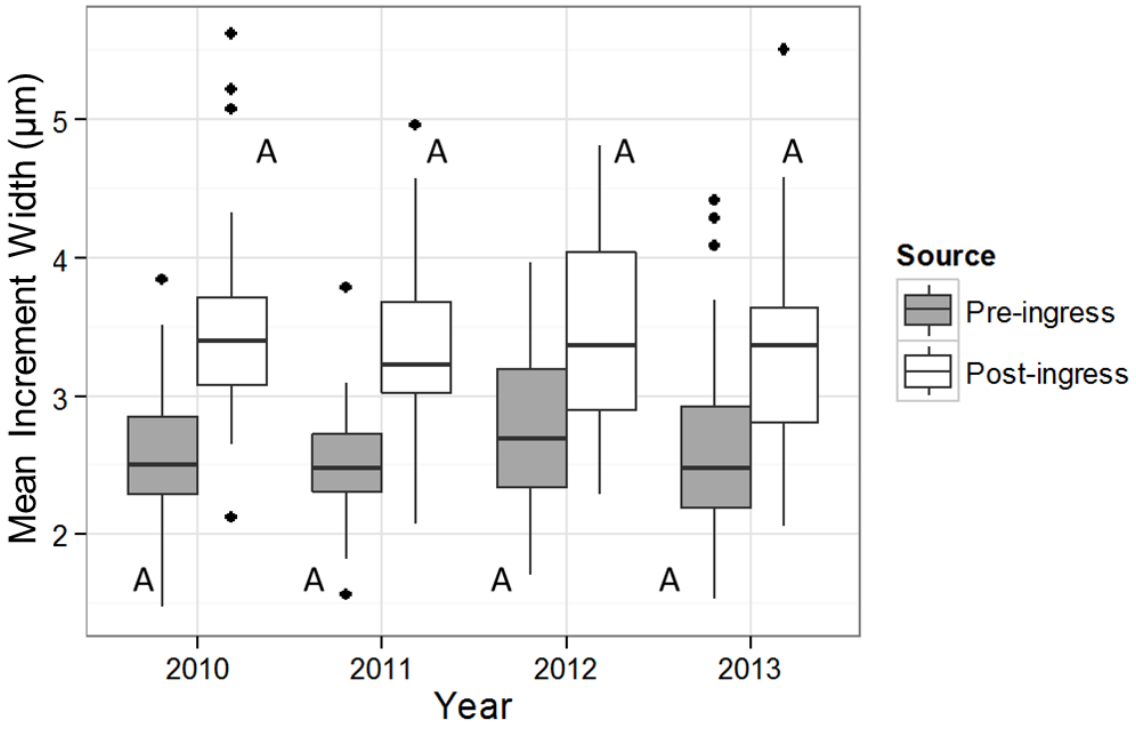

Figure 14 – Boxplot of YOY Atlantic menhaden otolith increment widths before (gray bars) and after (white bars) 50 days (ingress) for all years sampled in the Choptank River, MD. Sample sizes from 2010 – 2013 are 45, 41, 37, and 44, respectively. Box covers from 25th – 75th percentile, horizontal bar marks the mean, and whiskers extend to the highest/lowest value within 1.5 * inter-quartile range.

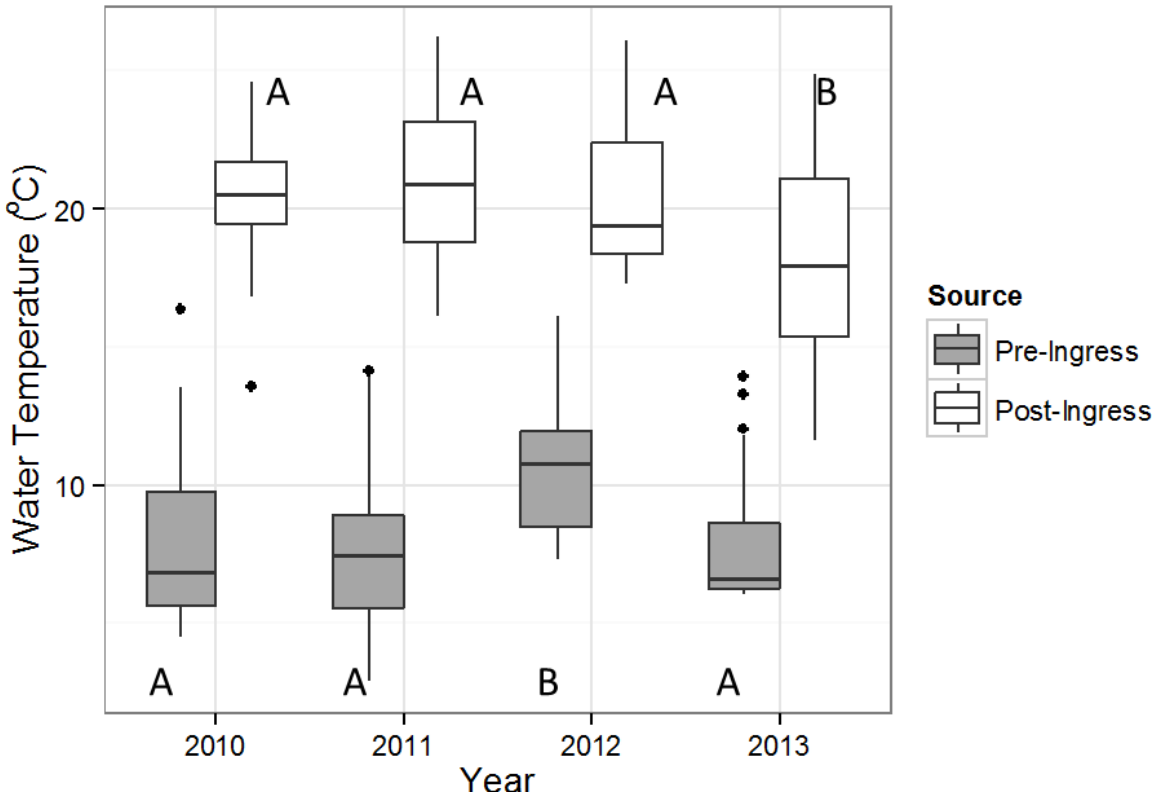

Figure 15 - Pre- and post-ingress water temperatures (°C) calculated per individual based on dates of hatch, approximated dates of ingress (50 days after hatch), and capture dates for 2010 – 2013 Atlantic menhaden samples (N=167). Sample sizes from 2010 – 2013 are 45, 41, 37, and 44, respectively. Box covers from 25th – 75th percentile, horizontal bar marks the mean, and whiskers extend to the highest/lowest value within 1.5 * inter-quartile range. Pre-ingress temperatures from Chesapeake Bay Bridge Tunnel (NOAA Tides & Currents site # 8638863) and Stingray Point and First Landing sites (Chesapeake Bay Interpretive Buoy System). Post-ingress temperatures from Goose's Reef (CBIBS) and Cambridge, MD (NOAA Tides & Currents) sites. Different years, as measured by Tukey HSD, are marked with differing letters (post-ingress: above; pre-ingress: below).

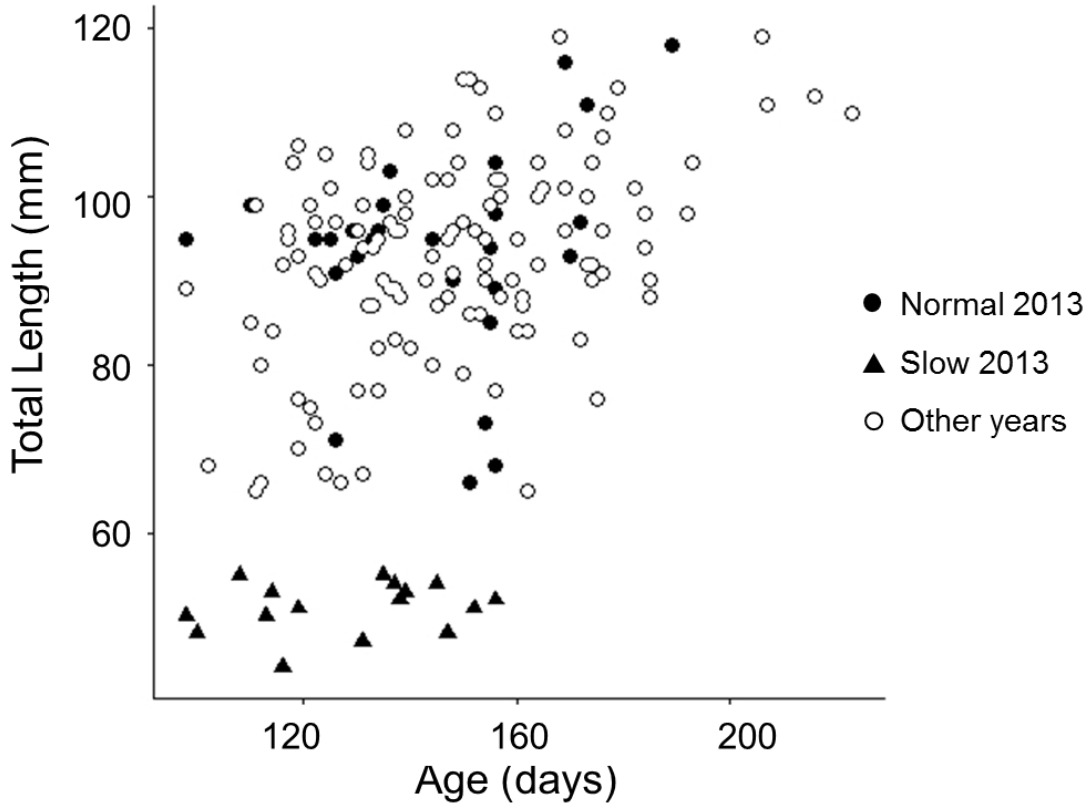

Figure 16 – Length at age for 2010 – 2013 sample of YOY Atlantic menhaden from the Choptank River, MD. All 2013 specimens are plotted with solid figures with slow growing individuals denoted by triangles and others are denoted by circles.

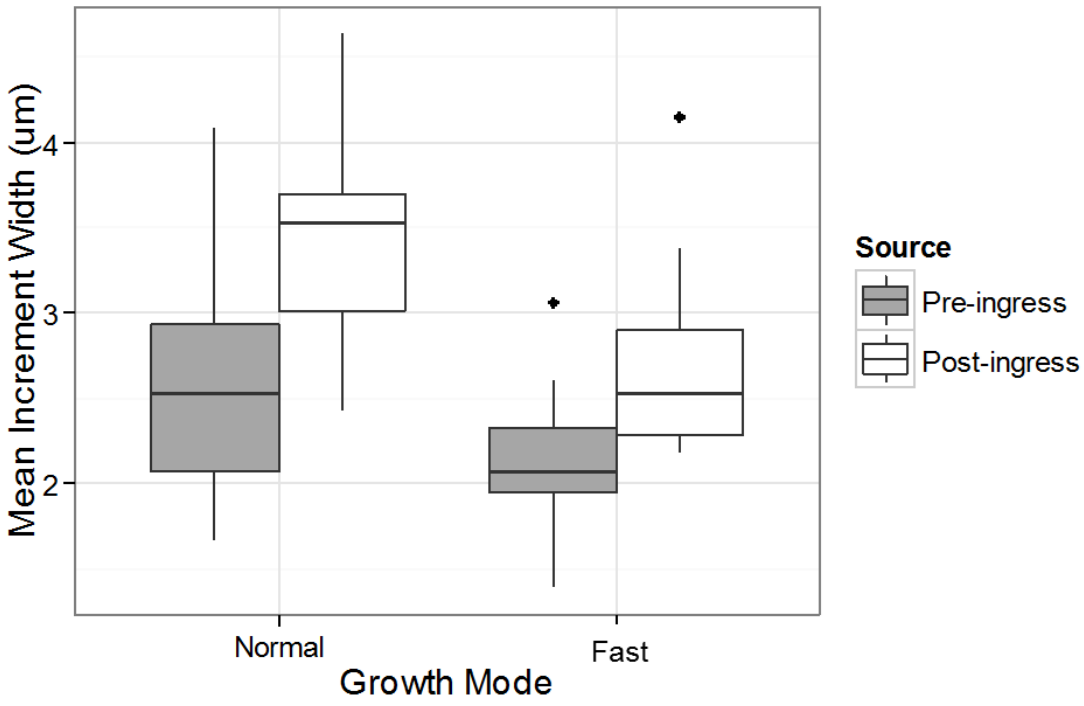

Figure 17 – YOY menhaden otolith increment widths before (gray bars) and after (white bars) 50 days (ingress) for the two growth sub-cohorts observed in 2013. Box covers from 25^{th} – 75^{th} percentile, horizontal bar marks the mean, and whiskers extend to the highest/lowest value within 1.5 * inter-quartile range.

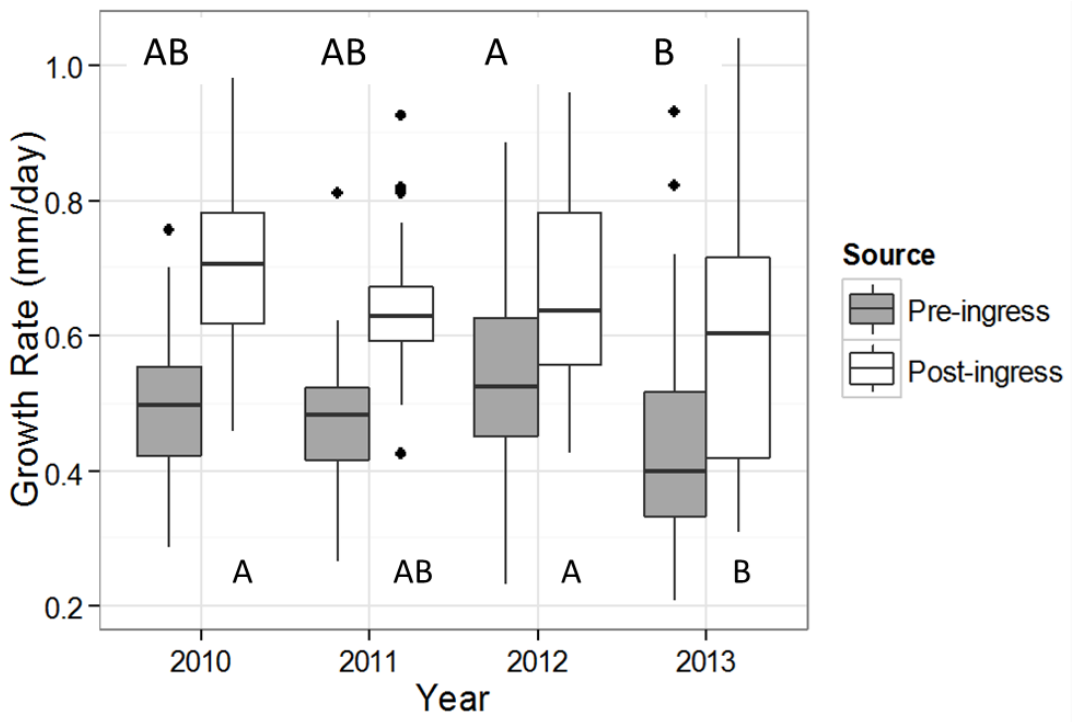

Figure 18 – Pre- and post-ingress growth rates of YOY Atlantic menhaden. Different years, as measured by Tukey HSD, are marked with differing letters (pre-ingress: above; post-ingress: below). Box covers from 25th – 75th percentile, horizontal bar marks the mean, and whiskers extend to the highest/lowest value within 1.5 * inter-quartile range.

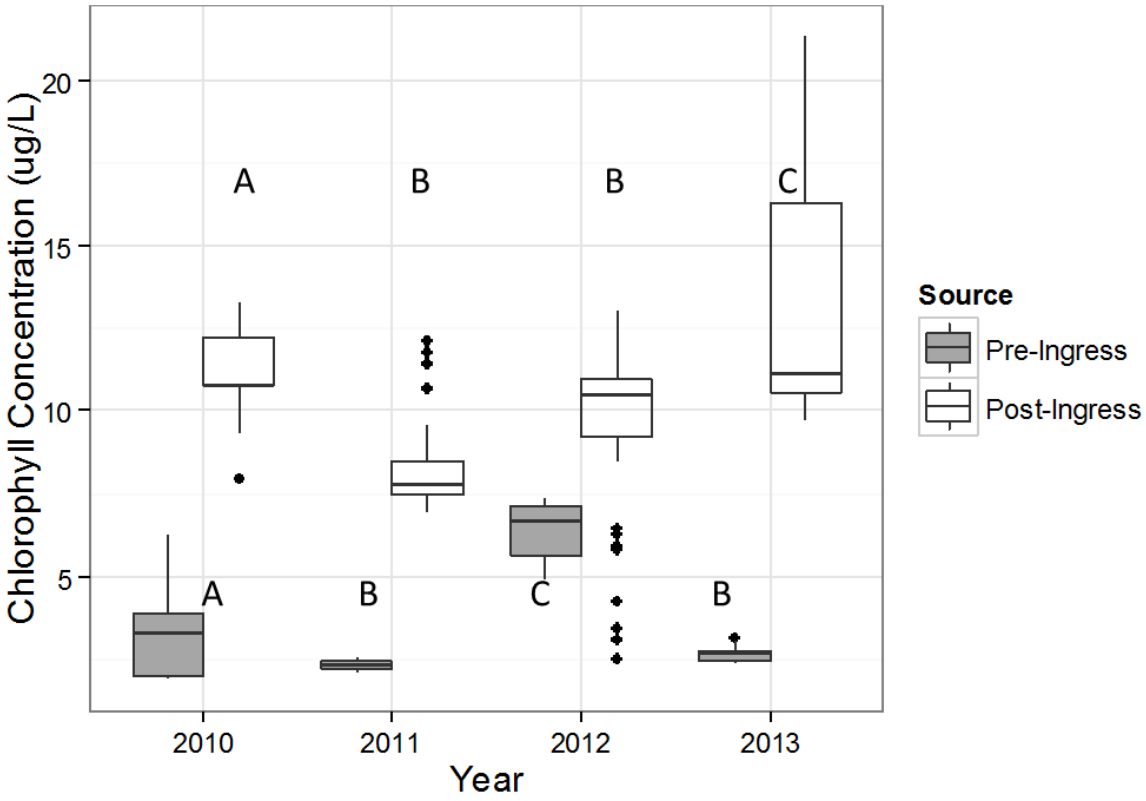

Figure 19 – Pre- and post-ingress chlorophyll concentration (µg L^{-1}) calculated per individual based on dates of hatch and approximated dates of ingress for 2010 – 2013 Atlantic menhaden samples (N=167). Box covers from 25th – 75th percentile, horizontal bar marks the mean, and whiskers extend to the highest/lowest value within 1.5 * inter-quartile range. Pre-ingress chlorophyll measures from Chesapeake Bay Bridge Tunnel (NOAA Tides & Currents site # 8638863) and Stingray Point and First Landing sites (Chesapeake Bay Interpretive Buoy System). Post-ingress chlorophyll measures from Goose's Reef (CBIBS) and Cambridge, MD (NOAA Tides & Currents) sites. Different years, as measured by Tukey HSD, are marked with differing letters (post-ingress: above; pre-ingress: below).

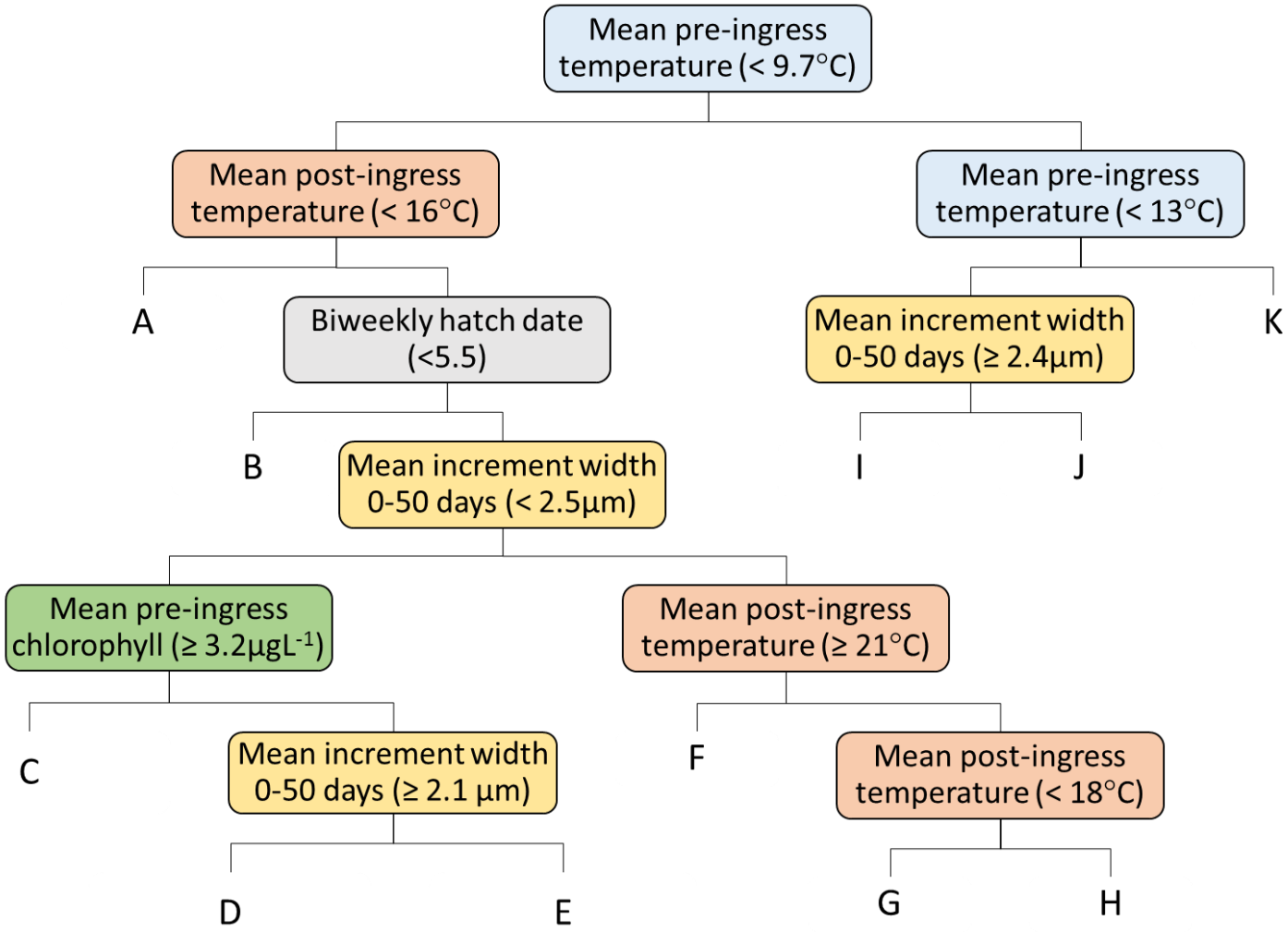

Figure 20 – Pruned regression tree of factors that influence post-ingress mean otolith increment widths for Atlantic menhaden. Variables tested included: pre/post-temperature, pre/post-chlorophyll densities, pre-ingress mean otolith increment width and biweekly hatch date. For specific estimates of terminal group characteristics see Table 8.

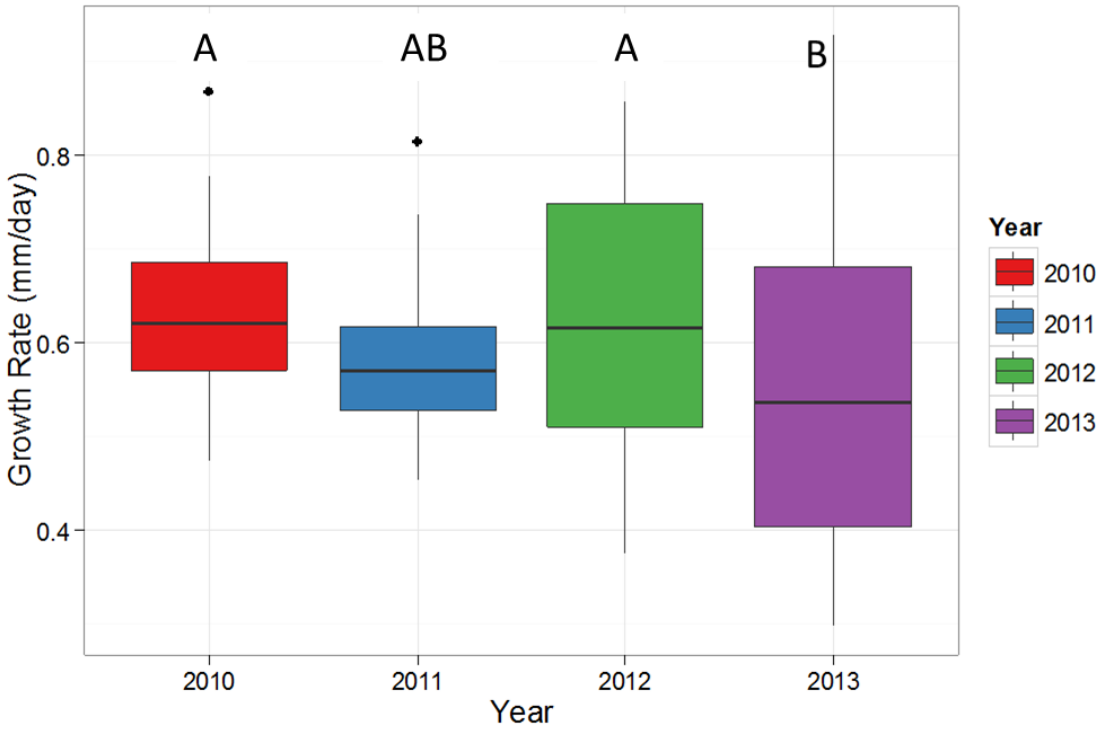

Figure 21 – Box whisker plots of growth rates (mm d^{-1}) from length at age data for summer-captured YOY Atlantic menhaden in the Choptank River, MD 2010 – 2013. Box covers from 25^{th} – 75^{th} percentile, horizontal bar marks the mean, and whiskers extend to the highest/lowest value within 1.5 * inter-quartile range.

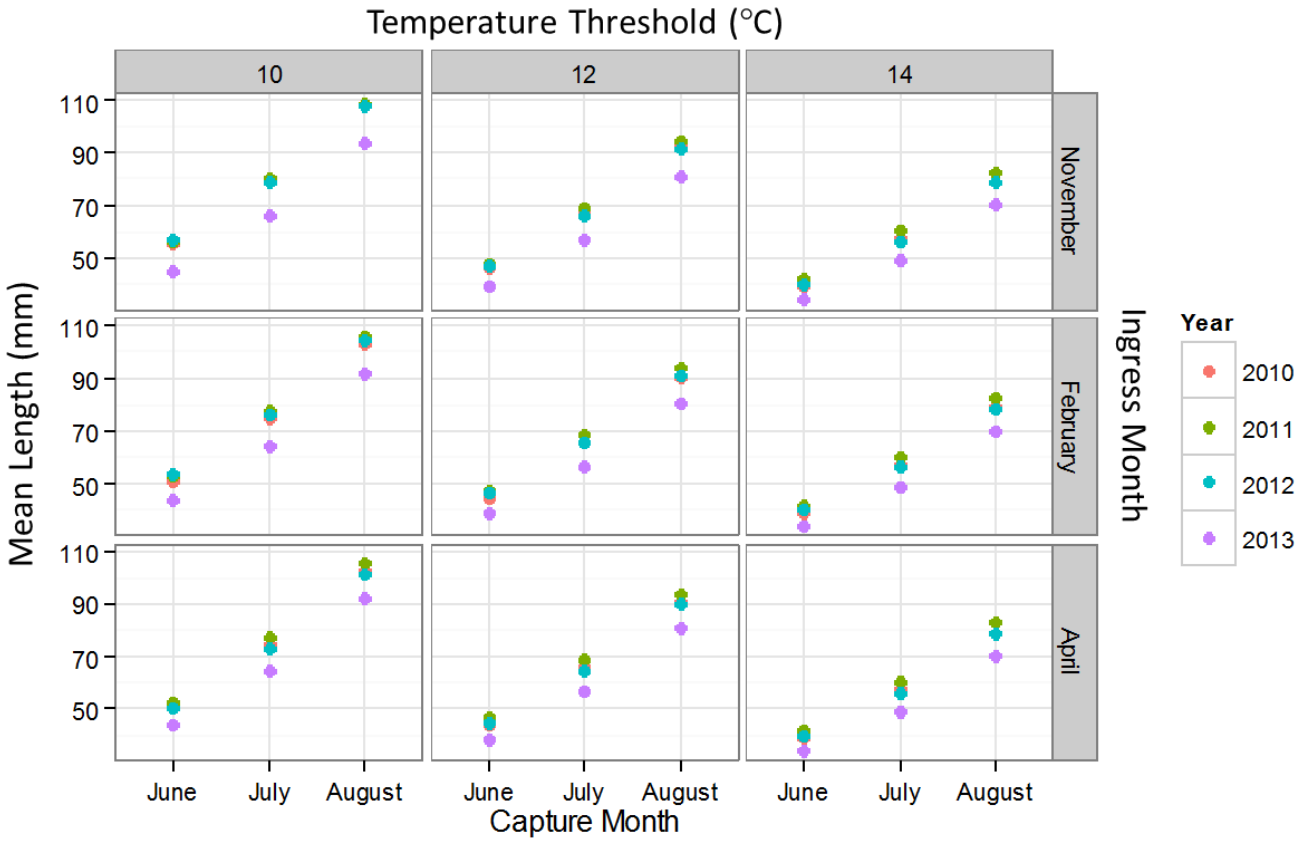

Figure 22 – Growing degree-day model simulation results for three dates of ingress (right y-axis: 1 November, 1 February, and 1 April) and for three dates of capture (lower x-axis: 1 June, 1 July, and 1 August) for Chesapeake Bay Atlantic menhaden YOY. Upper x-axis represents three growth temperature thresholds tested (10°, 12°, 14°C).

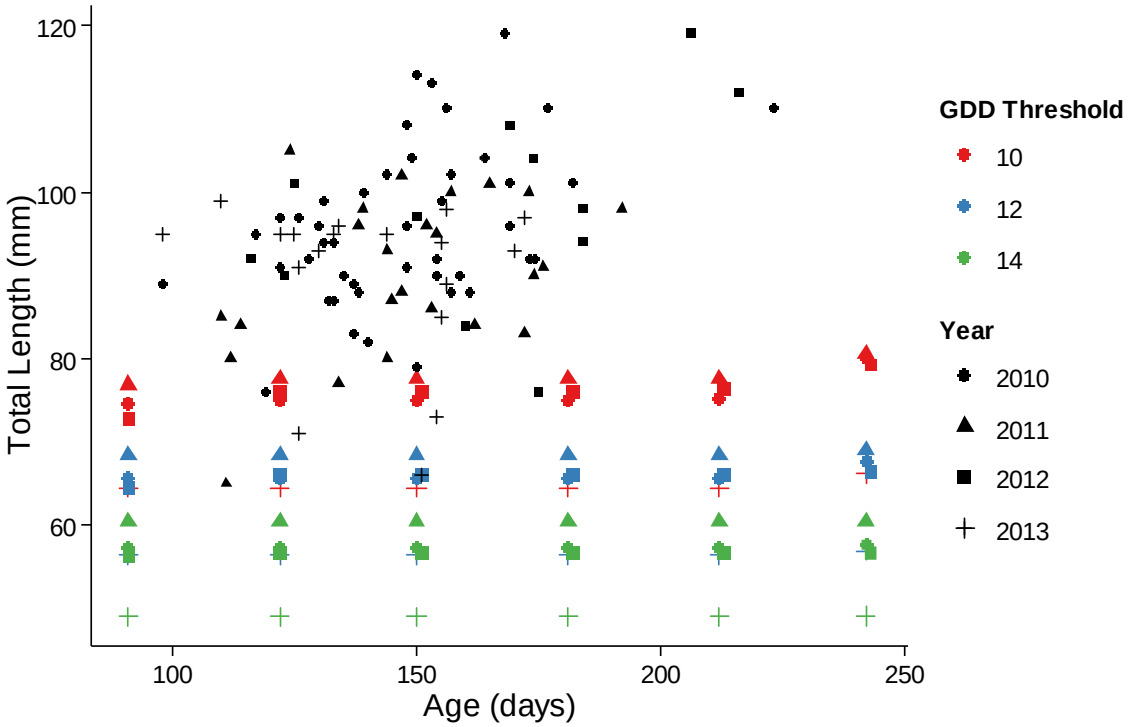

Figure 23 – Length at age for YOY Atlantic menhaden from growing degree-day (GDD) model for December - April ingress months, July capture month (see Tables 10-13), and 10, 12 and 14°C growth thresholds (red, blue, and green symbols). Overlain are empirically observed (July capture month) data (black symbols) from 2010 – 2013.

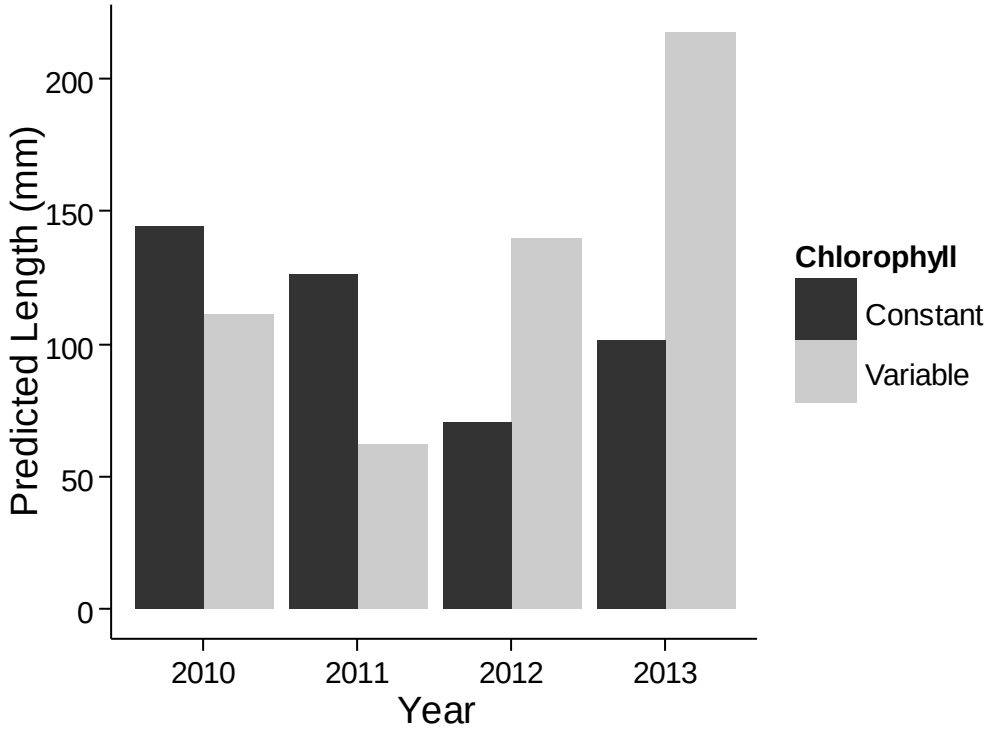

Figure 24 – Bioenergetics model length predictions for Atlantic menhaden YOY in 2010 – 2013 with constant or variable consumption.

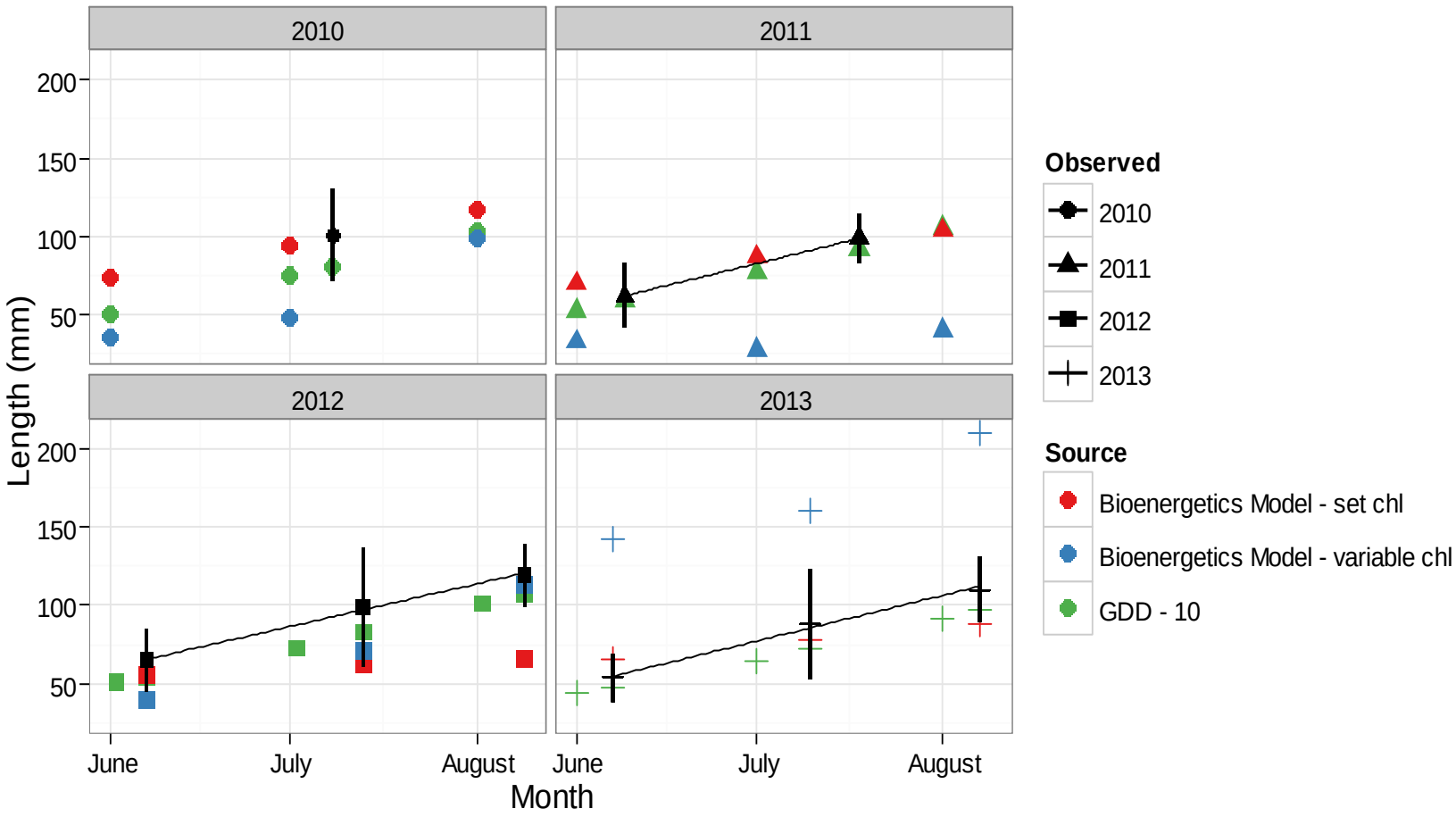

Figure 25a – Length at age for observed (black symbols) and modeled (red, green, and blue symbols) YOY Atlantic menhaden in 2010-2013. Observed lengths are plotted as a mean ± 2 standard deviations and, when possible, multiple sampling months means are regressed to infer growth rates (mm d^{-1}).

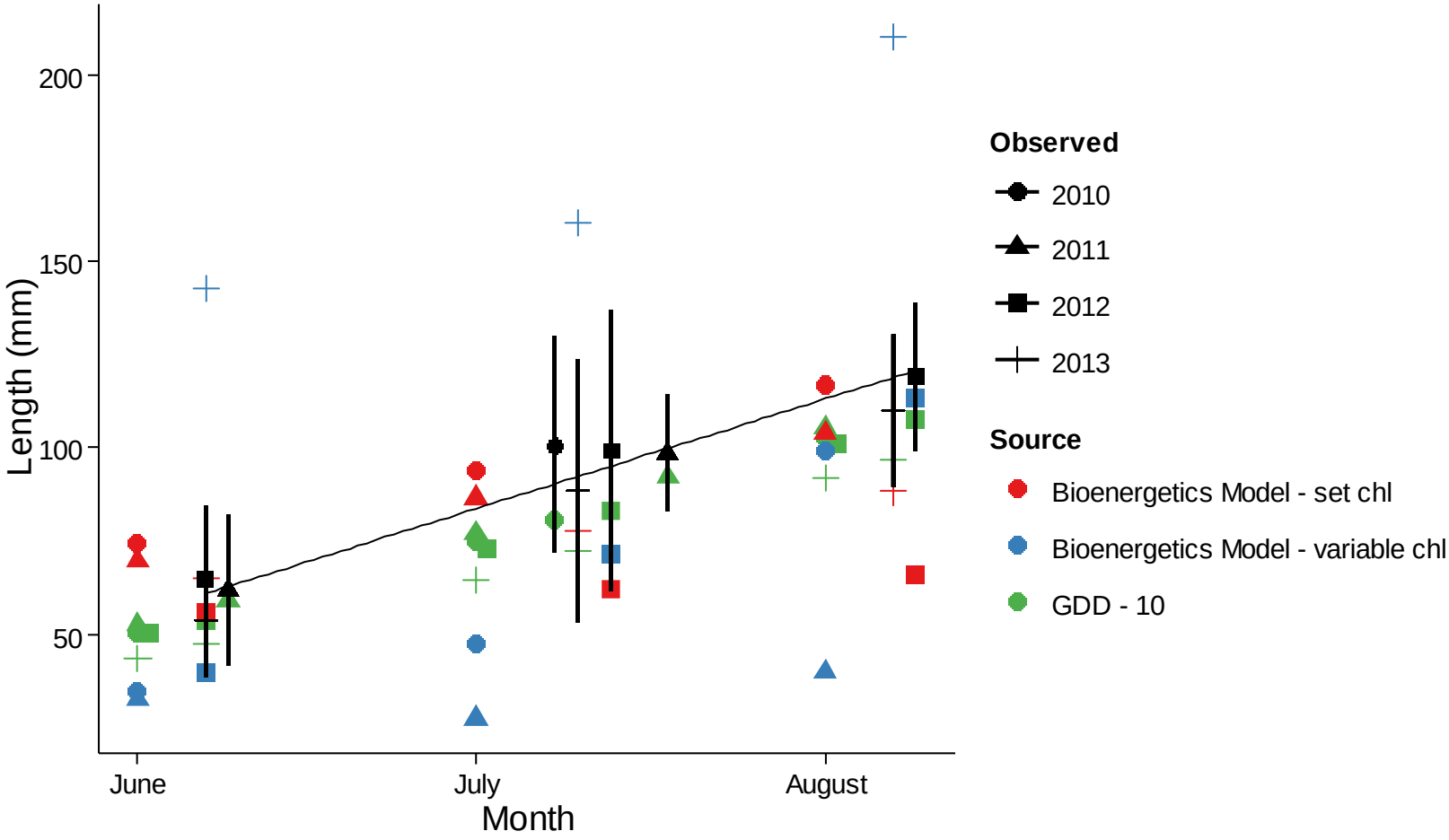

Figure 25b – Length at age for observed (black symbols) and modeled (red, green, and blue symbols) YOY Atlantic menhaden in 2010-2013. Observed lengths (black symbols) represent the mean length ± two standard deviations collected during monthly sampling events. A regression was performed on all years combined to infer growth rate from the slope (mm d^{-1}).

Appendix

Figure A1 – Principal Component Analysis of otolith, growth, hatch, and environmental variables used to evaluate the performance of a stipulated 50 days at ingress versus one that was estimated directly from the otolith transition point for Atlantic menhaden YOY captured in the Choptank River.

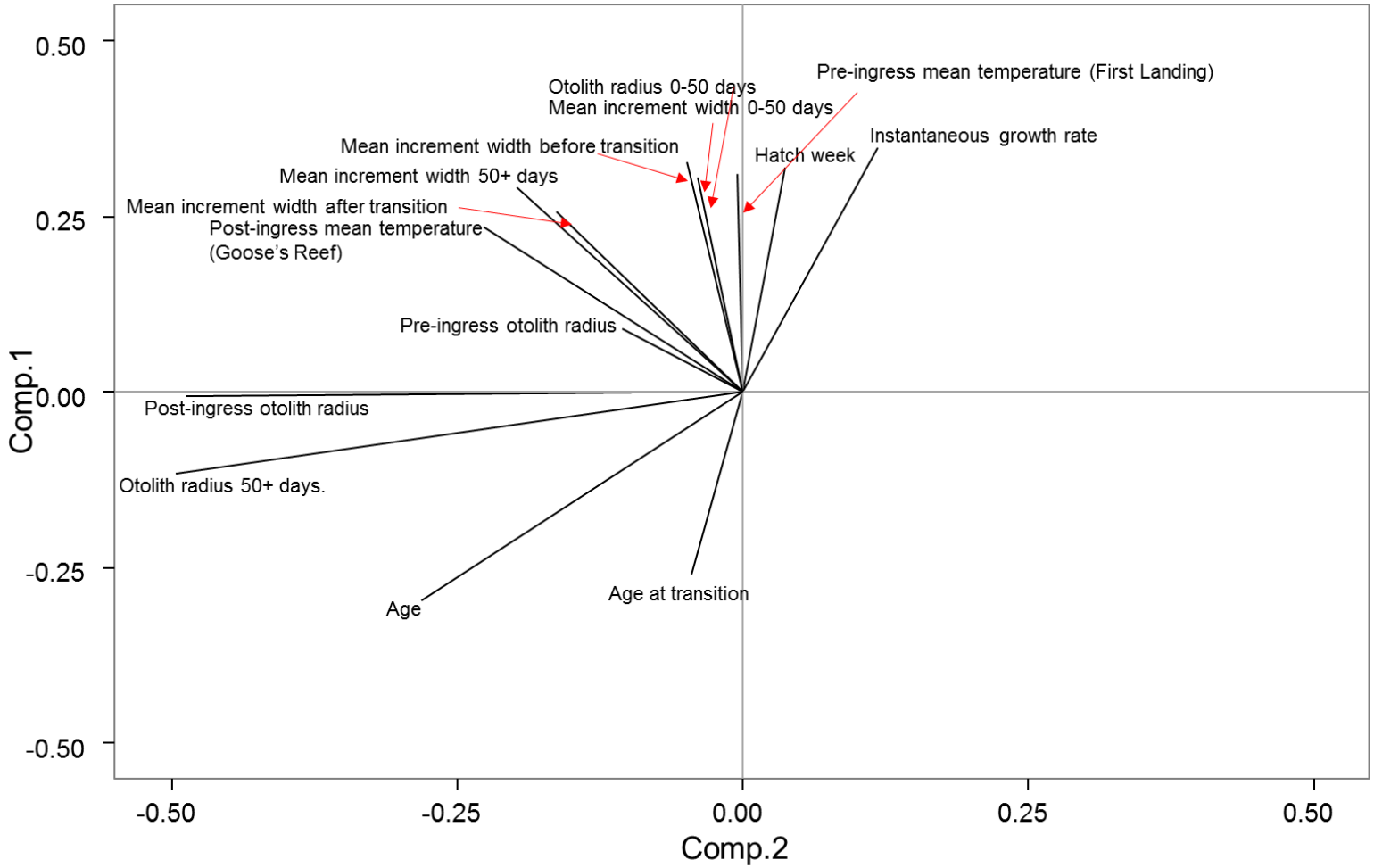

Table A1 – Growing degree-day model simulation summary and results (minimum, maximum, and mean lengths) for 2010 YOY Atlantic menhaden.

Start Month	End Month	End Date	Year	Threshold	Min Lt (mm)	Mean Lt (mm)	Max Lt (mm)
November	June	6/1	2010	10	34.3	55.5	67.3
November	June	6/1	2010	12	24.9	46.1	57.9
November	June	6/1	2010	14	17.9	39.1	50.9
November	July	7/1	2010	10	58.8	80.0	91.8
November	July	7/1	2010	12	46.4	67.6	79.4
November	July	7/1	2010	14	36.3	57.5	69.3
November	July	7/8	2010	10	64.7	85.9	97.7
November	July	7/8	2010	12	51.6	72.8	84.6
November	July	7/8	2010	14	40.8	62.0	73.8
November	August	8/1	2010	10	86.6	107.8	119.6
November	August	8/1	2010	12	71.1	92.3	104.1
November	August	8/1	2010	14	58.0	79.2	91.0
December	June	6/1	2010	10	29.6	50.7	62.6
December	June	6/1	2010	12	23.0	44.2	56.0
December	June	6/1	2010	14	17.5	38.7	50.5
December	July	7/1	2010	10	54.0	75.2	87.0
December	July	7/1	2010	12	44.5	65.7	77.5
December	July	7/1	2010	14	35.9	57.1	68.9
December	July	7/8	2010	10	59.9	81.1	92.9
December	July	7/8	2010	12	49.7	70.9	82.7
December	July	7/8	2010	14	40.5	61.6	73.5
December	August	8/1	2010	10	81.9	103.1	114.9
December	August	8/1	2010	12	69.2	90.4	102.2
December	August	8/1	2010	14	57.6	78.8	90.6
January	June	6/1	2010	10	29.3	50.5	62.3
January	June	6/1	2010	12	23.0	44.2	56.0
January	June	6/1	2010	14	17.5	38.7	50.5
January	July	7/1	2010	10	53.8	75.0	86.8
January	July	7/1	2010	12	44.5	65.7	77.5
January	July	7/1	2010	14	35.9	57.1	68.9
January	July	7/8	2010	10	59.7	80.9	92.7
January	July	7/8	2010	12	49.7	70.9	82.7
January	July	7/8	2010	14	40.5	61.6	73.5
January	August	8/1	2010	10	81.6	102.8	114.6
January	August	8/1	2010	12	69.2	90.4	102.2
January	August	8/1	2010	14	57.6	78.8	90.6
February	June	6/1	2010	10	29.3	50.5	62.3

February	June	6/1	2010	12	23.0	44.2	56.0
February	June	6/1	2010	14	17.5	38.7	50.5
February	July	7/1	2010	10	53.8	75.0	86.8
February	July	7/1	2010	12	44.5	65.7	77.5
February	July	7/1	2010	14	35.9	57.1	68.9
February	July	7/8	2010	10	59.7	80.9	92.7
February	July	7/8	2010	12	49.7	70.9	82.7
February	July	7/8	2010	14	40.5	61.6	73.5
February	August	8/1	2010	10	81.6	102.8	114.6
February	August	8/1	2010	12	69.2	90.4	102.2
February	August	8/1	2010	14	57.6	78.8	90.6
March	June	6/1	2010	10	29.3	50.5	62.3
March	June	6/1	2010	12	23.0	44.2	56.0
March	June	6/1	2010	14	17.5	38.7	50.5
March	July	7/1	2010	10	53.8	75.0	86.8
March	July	7/1	2010	12	44.5	65.7	77.5
March	July	7/1	2010	14	35.9	57.1	68.9
March	July	7/8	2010	10	59.7	80.9	92.7
March	July	7/8	2010	12	49.7	70.9	82.7
March	July	7/8	2010	14	40.5	61.6	73.5
March	August	8/1	2010	10	81.6	102.8	114.6
March	August	8/1	2010	12	69.2	90.4	102.2
March	August	8/1	2010	14	57.6	78.8	90.6
April	June	6/1	2010	10	29.0	50.2	62.0
April	June	6/1	2010	12	23.0	44.2	56.0
April	June	6/1	2010	14	17.5	38.7	50.5
April	July	7/1	2010	10	53.5	74.7	86.5
April	July	7/1	2010	12	44.5	65.7	77.5
April	July	7/1	2010	14	35.9	57.1	68.9
April	July	7/8	2010	10	59.4	80.6	92.4
April	July	7/8	2010	12	49.7	70.9	82.7
April	July	7/8	2010	14	40.5	61.6	73.5
April	August	8/1	2010	10	81.3	102.5	114.3
April	August	8/1	2010	12	69.2	90.4	102.2
April	August	8/1	2010	14	57.6	78.8	90.6

Table A2 – Growing degree-day model simulation summary and results (minimum, maximum, and mean lengths) for 2011 YOY Atlantic menhaden.

Start Month	End Month	End Date	Year	Threshold	Min Lt (mm)	Mean Lt (mm)	Max Lt (mm)
November	June	6/1	2011	10	34.9	56.1	67.9
November	June	6/1	2011	12	26.4	47.5	59.4
November	June	6/1	2011	14	20.8	42.0	53.8
November	July	6/9	2011	10	41.3	62.5	74.3
November	July	6/9	2011	12	31.9	53.1	64.9
November	July	6/9	2011	14	25.6	46.7	58.6
November	July	7/1	2011	10	59.3	80.5	92.3
November	July	7/1	2011	12	47.8	69.0	80.8
November	July	7/1	2011	14	39.2	60.4	72.2
November	July	7/18	2011	10	74.5	95.7	107.5
November	July	7/18	2011	12	61.2	82.4	94.2
November	July	7/18	2011	14	51.0	72.1	84.0
November	August	8/1	2011	10	87.8	108.9	120.8
November	August	8/1	2011	12	73.1	94.3	106.1
November	August	8/1	2011	14	61.4	82.6	94.4
December	June	6/1	2011	10	32.0	53.1	65.0
December	June	6/1	2011	12	25.7	46.9	58.7
December	June	6/1	2011	14	20.7	41.9	53.7
December	July	6/9	2011	10	38.3	59.5	71.3
December	July	6/9	2011	12	31.3	52.5	64.3
December	July	6/9	2011	14	25.5	46.7	58.5
December	July	7/1	2011	10	56.4	77.6	89.4
December	July	7/1	2011	12	47.2	68.3	80.2
December	July	7/1	2011	14	39.2	60.3	72.2
December	July	7/18	2011	10	71.5	92.7	104.5
December	July	7/18	2011	12	60.6	81.8	93.6
December	July	7/18	2011	14	50.9	72.1	83.9
December	August	8/1	2011	10	84.8	106.0	117.8
December	August	8/1	2011	12	72.5	93.7	105.5
December	August	8/1	2011	14	61.4	82.6	94.4
January	June	6/1	2011	10	32.0	53.1	65.0
January	June	6/1	2011	12	25.7	46.9	58.7
January	June	6/1	2011	14	20.7	41.9	53.7
January	July	6/9	2011	10	38.3	59.5	71.3
January	July	6/9	2011	12	31.3	52.5	64.3
January	July	6/9	2011	14	25.5	46.7	58.5
January	July	7/1	2011	10	56.4	77.6	89.4

January	July	7/1	2011	12	47.2	68.3	80.2
January	July	7/1	2011	14	39.2	60.3	72.2
January	July	7/18	2011	10	71.5	92.7	104.5
January	July	7/18	2011	12	60.6	81.8	93.6
January	July	7/18	2011	14	50.9	72.1	83.9
January	August	8/1	2011	10	84.8	106.0	117.8
January	August	8/1	2011	12	72.5	93.7	105.5
January	August	8/1	2011	14	61.4	82.6	94.4
February	June	6/1	2011	10	32.0	53.1	65.0
February	June	6/1	2011	12	25.7	46.9	58.7
February	June	6/1	2011	14	20.7	41.9	53.7
February	July	6/9	2011	10	38.3	59.5	71.3
February	July	6/9	2011	12	31.3	52.5	64.3
February	July	6/9	2011	14	25.5	46.7	58.5
February	July	7/1	2011	10	56.4	77.6	89.4
February	July	7/1	2011	12	47.2	68.3	80.2
February	July	7/1	2011	14	39.2	60.3	72.2
February	July	7/18	2011	10	71.5	92.7	104.5
February	July	7/18	2011	12	60.6	81.8	93.6
February	July	7/18	2011	14	50.9	72.1	83.9
February	August	8/1	2011	10	84.8	106.0	117.8
February	August	8/1	2011	12	72.5	93.7	105.5
February	August	8/1	2011	14	61.4	82.6	94.4
March	June	6/1	2011	10	32.0	53.1	65.0
March	June	6/1	2011	12	25.7	46.9	58.7
March	June	6/1	2011	14	20.7	41.9	53.7
March	July	6/9	2011	10	38.3	59.5	71.3
March	July	6/9	2011	12	31.3	52.5	64.3
March	July	6/9	2011	14	25.5	46.7	58.5
March	July	7/1	2011	10	56.4	77.6	89.4
March	July	7/1	2011	12	47.2	68.3	80.2
March	July	7/1	2011	14	39.2	60.3	72.2
March	July	7/18	2011	10	71.5	92.7	104.5
March	July	7/18	2011	12	60.6	81.8	93.6
March	July	7/18	2011	14	50.9	72.1	83.9
March	August	8/1	2011	10	84.8	106.0	117.8
March	August	8/1	2011	12	72.5	93.7	105.5
March	August	8/1	2011	14	61.4	82.6	94.4
April	June	6/1	2011	10	31.3	52.4	64.3
April	June	6/1	2011	12	25.7	46.9	58.7
April	June	6/1	2011	14	20.7	41.9	53.7

April	July	6/9	2011	10	37.6	58.8	70.6
April	July	6/9	2011	12	31.3	52.5	64.3
April	July	6/9	2011	14	25.5	46.7	58.5
April	July	7/1	2011	10	55.7	76.9	88.7
April	July	7/1	2011	12	47.1	68.3	80.1
April	July	7/1	2011	14	39.2	60.3	72.2
April	July	7/18	2011	10	70.8	92.0	103.8
April	July	7/18	2011	12	60.6	81.8	93.6
April	July	7/18	2011	14	50.9	72.1	83.9
April	August	8/1	2011	10	84.1	105.3	117.1
April	August	8/1	2011	12	72.5	93.7	105.5
April	August	8/1	2011	14	61.4	82.6	94.4

Table A3 – Growing degree-day model simulation summary and results (minimum, maximum, and mean lengths) for 2012 YOY Atlantic menhaden.

Start Month	End Month	End Date	Year	Threshold	Min Lt (mm)	Mean Lt (mm)	Max Lt (mm)
November	June	6/1	2012	10	35.5	56.7	68.5
November	June	6/1	2012	12	25.7	46.9	58.7
November	June	6/1	2012	14	18.8	40.0	51.8
November	June	6/6	2012	10	39.1	60.3	72.1
November	June	6/6	2012	12	28.8	50.0	61.8
November	June	6/6	2012	14	21.4	42.6	54.4
November	July	7/1	2012	10	58.1	79.3	91.1
November	July	7/1	2012	12	45.3	66.4	78.3
November	July	7/1	2012	14	35.3	56.5	68.3
November	July	7/12	2012	10	68.3	89.5	101.3
November	July	7/12	2012	12	54.4	75.6	87.4
November	July	7/12	2012	14	43.4	64.5	76.4
November	August	8/1	2012	10	86.4	107.5	119.4
November	August	8/1	2012	12	70.4	91.6	103.4
November	August	8/1	2012	14	57.4	78.6	90.4
November	August	8/8	2012	10	92.8	114.0	125.8
November	August	8/8	2012	12	76.2	97.3	109.2
November	August	8/8	2012	14	62.4	83.6	95.4
December	June	6/1	2012	10	32.6	53.8	65.6
December	June	6/1	2012	12	25.2	46.4	58.2
December	June	6/1	2012	14	18.8	40.0	51.8
December	June	6/6	2012	10	36.2	57.4	69.2
December	June	6/6	2012	12	28.3	49.5	61.3
December	June	6/6	2012	14	21.4	42.6	54.4
December	July	7/1	2012	10	55.1	76.3	88.1
December	July	7/1	2012	12	44.8	66.0	77.8
December	July	7/1	2012	14	35.3	56.5	68.3
December	July	7/12	2012	10	65.3	86.5	98.3
December	July	7/12	2012	12	53.9	75.1	86.9
December	July	7/12	2012	14	43.4	64.5	76.4
December	August	8/1	2012	10	83.4	104.6	116.4
December	August	8/1	2012	12	70.0	91.1	103.0
December	August	8/1	2012	14	57.4	78.6	90.4
December	August	8/8	2012	10	89.8	111.0	122.8
December	August	8/8	2012	12	75.7	96.9	108.7
December	August	8/8	2012	14	62.4	83.6	95.4
January	June	6/1	2012	10	32.2	53.4	65.2

January	June	6/1	2012	12	25.2	46.4	58.2
January	June	6/1	2012	14	18.8	40.0	51.8
January	June	6/6	2012	10	35.8	57.0	68.8
January	June	6/6	2012	12	28.3	49.5	61.3
January	June	6/6	2012	14	21.4	42.6	54.4
January	July	7/1	2012	10	54.8	75.9	87.8
January	July	7/1	2012	12	44.8	66.0	77.8
January	July	7/1	2012	14	35.3	56.5	68.3
January	July	7/12	2012	10	65.0	86.2	98.0
January	July	7/12	2012	12	53.9	75.1	86.9
January	July	7/12	2012	14	43.4	64.5	76.4
January	August	8/1	2012	10	83.0	104.2	116.0
January	August	8/1	2012	12	70.0	91.1	103.0
January	August	8/1	2012	14	57.4	78.6	90.4
January	August	8/8	2012	10	89.5	110.6	122.5
January	August	8/8	2012	12	75.7	96.9	108.7
January	August	8/8	2012	14	62.4	83.6	95.4
February	June	6/1	2012	10	32.2	53.4	65.2
February	June	6/1	2012	12	25.2	46.4	58.2
February	June	6/1	2012	14	18.8	40.0	51.8
February	June	6/6	2012	10	35.8	57.0	68.8
February	June	6/6	2012	12	28.3	49.5	61.3
February	June	6/6	2012	14	21.4	42.6	54.4
February	July	7/1	2012	10	54.8	75.9	87.8
February	July	7/1	2012	12	44.8	66.0	77.8
February	July	7/1	2012	14	35.3	56.5	68.3
February	July	7/12	2012	10	65.0	86.2	98.0
February	July	7/12	2012	12	53.9	75.1	86.9
February	July	7/12	2012	14	43.4	64.5	76.4
February	August	8/1	2012	10	83.0	104.2	116.0
February	August	8/1	2012	12	70.0	91.1	103.0
February	August	8/1	2012	14	57.4	78.6	90.4
February	August	8/8	2012	10	89.5	110.6	122.5
February	August	8/8	2012	12	75.7	96.9	108.7
February	August	8/8	2012	14	62.4	83.6	95.4
March	June	6/1	2012	10	32.2	53.4	65.2
March	June	6/1	2012	12	25.2	46.4	58.2
March	June	6/1	2012	14	18.8	40.0	51.8
March	June	6/6	2012	10	35.8	57.0	68.8
March	June	6/6	2012	12	28.3	49.5	61.3
March	June	6/6	2012	14	21.4	42.6	54.4

March	July	7/1	2012	10	54.8	75.9	87.8
March	July	7/1	2012	12	44.8	66.0	77.8
March	July	7/1	2012	14	35.3	56.5	68.3
March	July	7/12	2012	10	65.0	86.2	98.0
March	July	7/12	2012	12	53.9	75.1	86.9
March	July	7/12	2012	14	43.4	64.5	76.4
March	August	8/1	2012	10	83.0	104.2	116.0
March	August	8/1	2012	12	70.0	91.1	103.0
March	August	8/1	2012	14	57.4	78.6	90.4
March	August	8/8	2012	10	89.5	110.6	122.5
March	August	8/8	2012	12	75.7	96.9	108.7
March	August	8/8	2012	14	62.4	83.6	95.4
April	June	6/1	2012	10	29.0	50.2	62.0
April	June	6/1	2012	12	23.7	44.9	56.7
April	June	6/1	2012	14	18.5	39.7	51.5
April	June	6/6	2012	10	32.6	53.8	65.6
April	June	6/6	2012	12	26.8	48.0	59.8
April	June	6/6	2012	14	21.1	42.3	54.1
April	July	7/1	2012	10	51.6	72.8	84.6
April	July	7/1	2012	12	43.3	64.5	76.3
April	July	7/1	2012	14	35.0	56.2	68.0
April	July	7/12	2012	10	61.8	83.0	94.8
April	July	7/12	2012	12	52.4	73.6	85.4
April	July	7/12	2012	14	43.0	64.2	76.0
April	August	8/1	2012	10	79.9	101.1	112.9
April	August	8/1	2012	12	68.5	89.7	101.5
April	August	8/1	2012	14	57.1	78.3	90.1
April	August	8/8	2012	10	86.3	107.5	119.3
April	August	8/8	2012	12	74.2	95.4	107.2
April	August	8/8	2012	14	62.1	83.3	95.1

Table A4 – Growing degree-day model simulation summary and results (minimum, maximum, and mean lengths) for 2013 YOY Atlantic menhaden.

Start Month	End Month	End Date	Year	Threshold	Min Lt (mm)	Mean Lt (mm)	Max Lt (mm)
November	June	6/1	2013	10	24.1	45.3	57.1
November	June	6/1	2013	12	17.8	39.0	50.8
November	June	6/1	2013	14	13.0	34.2	46.0
November	June	6/7	2013	10	27.8	49.0	60.8
November	June	6/7	2013	12	20.9	42.1	53.9
November	June	6/7	2013	14	15.5	36.7	48.5
November	July	7/1	2013	10	45.0	66.2	78.0
November	July	7/1	2013	12	35.7	56.8	68.7
November	July	7/1	2013	14	27.9	49.1	60.9
November	July	7/10	2013	10	52.7	73.9	85.7
November	July	7/10	2013	12	42.4	63.6	75.4
November	July	7/10	2013	14	33.7	54.9	66.7
November	August	8/1	2013	10	72.5	93.6	105.5
November	August	8/1	2013	12	60.0	81.2	93.0
November	August	8/1	2013	14	49.1	70.3	82.1
November	August	8/7	2013	10	77.2	98.4	110.2
November	August	8/7	2013	12	64.2	85.4	97.2
November	August	8/7	2013	14	52.7	73.9	85.7
December	June	6/1	2013	10	22.4	43.6	55.4
December	June	6/1	2013	12	17.3	38.5	50.3
December	June	6/1	2013	14	12.9	34.1	45.9
December	June	6/7	2013	10	26.1	47.3	59.1
December	June	6/7	2013	12	20.4	41.5	53.4
December	June	6/7	2013	14	15.4	36.6	48.4
December	July	7/1	2013	10	43.3	64.5	76.3
December	July	7/1	2013	12	35.2	56.3	68.2
December	July	7/1	2013	14	27.8	49.0	60.8
December	July	7/10	2013	10	50.9	72.1	83.9
December	July	7/10	2013	12	41.9	63.1	74.9
December	July	7/10	2013	14	33.7	54.8	66.7
December	August	8/1	2013	10	70.7	91.9	103.7
December	August	8/1	2013	12	59.5	80.7	92.5
December	August	8/1	2013	14	49.0	70.2	82.0
December	August	8/7	2013	10	75.5	96.7	108.5
December	August	8/7	2013	12	63.7	84.8	96.7
December	August	8/7	2013	14	52.6	73.8	85.6
January	June	6/1	2013	10	22.4	43.6	55.4

January	June	6/1	2013	12	17.3	38.5	50.3
January	June	6/1	2013	14	12.9	34.1	45.9
January	June	6/7	2013	10	26.1	47.3	59.1
January	June	6/7	2013	12	20.4	41.5	53.4
January	June	6/7	2013	14	15.4	36.6	48.4
January	July	7/1	2013	10	43.3	64.5	76.3
January	July	7/1	2013	12	35.2	56.3	68.2
January	July	7/1	2013	14	27.8	49.0	60.8
January	July	7/10	2013	10	50.9	72.1	83.9
January	July	7/10	2013	12	41.9	63.1	74.9
January	July	7/10	2013	14	33.7	54.8	66.7
January	August	8/1	2013	10	70.7	91.9	103.7
January	August	8/1	2013	12	59.5	80.7	92.5
January	August	8/1	2013	14	49.0	70.2	82.0
January	August	8/7	2013	10	75.5	96.7	108.5
January	August	8/7	2013	12	63.7	84.8	96.7
January	August	8/7	2013	14	52.6	73.8	85.6
February	June	6/1	2013	10	22.4	43.6	55.4
February	June	6/1	2013	12	17.3	38.5	50.3
February	June	6/1	2013	14	12.9	34.1	45.9
February	June	6/7	2013	10	26.1	47.3	59.1
February	June	6/7	2013	12	20.4	41.5	53.4
February	June	6/7	2013	14	15.4	36.6	48.4
February	July	7/1	2013	10	43.3	64.5	76.3
February	July	7/1	2013	12	35.2	56.3	68.2
February	July	7/1	2013	14	27.8	49.0	60.8
February	July	7/10	2013	10	50.9	72.1	83.9
February	July	7/10	2013	12	41.9	63.1	74.9
February	July	7/10	2013	14	33.7	54.8	66.7
February	August	8/1	2013	10	70.7	91.9	103.7
February	August	8/1	2013	12	59.5	80.7	92.5
February	August	8/1	2013	14	49.0	70.2	82.0
February	August	8/7	2013	10	75.5	96.7	108.5
February	August	8/7	2013	12	63.7	84.8	96.7
February	August	8/7	2013	14	52.6	73.8	85.6
March	June	6/1	2013	10	22.4	43.6	55.4
March	June	6/1	2013	12	17.3	38.5	50.3
March	June	6/1	2013	14	12.9	34.1	45.9
March	June	6/7	2013	10	26.1	47.3	59.1
March	June	6/7	2013	12	20.4	41.5	53.4
March	June	6/7	2013	14	15.4	36.6	48.4

March	July	7/1	2013	10	43.3	64.5	76.3
March	July	7/1	2013	12	35.2	56.3	68.2
March	July	7/1	2013	14	27.8	49.0	60.8
March	July	7/10	2013	10	50.9	72.1	83.9
March	July	7/10	2013	12	41.9	63.1	74.9
March	July	7/10	2013	14	33.7	54.8	66.7
March	August	8/1	2013	10	70.7	91.9	103.7
March	August	8/1	2013	12	59.5	80.7	92.5
March	August	8/1	2013	14	49.0	70.2	82.0
March	August	8/7	2013	10	75.5	96.7	108.5
March	August	8/7	2013	12	63.7	84.8	96.7
March	August	8/7	2013	14	52.6	73.8	85.6
April	June	6/1	2013	10	22.4	43.6	55.4
April	June	6/1	2013	12	17.3	38.5	50.3
April	June	6/1	2013	14	12.9	34.1	45.9
April	June	6/7	2013	10	26.1	47.3	59.1
April	June	6/7	2013	12	20.4	41.5	53.4
April	June	6/7	2013	14	15.4	36.6	48.4
April	July	7/1	2013	10	43.3	64.5	76.3
April	July	7/1	2013	12	35.2	56.3	68.2
April	July	7/1	2013	14	27.8	49.0	60.8
April	July	7/10	2013	10	50.9	72.1	83.9
April	July	7/10	2013	12	41.9	63.1	74.9
April	July	7/10	2013	14	33.7	54.8	66.7
April	August	8/1	2013	10	70.7	91.9	103.7
April	August	8/1	2013	12	59.5	80.7	92.5
April	August	8/1	2013	14	49.0	70.2	82.0
April	August	8/7	2013	10	75.5	96.7	108.5
April	August	8/7	2013	12	63.7	84.8	96.7
April	August	8/7	2013	14	52.6	73.8	85.6

References

Ahrenholz, D.W. 1991. Population biology and life history of the North American menhadens, *Brevoortia spp*. Marine Fisheries Review 53(4):3-19.

Ahrenholz, D.W., Guthrie, J.F, and C.W. Krouse. 1989. Results of abundance surveys of juvenile Atlantic and Gulf menhaden, *Brevoortia tyrannus* and *Brevoortia patronus*. U.S. Department of Commerce NOAA Technical Report. National Marine Fisheries Service No. 84, 14 p.

Ahrenholz, D.W., Fitzhugh, G.R., Rice, J. A, Nixon, S.W., and C.W. Pritchard. 1995. Confidence of otolith ageing through the juvenile stage for Atlantic menhaden, *Brevoortia tyrannus*. Fishery Bulletin 93: 209–216.

Ahrenholz, D.W., Squires, D.D., Rice, J.A., Nixon, S.W., Carolina, N., and G.R. Fitzhugh. 2000. Periodicity of increment formation in otoliths of overwintering postlarval and prejuvenile Atlantic menhaden, *Brevoortia tyrannus*. Fishery Bulletin 426: 421–426.

Alheit, J., and A. Bakun. 2010. Population synchronies within and between ocean basins: Apparent teleconnections and implications as to physical–biological linkage mechanisms. Journal of Marine. Systems 79: 267–285.

Anderson, J.T. 1988. A review of size dependent survival during pre-recruit stages of fishes in relation to recuritment. Journal of Northwest Atlantic Fisheries Science 8: 55–66.

Annis, E., Houde, E., Harding, L., Mallonee, M., and M. Wilberg. 2011. Calibration of a bioenergetics model linking primary production to Atlantic menhaden, *Brevoortia tyrannus*, growth in Chesapeake Bay. Marine Ecology Progress Series 437: 253–267.

ASMFC. 2004. Atlantic menhaden stock assessment report for peer review. Atlantic States Marine Fisheries Commission, Stock Assessment Report 04-01 (Supplement). ASMFC, Washington, DC.

Austin, H.M. 2002. Decadal oscillations and regime shifts, a characterization of the Chesapeake Bay marine climate. American Fisheries Society Symposium 155–169.

Bakun, A., Babcock, E. A., and C. Santora. 2009. Regulating a complex adaptive system via its wasp-waist: grappling with ecosystem-based management of the New England herring fishery. ICES Journal of Marine. Science 66: 1768–1775.

Bergenius, M., Meekan, M., Robertson, R., and M. McCormick. 2002. Larval growth

predicts the recruitment success of a coral reef fish. Oecologia 131: 521–525.

Berrien, P., and J. Sibunka. 1999. Distribution patterns of fish eggs in the U.S. northeast continental shelf ecosystem, 1977-1987. NOAA Technical Report National Marine Fisheries Service 145.

Buchheister, A., Miller, T.J., Houde, E.D., Secor, D.H., and R. Latour. In Press. Spatial and temporal dynamics of Atlantic menhaden (*Brevoortia tyrannus*) recruitment in the Northwest Atlantic Ocean. ICES Journal of Marine Science.

Callihan, J.L, Takata, L T., Woodland, R.J., and D.H. Secor. 2008. Cohort splitting in bluefish, *Pomatomus saltatrix*, in the US mid-Atlantic bight. Fisheries Oceanography. 17(3):191-205.

Campana, S.E., and J.D. Neilson. 1985. Microstructure of Fish Otoliths. Canadian Journal of Fisheries and Aquatic Science 42: 1014–1032.

Campana, S.E., and S.R. Thorrold. 2001. Otoliths, increments, and elements: keys to a comprehensive understanding of fish populations? Canadian Journal of Fisheries and Aquatic Science 58: 30–38.

Chambers, R.C. and T.J. Miller. 1995. Evaluating fish growth by means of otolith increment analysis: special properties of individual-level longitudinal data. Recent developments in fish otolith research 155-175.

Checkley Jr., D.M., Raman, S., Maillet, G.L. and K.M. Mason. 1988. Winter storm effects on the spawning and larval drift of a pelagic fish. Nature 335: 346-348.

Conroy, C.W., Piccoli, P.M. and D.H. Secor. In Press. Carryover effects of early growth and river flow on partial migration in striped bass *Morone saxatilis.* Marine Ecology Progress Series.

Cury, P. and C. Roy. 1989. Optimal environmental window and pelagic fish recruitment success in upwelling areas. Canadian Journal of Fisheries and Aquatic Sciences 46(4): 670-680.

Cushing, D.H. 1975. Marine Ecology and Fisheries. Cambridge University Press, Cambridge, MA.

Cushing, D.H. 1990. Plankton production and year-class strength in fish populations: An update of the match mismatch hypothesis. Advances in Marine Biology 26: 249-293.

Deegan, L. A. 1990. Effects of estuarine environmental conditions on population dynamics of young-of-the-year gulf menhaden. Marine Ecology Progress Series 68: 195–205.

Edeline, E. 2007. Adaptive phenotypic plasticity of eel diadromy. Marine Ecology Progress Series 341: 229–232.

Epifanio, C.E. and R.W. Garvine. 2001. Larval transport on the Atlantic continental shelf of North America: a review. Estuarine, Coastal and Marine Science 52: 51-77.

Fey, D.P., and J.A. Hare. 2012. Temperature and somatic growth effects on otolith growth of larval Atlantic menhaden, *Brevoortia tyrannus* (Actinopterygii: Clupeiformes: Clupeidae). Acta Ichthyolgoica et Piscatoria 42: 215–222.

Fitzhugh, G.R., Nixon, S.W., Ahrenholz, D.W., and J.A. Rice. 1997. Temperature effects on otolith microstructure and birth month estimation from otolith increment patterns in Atlantic menhaden. Transactions of the American Fisheries Society 126: 579–593.

Flemer, D. 1970. Primary production in the Chesapeake Bay. Chesapeake Science 11: 117–129.

Food and Agriculture Organization of the United Nations. 2012. FAO Yearbook: Fishery and Aquaculture Statistics. Rome, Italy. 76 pp.

Friedland, K.D., Haas, L.W. and J.V. Merriner. 1984. Filtering rates of the juvenile Atlantic menhaden, *Brevoortia tyrannus*, (Pisces: Clupeidae), with consideration of the effects of detritus and swimming speed. Marine Biology 84: 109-117.

Friedland, K., Ahrenholz, D., and J.F. Guthrie. 1989. Influence of plankton on distribution patterns of the filter-feeder Brevoortia tyrannus (Pisces: Clupeidae) . Marine Ecology Progress Series 54: 1–11.

Friedland, K.D., Ahrenholz, D.W., and J.F. Guthrie. 1996. Formation and seasonal evolution of Atlantic menhaden juvenile nurseries in coastal estuaries. Estuaries 19(1): 105-114.

Fuiman, L. A., Poling, K.R., and D.M. Higgs. 1998. Quantifying developmental progress for comparative studies of larval fishes. Copeia 1998(3): 602–611.

Fuiman, L., and R. Batty. 1997. What a drag it is getting cold: partitioning the physical and physiological effects of temperature on fish swimming. Journal of Experimental Biology 200: 1745–1755.

Gagliano, M., McCormick, M.I., and M.G. Meekan. 2007. Survival against the odds:

ontogenetic changes in selective pressure mediate growth-mortality trade-offs in a marine fish. Proceedings of the Royal Society B: Biological Sciences 274: 1575–1582.

Gastwirth, J.L., Gel, Y.R., Wallace Hui, W.L., Lyubchich, V., Miao, W., and K. Noguchi. 2015. Lawstat:tools for biostatistics, public policy, and law. R package version 3.0.

Hanson, P.C., Johnson, T.B., Schindler, D.E., and J.F. Kitchell. 1997. Fish Bioenergetics 3.0. University of Wisconsin Sea Grant Institute.

Harding, L.W., Jr., Itsweire, E.C. and W.E. Esaias. 1994. Estimates of phytoplankton biomass in the Chesapeake Bay from aircraft remote sensing of chlorophyll concentrations. Remote Sensing of the Environment 49: 41-56.

Harding, L.W., Mallonee, M.E., and E.S. Perry. 2002. Toward a predictive understanding of primary productivity in a temperate, partially stratified estuary. Estuarine, Coastal and Shelf Science 55: 437–463.

Harding, L.W., Magnuson, A. and M.E. Mallonee. 2005. SeaWiFS retrievals of chlorophyll in Chesapeake Bay and the mid-Atlantic bight. Estuarine, Coastal and Shelf Science 62: 75-94.

Hare, J.A., Quinlan, J.A., Werner, F.E., Blanton, B.O., Govoni, J.J., Forward, R.B., Settle, L.R., and D.E. Hoss. 1999. Larval transport during winter in the SABRE study area: results of a coupled vertical larval behavior-3-dimensional circulation model. Fisheries Oceanography 8(Suppl.2): 57-76.

Hare, J. A., and K.W. Able. 2007. Mechanistic links between climate and fisheries along the east coast of the United States: explaining population outbursts of Atlantic croaker (*Micropogonias undulatus*). Fisheries Oceanography 16: 31–45.

Hare, J. A, Alexander, M. A, Fogarty, M.J., Williams, E.H., and J.D. Scott. 2010. Forecasting the dynamics of a coastal fishery species using a coupled climate-population model. Ecological Applications 20: 452–464.

Hettler, W.F. 1976. Influence of temperature and salinity on routine metabolic rate and growth of young Atlantic menhaden. Journal of Fish Biology 55–65.

Higham, J., and W. Nicholson. 1964. Sexual maturation and spawning of Atlantic menhaden. Fishery Bulletin 63: 255–271.

Hildebrand, H.H. 1948. A review of the American menhaden, genus *Brevoortia*, with a description of a new species. Smithsonian Publication 107(18): 1-39.

Hjort. J. 1914. Fluctuations in the great fisheries of Northern Europe. Conseil Permanent International pour L'Exploration de la Mer. 20: 1-228.

Hjort, J. 1926. Fluctuations in the year classes of important food fishes. Journal du Conseil International pour L'Exploration de la Mer 1: 1-38.

Hollowed, A.B., Barbeaux, S.J., Cokelet, E.D., Farley, E., Kotwicki, S., Ressler, P.H., Spital, C., and C.D. Wilson. 2012. Effects of climate variations on pelagic ocean habitats and their role in structuring forage fish distributions in the Bering Sea. Deep Sea Res. Part II Topical Studies in Oceanography 65-70: 230–250.

Houde, E.D. 1987. Fish early life dynamics and recruitment variability. American Fisheries Society Symposium 2, 17-29.

Houde, E.D. 1989. Subtleties and episodes in the early life of fishes. Journal of Fish Biology 35 (sa): 29–38.

Houde, E.D. 1997. Patterns and trends in larval-stage growth and mortality of teleost fish. Journal of Fish Biology. 57(A): 52-83.

Houde, E.D. 2008. Emerging from Hjort's Shadow. Journal of Northwest Atlantic Fisheries Science 41: 53–70.

Houde, E.D. 2009. Recruitment variability. pp. 91-171. In: Jakobsen, T., M.J. Fogarty, B.A. Megrey and E. Moksness. Fish reproductive biology. Implications for assessment and management. Wiley-Blackwell.

Houde, E.D., Secor, D.H. and M.J. Wilberg. 2010. Temporal and spatial variability in larval influx, production, and recruitment of young-of-the-year Atlantic menhaden and Bay anchovy in Chesapeake Bay: Year 3. NOAA Final Report Grant #: NA07NMF4570340, 49 pp.

Houde, E.D. Annis, E., Harding Jr., L. Mallonee, M and M. Wilberg. In Review. Factors affecting abundance of age-0 Atlantic menhaden (*Brevoortia tyrannus)* in Chesapeake Bay. ICES Journal of Marine Science.

Humphrey, J., Wilberg, M.J., Houde, E.D., and M.C. Fabrizio. 2014. Effects of temperature on age-0 Atlantic menhaden growth in Chesapeake Bay. Transactions of the American Fisheries Society 143: 1255–1265.

Hurst, T.P. 2007. Causes and consequences of winter mortality in fishes. Journal of Fish Biology 71: 315–345.

Hurst, T.P., and D.O. Conover. 1998. Winter mortality of young-of-the-year Hudson

River striped bass (*Morone saxatilis*): size-dependent patterns and effects on recruitment. Canadian Journal of Fisheries and Aquatic Science 55: 1122–1130.

Iles, T.D., and M. Sinclair. 1982. Atlantic herring: Stock discreteness and abundance. Science 215:627 633.

Juanes, F. 2007. Role of habitat in mediating mortality during the post-settlement transition phase of temperate marine fishes. Journal of Fish Biology 70(3) :661-677.

June, F.C., and F.T. Carlson. 1971. Food of young Atlantic menhaden, *Brevoortia tyrannus*, in relation to metamorphosis. Fishery Bulletin 68: 493–512.

Jung, S., and E.D. Houde. 2003. Spatial and temporal variabilities of pelagic fish community structure and distribution in Chesapeake Bay, USA. Estuarine, Coastal and Shelf Science 58: 335–351.

Jung, S., and E.D. Houde. 2005. Fish biomass size spectra in Chesapeake Bay. Estuaries 28(2): 226-240.

Kaufmann, R., and W. Wieser. 1992. Influence of temperature and ambient oxygen on the swimming energetics of cyprinid larvae and juveniles. Environmental Biology of Fishes 33: 87–95.

Kerr, L. A., and D.H. Secor. 2009. Bioenergetic trajectories underlying partial migration in Patuxent River (Chesapeake Bay) white perch (*Morone americana*). Canadian Journal of Fisheries and Aquatic Science 66: 602–612.

Kerr, L. A., and D.H. Secor. 2010. Latent effects of early life history on partial migration for an estuarine-dependent fish. Environmental Biology of Fishes 89: 479–492.

Kitchell, J.F., Stewart, D.J. and D. Weininger. 1977. Applications of a bioenergetics model to yellow perch (*Perca flavens)* and walleye (*Stizostedion vitreum vitreum)*. Journal of the Fishery Research Board Canada 34: 1922-1935.

Kimmel, D.G., Miller, W.D., Harding Jr., L.W., Houde, E.D. and M.R. Roman. 2009. Estuarine ecosystem response captured using a synoptic climatology. Estuaries and Coasts 32: 403–409.

Kroger, R.L., Guthrie, J.F., and M.H. Judy. 1974. Growth and first annulus formation of tagged and untagged Atlantic menhaden. Transactions of the American Fisheries Society 103: 292–296.

Lambert, T.C., and D.M. Ware. 1984. Reproductive strategies of demersal and

pelagic spawning fish. Canadian Journal of Fisheries and Aquatic Science 41: 1565–1569.

Lasker, R. 1975. Field criteria for survival of anchovy larvae: Relation between inshore chlorophyll maximum layers and successful first feeding. Fishery Bulletin 73(3): 453-462.

Lewis, R.M. 1965. The effect of minimum temperature on the survival of larval Atlantic menhaden, *Brevoortia tyrannus*. Transactions of the American Fisheries Society 94: 409–412.

Lewis, R.M., Ahrenholz, D.W., and S.P. Epperly. 1987. Fecundity of Atlantic menhaden, *Brevoortia tyrannus.* Coasta 10: 347–350.

Logan, D.T. 1985. Environmental variation and striped bass population dynamics : a size-dependent mortality model. Estuaries 8: 28–38.

Lozano, C. 2011. Dynamics of ingress, hatch dates, growth, and feeding of Atlantic menhaden, *Brevoortia tyrannus*, larvae at the Chesapeake Bay mouth. University of Maryland, College Park, MD. 175 pp.

Lozano, C., Houde, E.D., Wingate, R.L., and D.H. Secor. 2012. Age, growth and hatch dates of ingressing larvae and surviving juveniles of Atlantic menhaden *Brevoortia tyrannus*. Journal of Fish Biology 81: 1665–1685.

Ludsin, S. A., and D.R. Devries. 1997. First-year recruitment of largemouth bass: The interdependency of early life stages. Ecological Applications 7: 1024–1038.

Luo, J., Hartman, K.J., Brandt, S.B., Cerco, C.F., and T.H. Rippetoe. 2001. A spatially-explicit approach for estimating carrying capacity: an application for the Atlantic menhaden *(Brevoortia tyrannus*) in Chesapeake Bay. Estuaries 24: 545.

MacCall, A.D. 1990. Dynamic Geography of Marine Fish Populations. Washington Sea Grant, Seattle, WA.

Mackenzie, B.R., Miller, T.J., Cyr, S., and W.C. Leggett. 1994. Evidence for a dome shaped relationship between turbulence and larval fish ingestion rates. Limnology and Oceanography 39: 1790–1799.

Maillet, G.L., and D.M. Checkley Jr. 1990. Effects of starvation on the frequency of formation and width of growth increments in sagittae of laboratory-reared Atlantic menhaden *Brevoortia tyrannus* Larvae. Fishery Bulletin 88: 155–165.

Maillet, G.L., and D.M. Checkley Jr. 1991. Storm-related variation in the growth-rate

of otoliths of larval Atlantic menhaden, *Brevoortia tyrannus* - a time-series analysis of biological and physical variables and implications for larval growth and mortality. Marine Ecology Progress Series 79: 1–16.

Maryland Sea Grant. 2009. Ecosystem Based Fisheries Management for Chesapeake Bay: Menhaden Species Team Background and Issue Briefs. http://www.mdsg.umd.edu/sites/default/files/files/EBFM-Menhaden-Summary.pdf

Meekan, M.G., and L. Fortier. 1996. Selection for fast growth during the larval life of Atlantic cod *Gadus morhua* on the Scotian Shelf. Marine Ecology Progress Series 137: 25–37.

Miller, T.J., Crowder, L.B., Rice, J.A., and E.A. Marschall. 1988. Larval size and recruitment mechanisms in fishes: Toward a conceptual Framework. Canadian Journal of Fisheries and Aquatic Sciences 45: 1657–1670.

Miller, T. J. 2002. Chesapeake Bay fishery independent multispecies fisheries survey (CHESFIMS). 2001 Annual Report to NOAA-Chesapeake Bay Office, 1 March 2002. Ref. No. [UMCES]CBL 02-0079. Solomons, MD

Murdy, E.O., Birdsong, Ray S. and John A. Musick. 1996. Fishes of the Chesapeake Bay. Smithsonian Institution Press, Washington DC.

Najjar, R.G., Pyke, C.R., Adams, M.B., Breitburg, D., Hershner, C., Kemp, M., Howarth, R., Mulholland, M.R., Paolisso, M., Secor, D., Sellner, K., Wardrop, D., and R. Wood. 2010. Potential climate-change impacts on the Chesapeake Bay. Estuarine, Coastal and Shelf Science 86: 1–20.

Nicholson, W.R. 1978. Movements and Population Structure of Atlantic Menhaden Indicated by Tag Returns. Estuaries 1: 141–150.

O'Connor, C., Norris, D.R., Crossin, G.T., and S.J. Cooke. 2014. Biological carryover effects : linking common concepts and mechanisms in ecology and evolution. Ecosphere 5: 1–11.

Pacheco, A.L. and G.C. Grant. 1965. Studies of the early life histories of Atlantic menhaden in estuarine nurseries. Part I – Seasonal occurrence of juvenile menhaden and other small fishes in a tributary creek of Indian River, Delaware, 1957-1958. U.S. Fish and Wildlife Service Special Scientific Report. 504. 32 p.

Panella, G. 1971. Fish otoliths: daily growth layers and periodical patterns. Science 173(4002): 1124–1127.

Pechenik, J. A. 2006. Larval experience and latent effects--metamorphosis is not a

new beginning. Integrative and Comparative Biology 46: 323–333.

Pepin, P. 1991. Effect of temperature and size on development, mortality, and survival rates of the pelagic early life history stages of marine fish. Canadian Journal of Fisheries and Aquatic Science 48: 503–518.

Pikitch, E., Boersma, P.D., Boyd, I.L, Conover, D.O., Cury, P., Essington, T, Heppell, S.S., Houde, E.D., Mangel, M, Pauly, D., Plaganyl, E., Sainsbury, K., and R.S. Steneck. 2012. Little Fish, Big Impact: Managing a crucial link in ocean food webs. Lenfest Ocean Program. Washington, DC. 108 p.

Polgar, T.T. 1982. Factors affecting recruitment of Potomac River striped bass and resulting implications for management. Estuarine Comparisons Proceedings of the Sixth Biennial International Estuarine Research Conference 1981 p. 427-442.

Post, J.R., and D.O. Evans. 1989. Size-dependent overwinter mortality of young-of the-year yellow Perch (*Perca flavescens)*: Laboratory, *in situ* enclosure, and field experiments. Canadian Journal of Fisheries and Aquatic Science 46: 1958–1968.

Post, J.R., and A.B. Prankevicius. 1987. Size-selective mortality in young-of-the-year yellow perch (*Perca flavescens*): Evidence from otolith microstructure. Canadian Journal of Fisheries and Aquatic Science 44: 1840–1847.

Quinlan, J. A., Blanton, B.O., Miller, T.J., and F.E. Werner. 1999. From spawning grounds to the estuary: Using linked individual-based and hydrodynamic models to interpret patterns and processes in the oceanic phase of Atlantic menhaden Brevoortia tyrannus life history. Fisheries Oceanography 8: 224–246.

Quinlan, J.A., and B. Crowder. 1999. Searching for sensitivity in the life history of Atlantic menhaden: inferences from a matrix model. Fisheries Oceanography 8: 124–133.

R Core Team (2015). R: A language and environment for statistical computing. R Foundation for Statistical Computing, Vienna, Austria. URL http://www.R-project.org/.

Rankin, T.L., and S. Sponaugle. 2011. Temperature influences selective mortality during the early life stages of a coral reef fish. PLoS One 6: e16814.

Reintjes, J.W. 1960. Continuous distribution of menhaden along the South Atlantic and Gulf coasts of the United States. Bureau of Commercial Fisheries, Beaufort, NC.

Reish, R.L., Deriso, R.B., Ruppert, D., and R. J. Carroll. 1985. An investigation of the population dynamics of Atlantic menhaden (*Brevoortia tyrannus*). Canadian Journal of Fisheries and Aquatic Science 42: 147–157.

Rice, J.A., Quinlan, J.A., Nixon, S.W., Hettler Jr, W.F., Warlen, S.M., and P.M. Stegmann. 1999. Spawning and transport dynamics of Atlantic menhaden: inferences from characteristics of immigrating larvae and predictions of a hydrodynamic model. Fisheries Oceanography 8: 93–110.

Rippetoe, T.H. 1993. Production and energetics of Atlantic menhaden in Chesapeake Bay. Master's thesis, University of Maryland, College Park, MD. 113 p.

Rothschild, B.J. 1986. Dynamics of Marine Fish Populations. Harvard University Press, Cambridge, MA.

Rutherford, E.S., Houde, E.D. and R.M. Nyman. 1997. Relationship of larval-stage growth and mortality to recruitment of striped bass, *Morone saxatilis,* in Chesapeake Bay. Estuaries. 20: 174-198.

Sætre, R. 2002. Factors affecting the recruitment variability of the Norwegian spring spawning herring (*Clupea harengus L.*). ICES Journal of Marine Science 59: 725–736.

Schwartzlose, R.A. and 20 coauthors. 1999. Worldwide large-scale fluctuations of sardine and anchovy populations. South African Journal of Marine Science. 21: 289-347.

Secor, D.H., Dean, J.M., and E.H. Laban. 1991. Manual for otolith removal and preparation for microstructural examination. Electric Power Research Institute [Palo Alto, CA] and the Belle W. Baruch Institute for Marine Biology and Coastal Research [Columbia, SC]. 85 p.

Secor, D.H., and E.D. Houde. 1995. Temperature effects on the timing of striped bass egg production, larval viability, and recruitment potential in the Patuxent River (Chesapeake Bay). Estuaries 18: 527.

Secor, D.H. 2015. Migration ecology of marine fishes. Johns Hopkins University Press, Baltimore, MD.

SEDAR. 2015. SEDAR 40 – Atlantic Menhaden Stock Assessment Report. SEDAR, North Charleston SC. 643 pp. http://www.asmfc.org/uploads/file/55089931S40_AtlMenhadenSAR_CombinedFINAL_1.15.2015-reduced.pdf

Shima, J.S., and A.M. Findlay. 2002. Pelagic larval growth rate impacts benthic

settlement and survival of a temperate reef fish. Marine Ecology Progress Series 235: 303–309.

Shuter, B.J., Maclean, J.A., Fry, F.E.J., and H.A. Regier. 1980. Stochastic simulation of temperature effects on first-year survival of smallmouth bass. Transactions of the American Fisheries Society 109 (1): 1-34.

Shuter, B.J., Finstad, A.G., Helland, I.P., Zweimuller, I., and F. Holker. 2012. The role of winter phenology in shaping the ecology of freshwater fish and their sensitivities to climate change. Aquatic Sciences 74: 637-657.

Sogard, S.M. 1997. Size-selective mortality in the juvenile stage of teleost fishes: a review. Bulletin of Marine Science. 60: 1129–1157.

Stegmann, P.M., Quinlan, J.W., Werner, F.E., Blanton, B.O., and P. Berrien. 1999. Atlantic menhaden recruitment to a southern estuary: defining potential spawning regions. Fisheries Oceanography 8 (Suppl.2): 111-123.

Takasuka, A, Aoki, I., and I. Mitani. 2003. Evidence of growth-selective predation on larval Japanese anchovy *Engraulis japonicus* in Sagami Bay. Marine Ecology Progress Series 252: 223-238.

Therneau, T., Atkinson, B., and B. Ripley. 2015. Rpart: Recursive partitioning and regression trees. R package version 4.1-10. https://cran.r-project.org/web/packages/rpart/rpart.pdf

Townsend, D.W., Radtke, R.L., Morrison, M.A., and S.D. Folsom. 1989. Recruitment implications of larval herring overwintering distributions in the Gulf of Maine, inferred using a new otolith technique. Marine Ecology Progress Series 55: 1–13.

Uphoff J.H. Jr. 2003. Predator-prey analysis of striped bass and Atlantic menhaden in upper Chesapeake Bay. Fisheries Management and Ecology 10: 313-322.

Warlen, S.M. 1992. Age, growth, and size distribution of larval Atlantic menhaden off North Carolina. Transactions of the American Fisheries Society 121(5): 588–598.

Warlen, S.M. 1994. Spawning time and recruitment dynamics of larval Atlantic menhaden, *Brevoortia tyrannus*, into a North Carolina estuary. Fishery Bulletin 92: 420–433.

Warlen, S.M., Able, K.W., and E.H. Laban. 2002. Recruitment of larval Atlantic menhaden (*Brevoortia tyrannus)* to North Carolina and New Jersey estuaries: Evidence for larval transport northward along the east coast of the United States. Fishery Bulletin 100: 609–623.

Weatherly, A.H. 1990. Approaches to understanding fish growth. Transactions of the American Fisheries Society 119: 662–672.

Winemiller, K.O., and K.A. Rose. 1993. Why do most fish produce so many tiny offspring? The American Naturalist 142(4): 585–603.

Wood, R.J. 2000. Synoptic scale climate forcing of multispecies fish recruitment patterns in Chesapeake Bay. A Dissertation Presented to Doctor of Philosophy. College of William and Mary, Williamsburg, VA. 146 p.

Wood, R.J. and E.D. Houde. 2003. Variability in the dynamics of forage fish abundances in Chesapeake Bay: Retrospective analysis, models, and synthesis. NOAA Chesapeake Bay Office, Symposium Report pp. 97-107. http://www.eco-check.org/pdfs/asces_background.pdf

Wood, R.J., and H.M. Austin. 2009. Synchronous multidecadal fish recruitment patterns in Chesapeake Bay, USA. Canadian Journal of Fisheries and Aquatic Science 66: 496–508.